

---

Doctoral Dissertations

Student Theses and Dissertations


---

Spring 2015

## Synthesis, characterization and application of acrylic colloidal unimolecular polymer (CUP)

Ameya Manohar Natu

Follow this and additional works at: [https://scholarsmine.mst.edu/doctoral\\_dissertations](https://scholarsmine.mst.edu/doctoral_dissertations)

 Part of the [Polymer Chemistry Commons](#)

Department: Chemistry

---

### Recommended Citation

Natu, Ameya Manohar, "Synthesis, characterization and application of acrylic colloidal unimolecular polymer (CUP)" (2015). *Doctoral Dissertations*. 2391.

[https://scholarsmine.mst.edu/doctoral\\_dissertations/2391](https://scholarsmine.mst.edu/doctoral_dissertations/2391)

This thesis is brought to you by Scholars' Mine, a service of the Missouri S&T Library and Learning Resources. This work is protected by U. S. Copyright Law. Unauthorized use including reproduction for redistribution requires the permission of the copyright holder. For more information, please contact [scholarsmine@mst.edu](mailto:scholarsmine@mst.edu).

SYNTHESIS, CHARACTERIZATION AND APPLICATION OF ACRYLIC  
COLLOIDAL UNIMOLECULAR POLYMER (CUP)

by

AMEYA MANOHAR NATU

A DISSERTATION

Presented to the Faculty of the Graduate School of the  
MISSOURI UNIVERSITY OF SCIENCE AND TECHNOLOGY

In Partial Fulfilment of the Requirements for the Degree

DOCTOR OF PHILOSOPHY

in

CHEMISTRY

2015

Approved by

Dr. Michael R. Van De Mark, Advisor

Dr. Chariklia Sotiriou-Leventis

Dr. Thomas Schuman

Dr. Jeffrey Winiarz

Dr. John Myers

© 2015

AMEYA MANOHAR NATU

All Rights Reserved

### **PUBLICATION DISSERTATION OPTION**

The dissertation is divided into five chapters and has been prepared in the form of four manuscripts for publication. Papers included are prepared as per the requirements of the journal in which they are published or are submitted.

Paper I found on pages 12-42 is published Journal of Coatings Technology and Research.

Paper II found on pages 43-85 has been submitted to Progress in Organic Coatings.

Paper III found on pages 86-121 has been submitted to Colloid and Polymer Science.

Paper IV found on pages 122-160 will be submitted to a peer-reviewed journal.

## ABSTRACT

Colloidal Unimolecular Polymer (CUP) particles were prepared by the process of water reduction on amphiphilic acrylic copolymers prepared via free radical polymerization technique. The formation of CUP particles was driven by the polymer-polymer interaction being greater than the polymer-solvent interaction and entropically favored by release of the water. It was demonstrated by Dynamic Light Scattering technique that CUP particles based on copolymers below 13,000 MW were unstable and the particles aggregated to a higher particle size. For the polymers with molecular weight (MW) above 13,000, a good correlation between the theoretical and experimental CUP particle size was observed. The rheology behavior of CUPs was affected primarily by the tertiary electroviscous effects arising from the surface charged groups. At similar volume fraction, the CUP viscosity increased in the following order: quaternary ammonium > sulfonate > carboxylate which was directly related to the associated surface water fraction. The surface water was denser than bulk water and was the highest for sulfonate followed by carboxylate and quaternary ammonium functional CUP. The surface activity as measured by maximum bubble pressure tensiometer had the following trend: sulfonate > quaternary ammonium > carboxylate, at similar volume fraction which was attributed to the surface energy reduction because of electrostatic-repulsion. CUPs with sulfonate groups on the surface effectively catalyzed the acrylic-melamine crosslinking reactions and the cured films had mechanical properties similar to those obtained by using a commercial blocked p-toluene sulfonic acid catalyst. The CUP catalysts offered distinct advantages such as lower amount required on a molar equivalent basis and non-leachable in water after crosslinking, as compared to the commercial catalyst.

## ACKNOWLEDGMENTS

First and foremost, I would like to thank my advisor, Dr. Michael R. Van De Mark for his continuous guidance and support during my pursuit of graduate studies at Missouri S&T. His technical, professional and personal guidance has helped me to not only be successful academically but also to be a better human being. I admire his compassion and discipline which taught me to be passionate and hard-working.

I want to thank my advising committee members, Dr. Chariklia Sotiriou-Leventis, Dr. Thomas Schuman, Dr. Jeffrey Winiarz and Dr. John Myers for their support and guidance throughout the completion of my Ph.D. program. I thank the Department of Chemistry and the Missouri S&T Coatings Institute for financial support and other resources. I acknowledge fellow researchers: Dr. Minghang Chen, Dr. Jigar Mistry, Sagar Gade, and Yousef Dawib for their help and support at various occasions.

I am grateful to my friends; Abhishek, Pratik, Viswanaath and Sushrut who believed in me and my endeavors.

Last but not the least, I am truly indebted to my Family: my parents; Mr. Manohar Natu and Mrs. Veena Natu; grandmother: Mrs. Girija Vishwanath Natu; sister: Amala Natu and my wife Ar. Vrushali Lele, as well as my cousins and family for their unconditional love and support.

## TABLE OF CONTENTS

	Page
PUBLICATION DISSERTATION OPTION .....	iii
ABSTRACT .....	iv
ACKNOWLEDGMENTS .....	v
LIST OF ILLUSTRATIONS.....	x
LIST OF TABLES.....	xiv
<b>SECTION</b>	
1. INTRODUCTION.....	1
1.1. POLYMER NANOPARTICLES.....	1
1.2. POLYMERIC MICELLES .....	2
1.3. COLLOIDAL UNIMOLECULAR POLYMER (CUP) .....	5
1.3.1. Water-reduction Process For CUP Synthesis.....	7
1.3.2. Water-reduction Protocol.....	7
1.3.3. Determination Of Effective Charge .....	7
1.4. OBJECTIVE OF THIS RESEARCH.....	10
<b>PAPER</b>	
I MOLECULAR WEIGHT (MN) AND FUNCTIONALITY EFFECT ON CUP FORMATION AND STABILITY .....	12
ABSTRACT .....	12
INTRODUCTION.....	13
EXPERIMENTAL .....	16
Materials.....	16
Polymer synthesis.....	16
Synthesis for 12K polymer.....	17
Characterization of polymers synthesized.....	17
Water-Reduction of MMA-MAA based copolymers to form CUPs .....	18
Characterization of CUPs.....	20
RESULTS AND DISCUSSION .....	21
Acid Number .....	21
Molecular weight determination .....	22

Water-reduction of the polymers to prepare CUPs .....	23
Viscosity measurements of CUP solutions .....	27
Particle size analysis.....	31
CONCLUSIONS .....	39
ACKNOWLEDGEMENTS .....	40
REFERENCES.....	41
II. SYNTHESIS AND CHARACTERIZATION OF AN ACID CATALYST FOR ACRYLIC-MELAMINE RESIN SYSTEMS BASED ON COLLOIDAL UNIMOLECULAR POLYMER (CUP) PARTICLES OF MMA-AMPS .....	43
ABSTRACT .....	43
1. INTRODUCTION.....	44
2. MATERIALS AND METHODS .....	48
2.1. Characterization of Commercial Acrylic Resins.....	49
2.2. Synthesis of Random Copolymer of MMA and AMPS.....	49
2.3. Water-Reduction of MMA-AMPS Based Copolymer To Form CUPs.....	50
2.4. CO <sub>2</sub> H-CUP Synthesis.....	50
2.5. Characterization of Synthesized MMA-AMPS Copolymer.....	51
2.6. Characterization of CUPs.....	51
2.7. Coating Formulations and Testing .....	52
3. RESULTS AND DISCUSSION .....	57
3.1. Process of Water-reduction .....	57
3.2. Rheological Behavior.....	59
3.3. Role of Solvent and Divalent Cations .....	60
3.4. Particle Size Analysis Using DLS.....	62
3.5. Thermogravimetric Analysis and Differential Scanning Calorimetry (DSC)....	63
3.6. Effectiveness of CUP Catalyst In Curing OH-latex With Melamine Resin .....	65
3.7. Efficiency of CUP Catalyst In Curing OH-latex With Melamine Resin .....	71
3.8. Effectiveness of CUP Catalyst In Curing CO <sub>2</sub> H -latex and CO <sub>2</sub> H-CUP resin With Melamine Resin .....	72
3.9. Leaching Experiment .....	79
4. CONCLUSIONS .....	82
5. ACKNOWLEDGEMENTS .....	83



6. REFERENCES.....	83
III.SYNTHESIS AND CHARACTERIZATION OF CATIONIC COLLOIDAL UNIMOLECULAR POLYMER PARTICLES (CUPS).....	86
ABSTRACT.....	86
1. INTRODUCTION.....	87
2. THEORETICAL BASIS FOR RHEOLOGY BEHAVIOR.....	91
2.1. Primary Electroviscous Effect.....	91
2.2. Secondary Electroviscous Effect.....	91
2.3. Tertiary Electroviscous Effect.....	92
2.4. Determination of Intrinsic Viscosity of CUPs .....	92
3. MATERIALS AND METHODS.....	93
3.1. Materials.....	93
3.2. Polymer Synthesis and Characterization.....	93
3.3. Water-reduction.....	95
3.4. Particle Size and Distribution of CUPs .....	95
3.5. Absolute Viscosity of CUPs.....	96
3.6. Surface Tension.....	96
4. RESULTS AND DISCUSSION .....	97
4.1. Characterization of Polymer and CUPs .....	97
4.2. Water-reduction Process .....	99
4.3. Rheological Behavior.....	100
4.4. Particle Size Analysis Using DLS.....	101
4.5. Specific Viscosity Comparison .....	102
4.6. Density of Surface Water .....	108
4.7. Equilibrium Surface Tension Behavior.....	111
4.8. Dynamic Surface Tension Behavior.....	114
5. CONCLUSIONS.....	118
6. ACKNOWLEDGEMENTS .....	119
7. REFERENCES.....	120
IV.RHEOLOGY AND SURFACE TENSION BEHAVIOR OF SULFONATE FUNCTIONAL COLLOIDAL UNIMOLECULAR POLYMER (CUP).....	122
ABSTRACT.....	122

1. INTRODUCTION.....	123
2. THEORETICAL BASIS .....	126
2.1. Determination of Effective Charge .....	126
2.1.1. Nernst-Einstein model.....	126
2.1.2. Hessinger’s model.....	127
2.1.3. Charge renormalization.....	127
2.2. Theories Related With Rheology .....	129
2.3. Determination of Intrinsic Viscosity of CUPs .....	132
3. EXPERIMENTAL .....	133
3.1. Materials.....	133
3.2. Synthesis and Characterization of Copolymers .....	133
3.3. Preparation of CUPs.....	134
3.4. Characterization of CUPs.....	136
3.4.1. Shearing viscosity .....	136
3.4.2. Absolute viscosity of CUP solutions .....	136
3.4.3. Particle size of CUPs.....	136
3.4.4. Surface tension measurement.....	137
4. RESULTS AND DISCUSSION .....	137
4.1. Acid Number and Density.....	137
4.2. Particle Size Analysis.....	138
4.3. Specific Viscosity of CUP Suspension .....	139
4.4. Surface Water Density .....	144
4.5. Rheological Model Fitting .....	146
4.6. Surface Tension Measurement .....	150
5. CONCLUSIONS .....	157
6. ACKNOWLEDGEMENTS .....	158
7. REFERENCES.....	158
SECTION	
2. SUMMARY .....	161
BIBLIOGRAPHY .....	164
VITA .....	166

## LIST OF ILLUSTRATIONS

	Page
Figure 1.1 Process of formation of CUPs from poly(MMA-co-AMPS) .....	6
 <b>PAPER I</b>	
Figure 1. Comparison of size of latex, waterborne urethane and CUP particle.....	14
Figure 2. General Process of Formation of CUPs .....	19
Figure 3. Vial 1: CUP solution of Poly-1 before filtering; Vial 2: CUP solution of Poly-1 after filtering; Vial 3: CUP solution of Poly-5 (MW = 15K) .....	26
Figure 4. Viscosity against shear rate for Poly-4, Poly-7 and Poly-8 at 5.00% solids at 25 <sup>0</sup> C .....	28
Figure 5. Viscosity against shear rate for Poly-8 at 15% solids at 25 <sup>0</sup> C .....	29
Figure 6. Particle size distribution of Poly-1 after filtering .....	33
Figure 7. Particle size distribution of Poly-2 .....	35
Figure 8. Particle size distribution of Poly-3 .....	36
Figure 9. Particle size distribution of Poly-4 .....	37
Figure 10. Particle size distribution of Poly-5 .....	37
Figure 11. Particle size distribution of Poly-6 .....	38
Figure 12. Particle size distribution of Poly-7 .....	38
Figure 13. Particle size distribution of Poly-8 .....	39
Figure 14. Particle size distribution of Poly-9 .....	39
 <b>PAPER II</b>	
Figure 1. Incorporation of CUP catalyst in the acrylic-melamine resin via trans-esterification .....	47
Figure 2. Load-depth curve using the standard method for indentation testing of System 1. ....	56

Figure 3.	Load-depth curve using the ESP method for indentation testing of System 1. ....	56
Figure 4.	Process of formation of CUPs from copoly(MMA-AMPS).....	58
Figure 5.	Shear stress against shear rate for CUP catalyst solution at 5% solids at 1) 25 <sup>0</sup> C and 2) 29 <sup>0</sup> C.....	60
Figure 6.	Water reduction in presence of 50 ppm calcium for 1) CO <sub>2</sub> H-copolymer 2) SO <sub>3</sub> H-copolymer .....	62
Figure 7.	Particle size distribution of SO <sub>3</sub> H-CUPs in presence of 50 ppm of CaCl <sub>2</sub> ..	63
Figure 8.	Particle size distribution of SO <sub>3</sub> H-CUPs of poly(MMA-co-AMPS) without CaCl <sub>2</sub> .....	63
Figure 9.	TGA thermograms of CUP catalyst, OH-latex, CO <sub>2</sub> H-latex and CO <sub>2</sub> H-CUP. ....	65
Figure 10.	Modulated DSC thermogram of CUP catalyst, OH-latex, CO <sub>2</sub> H-latex and CO <sub>2</sub> H-CUP. ....	65
Figure 11.	MEK double rubs as a function of cure time for OH-latex cured with melamine resin at 150 <sup>0</sup> C.....	69
Figure 12.	A model for the stages involved in crosslinking of acrylic-melamine .....	72
Figure 13.	MEK double rubs against cure time for CO <sub>2</sub> H-latex cured with melamine resin .....	76
Figure 14.	MEK double rubs against cure time for CO <sub>2</sub> H-CUP cured with melamine resin .....	77
Figure 15.	Elastic modulus vs indentation depth for formulations based on OH-latex..	78
Figure 16.	Indentation Hardness vs indentation depth for formulations based on OH-latex .....	78
Figure 17.	NMR spectra of acrylic latex, melamine resin, blocked p-TSA, CUP catalyst, residue of acrylic film cured with blocked p-TSA and residue of acrylic film crosslinked with CUP catalyst .....	81
 PAPER III		
Figure 1.	Monomer structure .....	89

Figure 2.	CUP formation process.....	89
Figure 3.	NMR of polymer 1 (MW=36K) .....	98
Figure 4.	Plot of shear stress against shear rate for QUAT-CUP-55K at 25 °C and 29 °C.....	101
Figure 5.	Particle size distribution graphs using DLS for the three QUAT-CUPs....	102
Figure 6.	Plot of specific viscosity of the three quaternary ammonium functional and one carboxylate functional [14] CUP solutions as a function of volume fraction.....	103
Figure 7.	Plot of $\ln(\eta_{rel})$ versus volume fraction for quaternary ammonium functional CUPs.....	104
Figure 8.	Representative structure of QUAT and $\text{CO}_2^-$ -CUP surface with hydration layer.....	107
Figure 9.	Effect of weight fraction (f) on $1/\rho_s$ .....	110
Figure 10.	Surface tension versus concentration for the three QUAT-CUPs and $\text{CO}_2^-$ -CUP-36K.....	112
Figure 11.	Surface tension versus surface age for QUAT-CUPs and $\text{CO}_2^-$ -CUP-36K at 0.5 mole/m <sup>3</sup> .....	114
Figure 12.	Dynamic surface tension versus surface age at 4 different concentration for QUAT-CUPs (36K, 55K, 94K) .....	117
 PAPER IV		
Figure 1.	Process of CUP formation from poly(methyl methacrylate-co-2-acrylamido-2-methyl propane sulfonic acid).....	126
Figure 2.	Plot of specific viscosity of the three sulfonate functional and one carboxylate functional CUP solutions as a function of volume fraction....	139
Figure 3.	Plot of $\ln(\eta_{rel})$ versus volume fraction for sulfonate functional CUPs .....	140
Figure 4.	Representative structure of $\text{SO}_3^-$ and $\text{CO}_2^-$ -CUP surface with hydration layer .....	143
Figure 5.	Effect of weight fraction (f) on $1/\rho_s$ .....	146

Figure 6.	Comparison of experimental and theoretical specific viscosity for $\text{SO}_3^-$ -CUP (28K, 56K and 80K).....	149
Figure 7.	Surface tension of CUP suspensions as a function of concentration .....	151
Figure 8.	Dynamic surface tension versus surface age for the three $\text{SO}_3^-$ -CUPs and $\text{CO}_2^-$ -CUP-28K.....	153
Figure 9.	Dynamic surface tension versus surface age at various concentrations for the three $\text{SO}_3^-$ -CUPs: a) 28K, b) 56K and c) 80K CUP .....	155

## LIST OF TABLES

	Page
<b>PAPER I</b>	
Table 1. Formulation for MMA-MAA Polymers .....	18
Table 2. Percent Yield and Acid Value of Polymers .....	22
Table 3. Molecular Weight, Polydispersity Index and Number of Acid Groups Per Polymer Chain of the Synthesized Polymers .....	23
Table 4. Percent Solids and Viscosity at 25 °C and 29 °C for CUP Solutions .....	27
Table 5. Viscosity measurements at 25 °C for CUP solutions at 5.00% solids by weight .....	29
Table 6. Comparison of Theoretical and Experimental Particle Size of the CUPs .....	32
<b>PAPER II</b>	
Table 1. Important physical properties of the acrylic resins .....	48
Table 2. Formulations for OH-latex cured with melamine.....	53
Table 3. Formulations for CO <sub>2</sub> H-latex cured with melamine.....	53
Table 4. Formulations for CO <sub>2</sub> H-CUP cured with melamine.....	54
Table 5. Hardness and gloss values at 60° for the OH-latex system at different cure times (Curing Temperature: 150 °C) .....	67
Table 6. Pencil / Indentation hardness values for CO <sub>2</sub> H-latex and CO <sub>2</sub> H-CUP cured with melamine resin. ....	73
<b>PAPER III</b>	
Table 1. % Yield, density, diameter and molecular weight of the three QUAT-CUPs ....	98
Table 2. Intrinsic viscosity, associated water fraction and surface water thickness for the three QUAT-CUPs .....	105
Table 3. Surface tension fitting parameters .....	114

Table 4. Fitting parameters for dynamic surface tension versus surface age at 0.5 mole/m <sup>3</sup> .....	115
--	-----

Table 5. Relaxation time ( $\tau_k$ ) for the three CUPs at various concentrations.....	118
---	-----

#### PAPER IV

Table 1. % Yield, acid number and density of the copolymers .....	138
---	-----

Table 2. Particle size of CUP measured from Nanotrac 250 .....	138
--	-----

Table 3. Intrinsic viscosity, associated water fraction and surface water thickness of SO <sub>3</sub> <sup>-</sup> -CUPs .....	142
--	-----

Table 4. Effective Charge, surface potential, effective collision diameter, primary electroviscous coefficient and specific viscosity of CUP suspension at various volume fractions for carboxylate-CUP (28K) and the three sulfonate-CUPs.....	148
--	-----

Table 5. Fitting parameters for DST versus surface age at 0.5 mole/m <sup>3</sup> .....	154
---	-----

Table 6. Relaxation time ( $\tau_k$ ) for the three sulfonate-CUPs at various concentrations..	156
--	-----



# 1. INTRODUCTION

## 1.1. POLYMER NANOPARTICLES

In the recent years, the polymers and coatings industry has seen a remarkable growth in the application of nanotechnology via development of nano-polymers, nano-additives and nano-composites. The growth is based on the capacity of nano-technology to deliver enhanced physical and chemical properties in applications as diverse as biomedicine and surface coatings.<sup>1</sup> There is an increasing trend towards shifting from simply using nanomaterials as fillers to developing basic nanopolymer systems due its properties such as high surface area to volume ratio or surface functionalization and wide range of applications such as electronics, conducting materials, coatings, etc.<sup>2</sup>

Though the term nano is commonly used to refer anything less than 1000 nm, nanoparticles with particle size below 10 nm exhibit remarkable properties due to the precise and ultrafine dimensions.<sup>3,4</sup> To date, inorganic nanoparticles less than 10 nm have been extensively reported. But for polymeric nanoparticles, particle size less than 10 nm has been difficult to achieve because the nanoparticle systems have been mainly developed via self-aggregation of amphiphilic block copolymers with little control over the aggregation behavior.<sup>5-7</sup> Recently, Chen et al.<sup>8</sup> reported nanopolymer synthesis with particle size less than 10 nm via inverse microemulsion polymerization technique, but the particles aggregated to larger diameter on removal of the surfactant.

Van De Mark's research group has recently reported a facile route for synthesis of true nanoscale (size < 10 nm) polymeric material composed of amphiphilic acrylic copolymers and termed it as Colloidal Unimolecular Polymer (CUP).<sup>9</sup> Previous studies

have reported the use of carboxylic acid containing monomer as the hydrophilic group.<sup>10</sup> This thesis further explores the basic science of CUP formation with carboxylic acid containing monomers and reports for the first time, CUP formation based on sulfonic acid and quaternary ammonium functional monomers.

CUPs are composed of hydrophobic polymer backbone with hydrophilic pendant groups and bear a close resemblance to polyelectrolytes which are defined as macromolecular chains with a large number of ionizable groups.<sup>11</sup> The transition of a single flexible polyelectrolyte chain from a random coil conformation to a globular compact form, with particle diameter < 100 nm, serves as a fundamental model to study basic physical phenomena with wide-ranging implications to fields such as protein folding<sup>12</sup>, drug-delivery<sup>13</sup>, waterborne resins<sup>14</sup> and surface coatings<sup>15</sup> and therefore has been widely studied in the last few decades. Various methods have been implemented to trigger the coil to globule transition such as the change in solvent dielectric or a change in pH.<sup>16-19</sup> CUPs could be utilized as a model material for studying the coil to globule transition.

## **1.2. POLYMERIC MICELLES**

The conformational behavior of polyelectrolytes has also led to the synthesis of polymers that had the ability to form single chain nanoparticles (SCNPs). The particles can mimic micelle behavior and collapse inwardly due to a change in the regional environment, or collapse by intramolecular self-crosslinking. Li<sup>20</sup> investigated the use of multi-chain polymeric micelles as potential drug delivery systems. The hydrophobic blocks consisted of the anticancer drug paclitaxel, grafted onto blocks of hydrophilic polyether ester. The polymers were placed in an aqueous environment and upon adjusting the pH, the polyether ester portions of the chains oriented into the water phase and left the hydrophobic paclitaxel

oriented to the interior domain. The macromolecular polymeric micelles had an average diameter of 50-120 nm. The paclitaxel was released into the cell through hydrolysis of the ester bonds that linked the drug to the hydrophilic exterior.

In a study by Morishima<sup>21</sup>, polyelectrolyte chains composed of methacrylamide with bulky hydrophobic groups such as cyclododecyl and adamantyl and hydrophilic sulfonic acid groups were observed to be “self-assembled” to form spherical particles with a particle diameter of about 20 nm.

Mecerreyes et al.<sup>22</sup> used linear copolymers with pendant acryloyl or methacryloyl groups as reactive precursors. Aliphatic polyester were obtained through ring opening (ROP) copolymerization of 4-acryloyloxy caprolactone with  $\epsilon$ -caprolactone. The reactive precursor was then radically polymerized in ultra-dilute conditions to give single chain nanoparticles (SCNP's) with particle diameter in the range of 3.8 - 13.1 nm. If polymerized in concentrated conditions, a 3-dimensional polymer network rather than particles was formed.

Altintas et al.<sup>23</sup> utilized Diels Alder reactions by incorporating dienes precursors and dienophiles along the polymer backbone. The chains were then subjected to a UV-A fluorescent lamp at 320 nm causing intramolecular Diels Alder reaction. The SCNP's were successfully prepared at concentrations of 0.017 mg/mL and the diameters were dependent on the molecular weight of the polymer precursors.

Jiang et al.<sup>24</sup> demonstrated SCNP's synthesis via sulfonyl-azide functionalized polymer precursors. The polymers were then dissolved in benzyl ether and subjected to high heat causing the loss of nitrogen and forming nitrene groups which then reacted with the C-H bonds along the polymer backbone to give crosslinked product.

Non-unimolecular collapse has been observed in waterborne urethane resins used in the coatings industry. Resins have been synthesized by the reaction of isocyanates with either modified or unmodified polyester polyols, in acetone with water addition. Removal of the acetone from the resin-water blend caused the chains to collapse into aggregate particles with diameters of approximately 25 nm<sup>25</sup>. Collapse of polymer chains while still entangled has also been used in the coatings industry, as water-reducible resins<sup>26</sup>. Water-reducible resins were dissolved in high boiling water miscible solvents, the resins contained ionizable carboxylic acid groups that were neutralized with amines. Water was then added to the coating, until the solvent blend became a less-than theta solvent condition, which caused the chains to collapse.

CUP particles although similar in concept to Morishima's unimolecular micelles<sup>21</sup> and the currently used water-reducible resins, are also unique because of its method of synthesis. The CUP synthesis involves dissolving the polymer in a water miscible organic solvent, adding water slowly, and then complete evaporation of the organic solvent, leaving the CUP particles suspended in aqueous media, thereby achieving a zero-VOC (volatile organic compound) solution. Zero-VOC is especially important because of the continually decreasing acceptable limits of solvent emissions. The polymer itself is not water soluble, however, after the water reduction process, polymer particles are suspended in water and are stable long term.

The major challenge for achieving stability of collapsed polymer chain is the hydrophilic/hydrophobic balance of amphiphilic polymer. If the chains are too hydrophobic, then the collapsed chains tend to aggregate and if the chains are too hydrophilic, they tend to dissolve or maintain a chain-like conformation even after collapse. Only when all the factors such as the concentration of polymer in solvent, charge

fraction of polymer, temperature, pH and solubility of polymer in solvent are coordinated simultaneously, can the individual polymer chains collapse into a single compact globule.

### **1.3. COLLOIDAL UNIMOLECULAR POLYMER (CUP)**

CUPs are a two-phase colloidal system with solid unimolecular polymer as the dispersed phase and water as the continuous phase. Colloidal Unimolecular Polymer (CUP) particles are formed by the effect of hydrophilic/hydrophobic interactions of the polymer with a change in the solvent environment. CUP formation is driven by the polymer-polymer interaction being greater than the polymer-solvent interaction and entropically favored by release of the water similar to micelle formation with hydrophilic or charged groups creating the sphere-like shape.

Figure 1 shows the formation of CUP particles based on a copolymer of methyl methacrylate (MMA) and 2-acrylamido-2-methylpropane sulfonic acid (AMPS) with the sulfonate groups on the surface, preventing the particles from aggregation. The CUP suspension contains only charged particles, water and counterions and are free of surfactants or stabilizers unlike latex resins prepared by emulsion polymerization. As a result, there are several advantages of CUPs over other traditional materials treated as model nanomaterials.

First, CUP is formed by a single strand of polymer chain with ionizable groups on the surface, which is similar to the conformation of globular proteins. Second, CUP is free of surfactant and its preparation is quite simple while surface modified latex involves tedious dialysis to remove the surfactant. Third, the particle size and charge density of CUPs can be easily controlled by controlling the molecular weight of the copolymer. All of the functional groups are on the surface of particle and thus more readily available for further modification / reaction and incorporation into polymer and coating formulations.

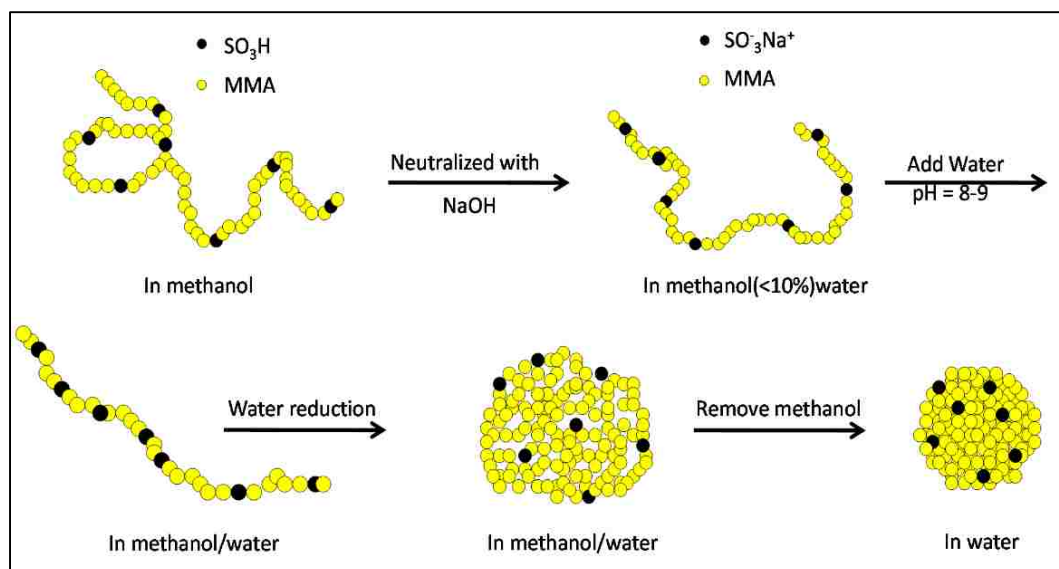


**Figure 1.1** Process of formation of CUPs from poly(MMA-co-AMPS)

The advantages make CUPs a very good model material to study the fundamental properties of protein or analogous particles. Among the basic properties of polyelectrolytes, rheology and surface tension are of great importance because of their correlation to the conformation, diffusion, surface behavior and application properties. The acrylic CUP resins based on carboxylic acid monomers could be potentially used as clear coats for coil coatings after crosslinking with melamine or aziridine crosslinkers.<sup>27</sup> Use of sulfonic acid functional monomers can lead to the synthesis of CUPs with sulfonic acid groups on the surface with potential application as novel polyfunctional acid catalyst. Other applications could include as surfactants or rheology modifiers. CUPs with quaternary ammonium groups on the surface could have potential applications in anti-bacterial coatings, polymeric flocculants etc. CUPs with cationic groups could be utilized as flocculants or in fabric softeners due to their surface activity.

**1.3.1. Water-reduction Process For CUP Synthesis.** Water-reducible polymers show a unique viscosity behavior during the water-reduction process. When the acid groups are neutralized, the viscosity increases slightly due to inter and intrapolymer ionic interactions and hydrogen bonding. As more water is added, the viscosity increases further due to repulsive interactions of solvated ions causing the polymer chain to take an extended rod-like conformation. At a critical ratio of water to THF, the individual polymer chains collapse to form spherical particles causing a dramatic decrease in viscosity.<sup>28,29</sup>

**1.3.2. Water-reduction Protocol.** Riddles et al.<sup>9</sup> have demonstrated that the purity of the water used for water-reduction was a critical factor and it should be free of polyvalent cations such as calcium. The calcium ions interact with the carboxylic acid groups on the polymer chain and cause multiple chains to aggregate and precipitate out of solution. The calcium salt of carboxylic acid does not readily dissociate and the polymer chains lose their ability to be stabilized and precipitate.<sup>30</sup> During the water-reduction, water had to be added slowly using peristaltic pump via a submerged tube and stirred continuously at a modest rate to prevent a large change in the regional solvent composition.

If the polymer chains were at a high concentration during water-reduction, they collapsed while entangled, resulting in particle diameters larger than expected. If the concentration was low, the individual polymer chain was able to collapse on itself. The hydrophobic: hydrophilic monomer ratio of 7:1 to 12:1 was found to be suitable to achieve CUP formation. A higher ratio gave non-unimolecular collapse due to increased hydrophobic aggregation while a lower ratio made the polymer water-soluble.<sup>9</sup>

**1.3.3. Determination Of Effective Charge.** As reported by Chen et al.,<sup>31</sup> the carboxylate functional CUP displayed interesting rheological behavior dominated by the tertiary electroviscous effect because of the presence of surface water layer. The

electroviscous effects occurring due to the presence of surface charge gives rise to electrophoresis. Electrophoresis is defined as the migration of charged colloidal particles through a solution under the influence of an applied electric field and has a profound effect on the rheological behavior of a colloidal dispersion.<sup>32</sup> The fundamental parameters involved in electrophoresis are the zeta potential ( $\zeta$ ), the Debye-Hückel parameter ( $\kappa$ ) and the electrophoretic mobility ( $\mu$ ). The zeta potential is the potential at the surface of shear of a particle which is the layer of liquid immediately adjacent to a particle and moves with the same velocity as the surface. The boundary of the surface of shear is assumed to be within a couple of molecular diameters away from the surface of particle. For regular suspensions where the ionic strength is dominated by added electrolytes,  $\kappa$  is expressed as follows<sup>32</sup>:

$$\kappa^2 = \left[ \left( \frac{e^2}{\epsilon k_B T} \right) \sum_i z_i^2 n_{i\infty} \right] \quad (1)$$

Where,  $e$  is the elementary charge,  $\epsilon$  is the permittivity of the solvent,  $k_B$  is the Boltzmann constant,  $T$  is the temperature,  $z_i$  is the charge number of the electrolyte ions in the solution and  $n_{i\infty}$  is the number of each ion. The unit of  $\kappa^2$  is  $\text{m}^{-2}$ , so  $\kappa^{-1}$  has the unit of meter and is known as the thickness of electrical double layer.

The relation between zeta potential, electrophoretic mobility and Debye-Hückel parameters forms the basis of the electrophoretic properties of CUP. If the surface potential is low enough to justify  $\frac{e\psi}{k_B T} < 1$ , and the ion atmosphere is undistorted by the external field, then the mobility can be expressed as<sup>33</sup>:

$$\mu = \frac{2\epsilon\zeta}{3\eta} f(\alpha) \quad (2a)$$

Where,  $\alpha$  is the ratio of radius of particle to Debye length, i.e.  $\alpha = \kappa a$ , and when  $\alpha < 1$ ,



$$f(\alpha) = \left(1 + \frac{1}{16}\alpha^2 - \frac{5}{48}\alpha^3 - \frac{1}{96}\alpha^4 - \frac{1}{96}\alpha^5 - \left(\frac{1}{8}\alpha^4 - \frac{1}{96}\alpha^6\right) \exp(\alpha) \int_{\infty}^{\alpha} \frac{e^{-t}}{t} dt\right) \quad (2b)$$

For  $\alpha > 1$ ,

$$f(\alpha) = \left(\frac{3}{2} - \frac{9}{2}\alpha^{-1} + \frac{75}{2}\alpha^{-2} - 330\alpha^{-3}\right) \quad (2c)$$

The equations 2a, 2b and 2c are Henry's equations based on which, Ohshima corrected the factor  $f(\alpha)$  to  $\zeta$ .<sup>34</sup> The equations are applicable to particles with constant charge density and work well for the dilute concentration regime, where the particle-particle interaction can be considered negligible. When the particle concentration increases, the inter-particle distance decreases and the electrostatic repulsion increases until at a critical point, the counterion collapses on the surface of particles. The entire process, known as counterion condensation, decreases the surface charge density and enables the particles to further approach each other.<sup>35</sup>

For the salt-free CUPs, the counterion comes from the dissociation of functional groups on the surface. As the concentration of CUP increases, the concentration of counterions also increase causing the Debye-Hückel parameter to increase, and compressing the electrical double layer. The effective diameter of the charged particle decreases which counters the effect of counterion condensation. Due to the complicated nature of the ionic and the electrokinetic environment, the average effective charge on each particle is difficult to determine experimentally.

The effective charge is a very important parameter in colloidal systems as it is related to its stability and also its rheology and surface tension properties. To the knowledge of the author, there is no common method to measure the effective charge and the results from different methods can vary significantly. The effective charge for the CUP particles has been calculated using Belloni's<sup>36</sup> program which requires the knowledge of

the particle size, maximum bare charge, pH of the system and the salinity. The program uses a model based on the assumption that each colloidal particle occupies the center of a spherical Wigner–Seitz (WS) cell<sup>37</sup> with the presence of counterions and that two electro repulsive surfaces tend to minimize the total free energy.

#### **1.4. OBJECTIVE OF THIS RESEARCH**

Zero-VOC, aqueous colloidal unimolecular polymer particles based on methacrylic acid monomer as the hydrophilic group have been reported and characterized for the viscosity behavior and gel formation. The main objective of the present work was to further evaluate the basic physical properties of CUPs with different surface functional groups and explore some applications. The following studies were planned to attain the objective:

1. Synthesize a series of copolymers based on methyl methacrylate and methacrylic acid, with different molecular weight (MW) in the range of 2,000 to 160,000 and evaluate the effect of MW on CUP formation and stability. Different molecular weight corresponds to different surface charge density
2. Develop novel sulfonate functional CUPs based on copolymers with sulfonic acid functional groups and evaluate their application as an acid catalyst for crosslinking of three different acrylic resins including, OH-functional-latex, CO<sub>2</sub>H-functional-latex and CO<sub>2</sub>H-functional-CUP with melamine resin systems. The performance of CUP catalyst in curing acrylic-melamine films would be evaluated in terms of mechanical properties such as pencil hardness, indentation hardness and solvent resistance via MEK double rubs and the non-leachability of CUP catalyst in water. Performance comparison would be performed with respect to a commercial blocked sulfonic acid catalyst.

3. Synthesize novel cationic CUPs based on [2-(methacryloyloxy)ethyl]trimethylammonium chloride (QUAT) hydrophilic groups and evaluate its rheology and surface tension behavior.
4. Investigate the basic physical properties including rheology, surface tension and surface water density of sulfonate functional CUPs.

## I MOLECULAR WEIGHT (MN) AND FUNCTIONALITY EFFECT ON CUP FORMATION AND STABILITY

Michael R Van De Mark, Ameya M Natu, Sagar V Gade, Minghang Chen,

Catherine Hancock and Cynthia Riddles

Department of Chemistry, Missouri S&T Coatings Institute,

Missouri University of Science & Technology,

Rolla, MO 65409

Michael R Van De Mark, [mvandema@mst.edu](mailto:mvandema@mst.edu), 573-341-4882

### ABSTRACT

The formation of colloidal unimolecular polymer (CUP) particles from single polymer strands was investigated as a function of molecular weight. The CUP particle size was correlated with the absolute molecular weight and its distribution. The characteristics of the particles were evaluated with respect to viscosity, acid number, size distribution and stability. The particle size varied from less than three nanometers to above eight nanometers representing polymers with molecular weight in the range of 3,000 to 153,000. Lower molecular weight polymers were found to be unstable. Particle size measurements using Dynamic Light Scattering technique indicated a normal distribution which corresponded to the molecular weight distribution of the copolymer. The statistical distribution of the acid groups in the polymer chains played a significant role in the stability of low molecular weight polymers.

### Keywords

Colloidal unimolecular polymer (CUP), Molecular weight, Stability, Particle size distribution

## INTRODUCTION

Micelle formation of amphiphilic polymers has been a topic of huge interest because of its diverse applications ranging from an understanding of protein folding and drug delivery to its application in polymers and coatings in general. Kabanov et al. studied micelle formation of block copolymer based on hydrophilic poly(ethylene oxide) and hydrophobic poly(propylene oxide).<sup>1</sup> Kataoka et al. demonstrated micelle formation of diblock copolymers of poly(aspartic acid) as the hydrophobic block and poly(ethylene glycol) as the hydrophilic block.<sup>2</sup> The aspartic acid-PEG copolymers and similar other amphiphilic diblock copolymers which form polymeric micelles suffer from a major drawback in the sense that they are dynamic entities and demonstrate micelle-like properties only above a critical micelle concentration (CMC).

As a solution to the problem, Uhrich et al. synthesized hyperbranched polymers with a hydrophobic core and a hydrophilic shell, which, because of its covalently bound structure gave stable micelle-like structures.<sup>3-5</sup> Moroshima et al. studied micelle formation through intramolecular aggregation of random copolymers of 2-acrylamido-2-methylpropanesulfonate (AMPS) and methacrylamides, N-substituted with bulky hydrophobic groups with cyclic structures like cyclodecyl, adamantyl and 1-naphthyl.<sup>6,7</sup> In both the cases, the polymers studied were readily soluble in water which hampers its application in paints and coatings and also the particle size of the polymeric micelle were not in the true nano-scale region (<10 nm).

Recently, Van De Mark et al.<sup>8</sup> have reported the synthesis of a new type of micelle-like, true nano-scale polymer and termed as colloidal unimolecular polymer particles (CUPS). Some of the interesting features of CUPS include zero volatile organic content

(VOC), particle size in the range of 3–9 nm and an easy and efficient synthesis. The CUPs are self-stabilized by electrostatic repulsion of the surface functional groups which obviates the use of any surfactant. Also, CUPs have all of the functional groups on the surface making them more available for further modification.

In paint formulations, smaller the particle size of the resin, the faster its coalescence into a film. As Kan has observed, the minimum film forming temperature (MFFT) of waterborne resins increases with increasing particle size of the resin.<sup>9</sup> So, CUPs could possibly provide faster coalescence compared to latex resins and provide a major advantage for use in paint formulations.

CUPs are solid unimolecular polymer particles suspended in an aqueous phase.<sup>10</sup> Figure 1 illustrates the size comparison of a conventional latex particle, waterborne urethane resin and Colloidal Unimolecular Polymer (CUPs) particle.

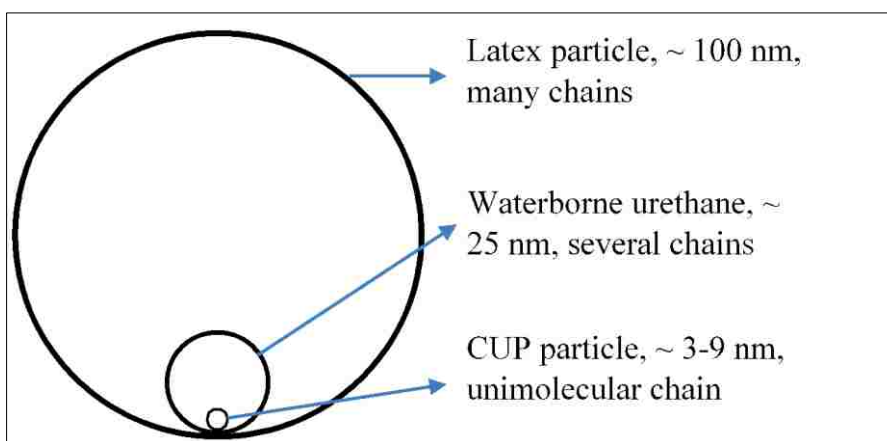


**Fig. 1: Size comparison of latex, waterborne urethane and CUP particle**

CUPs are typically prepared from polymers containing hydrophilic groups such as carboxylic acid salts or sulfonic acid salts on the hydrophobic polymer backbone. The amount of hydrophobic and hydrophilic groups on the polymer chain (HLB value) plays a critical role in the unimolecular collapse of the random acrylic polymer chains during the process of water reduction. The collapse of polymer chains in the aqueous solution is favored by a higher polymer-polymer interaction as compared to polymer-solvent interaction and entropically favored by the release of water which is associated with the surface of polymer chains.

The polymer chains which are in a state of random coils in THF undergo a conformational change as the solvent environment around the polymer is changed by way of neutralization with a base and addition of water. The random coil conformation in THF transits to an extended chain conformation with neutralization of acid groups and water addition because of the ionic repulsion along the polymer chain and then finally to a collapsed globule like conformation. When the concentration of polymer in the solution is dilute, the polymer chains collapse unimolecularly and the CUPs are then stabilized by the carboxylate groups through electrostatic repulsion.<sup>11</sup>

In the present study, the effect of molecular weight of the acrylic copolymers on the formation and stability of colloidal unimolecular polymer particles was explored. Nine random copolymers of methyl methacrylate and methacrylic acid with a molecular weight in the range of 3000 to 153000 were synthesized and investigated for their ability to water-reduce to form colloidal unimolecular polymer particles with a stable particle size in the true nano-scale region (<10 nm).

## EXPERIMENTAL

### *Materials*

Methacrylic acid (MAA), methyl methacrylate (MMA), 2,2'-azobis (2-methylpropionitrile) (AIBN) and 1-butanethiol were purchased from Aldrich. Inhibitors from MMA were removed by washing with 10% aqueous solution of sodium bicarbonate (NaHCO<sub>3</sub>), distilled water and brine solution respectively and further purified by distillation. MAA was purified by distillation with copper (I) bromide under vacuum. AIBN was re-crystallized from methanol prior to use and n-butanethiol was used as received. Tetrahydrofuran (THF) was purchased from J. T. Baker and purified by distillation before use.

### *Polymer synthesis*

Copolymers of MMA and MAA were prepared in a 3-neck flask equipped with thermometer, nitrogen inlet and condenser fitted with a mineral oil isolation positive pressure bubbler. MMA and MAA monomers were charged into the flask in a molar ratio of 9:1 along with the solvent THF and n-butanethiol as a chain transfer agent. AIBN was used as the free radical initiator and the polymerization reaction was carried out under refluxing conditions for 24 hrs. The polymer solution was then cooled to room temperature and precipitated in cold de-ionized water under high shear and then filtered.

For further purification, the polymer was re-dissolved in distilled THF and precipitated in cold water under high shear, primarily done to get rid of most of the unreacted MAA monomer as it was water-soluble. The traces of un-reacted MMA and THF were removed by placing the polymer in a desiccator under high vacuum. The polymers



were thoroughly dried using a freeze-drier. Polymers with different molecular weights were synthesized by controlling the amount of chain transfer agent n-butanethiol. The composition for the polymers synthesized is listed in Table 1.

### ***Synthesis for 12K polymer***

The monomers MMA (0.9 moles, 91.3 g), and MAA (0.1 moles, 8.7 g) and the solvent (THF) were charged in a 500 ml 3-necked round bottom flask fitted with a nitrogen inlet, a mechanical stirrer, a thermometer, and a reflux condenser with a gas bubbler tower at the top to allow a positive flow of nitrogen throughout the polymerization. Then the chain transfer agent i.e. n-butanethiol (0.008 moles, 0.75 g) was added to the reaction mixture. While stirring the reaction mixture, the 3-necked flask was purged with nitrogen gas for about 15 minutes to get rid of oxygen before adding the initiator. After purging, the freshly recrystallized free radical initiator i.e. AIBN (0.0007 moles, 0.12 g) was added. The flask was heated slowly to reflux and allowed to react for 24 hours. The polymer solution was then cooled to room temperature and the polymer was precipitated in cold de-ionized water under high shear. Then the polymers were dried completely using a freeze drier. All the polymers were synthesized similarly.

### ***Characterization of polymers synthesized***

Absolute number average molecular weights ( $M_n$ ) were measured by Gel Permeation Chromatography (GPC) on a Viscotek GPCmax from Malvern instruments coupled with a triple detector array TDA305 (static light scattering, differential refractometer and intrinsic viscosity). Acid value (AV - reported in mg of KOH/ g of polymer sample) for all polymers were measured by titration method mentioned in ASTM

D-974 which was modified by using potassium hydrogen phthalate (KHP) in place of hydrochloric acid, and phenolphthalein as an indicator in place of methyl orange.

**Table 1.** Formulation for MMA-MAA Polymers

Polymer	Acrylate: acid molar ratio	Monomer:Thiol ratio
Poly-1	9:1	28:1
Poly-2	9:1	55:1
Poly-3	9:1	106:1
Poly-4	9:1	155:1
Poly-5	9:1	201:1
Poly-6	9:1	246:1
Poly-7	9:1	824 :1
Poly-8	9:1	1030 :1
Poly-9	9:1	1648 :1

***Water-Reduction of MMA-MAA based copolymers to form CUPs***

The purified and dry acrylic copolymers were dissolved in dry and distilled THF; a low boiling and water miscible solvent. The polymer was stirred overnight for complete dissolution of polymer chains. Aqueous ammonium hydroxide solution (28% w/w) was added to neutralize all the acid groups on the copolymer based on the acid number of the copolymer. Deionized water modified to a pH of 8~9 using 28% aqueous NH<sub>4</sub>OH solution was then added to the polymer solution by a peristaltic pump at a rate of about 1.24g/minute. The pH of solution was maintained at 8-9 throughout the process of water reduction. THF was then stripped off under vacuum to give CUPs in VOC free aqueous

solution. The CUP solutions were then filtered through 0.45 $\mu$ m Millipore membrane to remove any impurities.

Water reduction process-Poly-4 (MW=12K): 10 g of poly (MMA-co-MAA) was dissolved in 40g of THF to make a 20% w/w solution. The carboxylic acid groups were neutralized by adding 28% aqueous  $\text{NH}_4\text{OH}$  solution and 90g of deionized water was then added by means of a peristaltic pump. The THF was then completely stripped off in vacuum. Then the sample was concentrated by stripping off water to give a 20% w/w CUP solution of poly (MMA-co-MAA) in water. Figure 2 shows the process of formation of CUP particles with carboxylate groups on the surface, preventing the particles from aggregating through electrostatic repulsion.

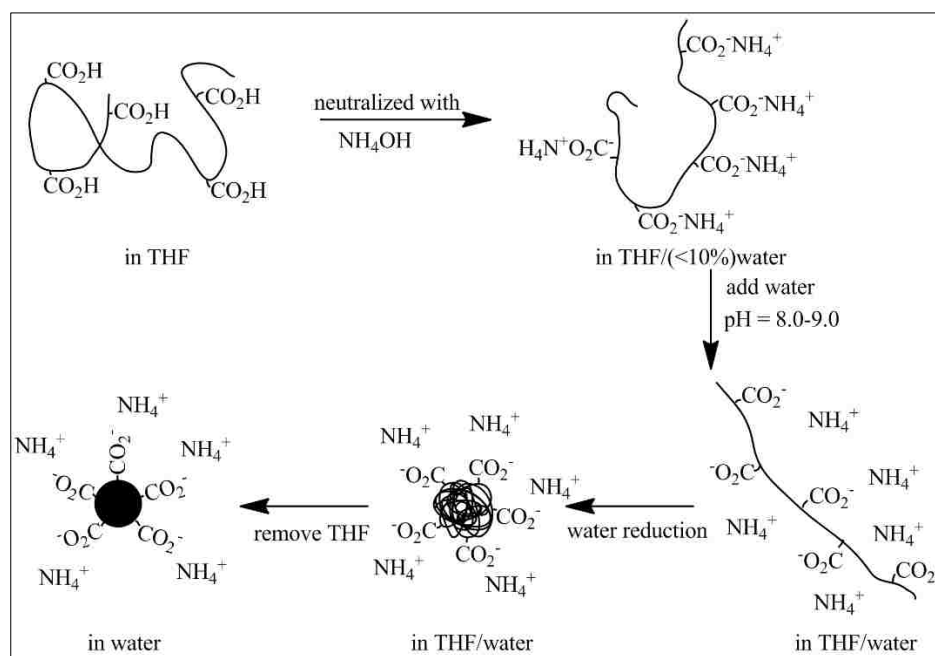


**Fig. 2: General Process of Formation of CUPs**

The water reduction process for CUP particle was depicted in Figure 2. The polymer had a hydrophobic backbone of methyl methacrylate and hydrophilic methacrylic acid units in a molar ratio of 9:1. When dissolved in THF (dielectric constant = 7.58 at 25°C) the polymer chain was a random coil based upon the Mark-Houwink exponent 'a'. The value of the Mark-Houwink constant 'a' for polymers was  $0.66 \pm 0.03$ . When base i.e. ammonium hydroxide was added to the solution, the carboxylic acid groups on polymer chain formed ion pairs of  $\text{COO}^-$  and  $\text{NH}_4^+$ . When pH modified water (pH = 8-9) was added using peristaltic pump, the formed ion pairs become solvated and separate. Negatively charged carboxylate groups then repelled each other due to the increasing dielectric caused by the added water (dielectric constant = 78.39 at 25°C)<sup>12</sup> and the polymer chain stretched causing an increase in the viscosity.

With continuous addition of water, at a critical point in the composition, the amphiphilic polymer chains collapse. The hydrophilic carboxylate groups orient into the water phase organizing to produce maximum separation of charge and the stretched hydrophobic polymer chain collapsed to the spheroidal CUP particle. The unimolecular collapse was also dependent on molecular weight and on the concentration of the amphiphilic polymer in THF and THF/water mixture. At higher concentration, polymer chains overlap and if overlapped polymer chains come in contact with each other at the critical point, non-unimolecular collapse occurs forming a larger particle size or coagulum. When carboxylic acid groups are used, the water must be free of polyvalent cations like calcium which cause aggregation and gelling.

### ***Characterization of CUPs***

After the water-reduction process which includes the removal of THF, viscosity measurements of CUP solutions were done using the Brookfield LV DVIII rheometer for

use in particle size measurements. Viscosity at two different temperatures was measured, one at 25<sup>0</sup> C and other at 29<sup>0</sup> C. Shearing viscosities of CUPs at different shear rate were measured. The shear rates were programmed to increase at set speed and viscosities were recorded after continuous shearing for 1 minute at each speed. Particle size and distribution were measured by dynamic light scattering on a Nanotracer 250 particle size analyzer from Microtrac with a laser diode of 780 nm wavelength, and 180° measuring angle. The viscosity of the solution was used instead of the viscosity of solvent for measuring the particle size.

## **RESULTS AND DISCUSSION**

### ***Acid Number***

The experimental value of acid number was slightly greater than the theoretical acid number which can be explained by the loss of some of the MMA monomer which was more volatile of the two monomers, through evaporation with solvent during the polymerization. The methacrylic acid monomer has a high boiling point of about 161 °C and therefore is lost to a lesser extent. Table 2 shows the values for the theoretical and experimental acid number and percent yield for all the nine polymers synthesized. The acid numbers were determined using standard titration methods.

**Table 2.** Percent Yield and Acid Value of Polymers

Polymer Synthesized	Percent Yield	Acid Value (mg KOH/g polymer)	
		Theoretical	Experimental
Poly-1	80	56.8	57.7
Poly-2	89	56.8	57.1
Poly-3	85	56.8	58.4
Poly-4	84	56.8	58.2
Poly-5	90	56.8	57.3
Poly-6	80	56.8	57.3
Poly-7	75	56.8	57.8
Poly-8	78	56.8	57.1
Poly-9	76	56.8	58.4

### ***Molecular weight determination***

Molecular weight and the polydispersity index for all the polymers synthesized were listed in Table 3. The number average molecular weight ( $M_n$ ) as determined by the GPC was close to the targeted molecular weight for all polymers. The molecular weight of the copolymers was controlled by changing the amount of chain transfer agent. The last column indicates the theoretical number of acid groups on each polymer chain which is explained further in the results and discussion section.

**Table 3** Molecular Weight, Polydispersity Index and Number of Acid Groups Per Polymer Chain of the Synthesized Polymers

Polymer Synthesized	Molecular Weight (Mn)	Polydispersity index	Number of acids group per polymer chain (calculated)
Poly-1	3.5K <sup>a</sup>	1.20	4
Poly-2	4.5K	2.02	5
Poly-3	8.5K	1.79	9
Poly-4	13K	1.48	13
Poly-5	15K	1.61	15
Poly-6	20K	1.32	21
Poly-7	72K	1.19	74
Poly-8	90K	1.15	92
Poly-9	153K	1.27	157

a- Polymers were run at 2 mg/cc in THF except Poly-1 which was 4mg/cc.

#### ***Water-reduction of the polymers to prepare CUPs***

All the polymers except the Poly-1 sample (MW = 3.5K) underwent water-reduction to give a clear, transparent CUP solution without any visible aggregate formation. For Poly-1 sample however, some polymer precipitated out during the solvent (THF) removal step to give a white, turbid solution with solid polymer particles. The molar ratio of MMA: MAA in the polymer was 9:1 which means that on an average, three carboxylic acid groups are present on an individual polymer chain of the Poly-1 sample with molecular weight of 3500. Simha and Branson first gave a general description of sequence distribution and chemical composition distribution in random copolymers<sup>13</sup> which was later simplified by Stockmayer<sup>14</sup>.

According to Stockmayer, for free radical random copolymerization, the composition of the copolymer at any instant depends upon the concentration of growing free radical chains which is a function of the reactivity ratios of monomers, monomer concentration and number average degree of polymerization. The concentration of growing radical can be expressed as a power series of composition deviation which leads to a statistical distribution of chain composition about the mean value. As a result, for the MMA-MAA copolymer synthesized, the acid groups on the polymer chains have a statistical distribution similar to the molecular weight distribution (polydispersity). The carboxylic acid groups after being neutralized to carboxylate groups provide the necessary stability to CUP particles through electrostatic repulsion.

The formation of solid polymer particles during the solvent removal step for Poly-1 sample indicated that some polymer chains had insufficient number of carboxyl groups on the chain to keep them stable via electrostatic repulsion for a unimolecular collapse. Insufficient stabilization lead to the aggregation of polymer chains which resulted in some portion of the water-reduced polymer precipitating out of the solution. The acid number of the precipitated Poly-1 was evaluated to provide evidence that the precipitated polymer had lower acid value than the original synthesized copolymer. The solid particles of the precipitated polymer were first filtered from the CUP solution and then dried to constant weight in vacuum. The acid value of the precipitated polymer was determined to be 28.4 mg KOH/ g of polymer which was considerably lower than the acid value of the synthesized polymer (Poly-1) and indicated that the polymer chains with low number of acid groups had precipitated out because of insufficient stabilization.

The remaining CUP solution was then filtered through a 0.45 micron filter and analyzed further for viscosity and particle size measurement. A pictorial comparison of the



turbid CUP solution of Poly-1 before filtering, the clear CUP solution of Poly-1 after filtering and the clear CUP solution of poly-5 (MW = 15K) was shown in Figure 3. A sample of the filtered CUP solution of Poly-1 was also analyzed for acid number. The acid number was 74.1mg KOH/g polymer and was larger than the acid number of the synthesized copolymer, Poly-1. Therefore, during water-reduction of Poly-1, the fraction of polymer with low acid number i.e. insufficient electrostatic stabilization precipitated out of the solution and the remaining fraction of polymer which stayed in solution had a larger acid number.

The molecular weight of the polymer that precipitated and the polymer that remained in solution after filtration was measured using GPC. The number average molecular weight of the precipitated polymer was 2.5K which corresponded to polymer chains with low acid number and hence insufficient electrostatic stabilization. The number average molecular weight of the fraction of polymer that stayed in solution after filtration was 4K which corresponded to polymer chains with sufficient electrostatic stabilization that prevented the polymers from precipitating out but still insufficient to prevent aggregation, giving dispersions with larger particle diameter. The acid number of the precipitated polymer and the polymer that remained in solution also corroborated the finding that low molecular weight copolymers had insufficient electrostatic repulsion and therefore were unstable.



**Fig. 3: Vial 1: CUP solution of Poly-1 before filtering; Vial 2: CUP solution of Poly-1 after filtering; Vial 3: CUP solution of Poly-5 (MW = 15K)**

The concentration of polymer in THF can affect the unimolecular collapse of the polymer chains during water reduction. Dilute concentration prevents the polymers from aggregating during water-reduction. So, polymers up to  $M_n = 20K$  were dissolved in THF at a concentration of 20% weight solids, Poly-7 (72K) and Poly-8 (90K) at 10% weight solids and Poly-9 (153K) was at 5% weight by solids to avoid overlap of polymer chains during water reduction process [10].

High molecular weight polymeric chains begin to overlap when the distance between them becomes on the order of the hydrodynamic size in solution which prevents the unimolecular collapse of polymer chains to form CUPs. So, low concentration was required only during the CUP formation process. Once formed, the CUP solution can be concentrated by removing water under vacuum.

### *Viscosity measurements of CUP solutions*

The viscosity values used for measuring the particle size of CUPs were listed in Table 4. For each CUP solution, at both 25<sup>0</sup> C and 29<sup>0</sup> C, the shear stress on CUP solution increased linearly with increasing shear rate. The viscosity values were constant for all values of shear rate which indicated that the CUP solutions behave as a Newtonian fluid at that concentration. A representative plot of viscosity against the shear rate for samples Poly-4, Poly-7 and Poly-8 was shown in Figure 4.

**Table 4.** Percent Solids and Viscosity at 25<sup>0</sup> C and 29<sup>0</sup> C for CUP Solutions

Polymer samples	% Solids	Viscosity (cP)at 25 <sup>0</sup> C	Viscosity (cP) at 29 <sup>0</sup> C
Poly-1	12.5	4.51	4.30
Poly-2	18.9	6.79	5.16
Poly-3	19.9	8.25	7.47
Poly-4	19.5	8.96	8.06
Poly-5	22.1	10.0	8.84
Poly-6	19.9	14.1	9.26
Poly-7	9.07	3.96	2.43
Poly-8	8.88	4.31	2.73
Poly-9	4.82	1.55	1.45

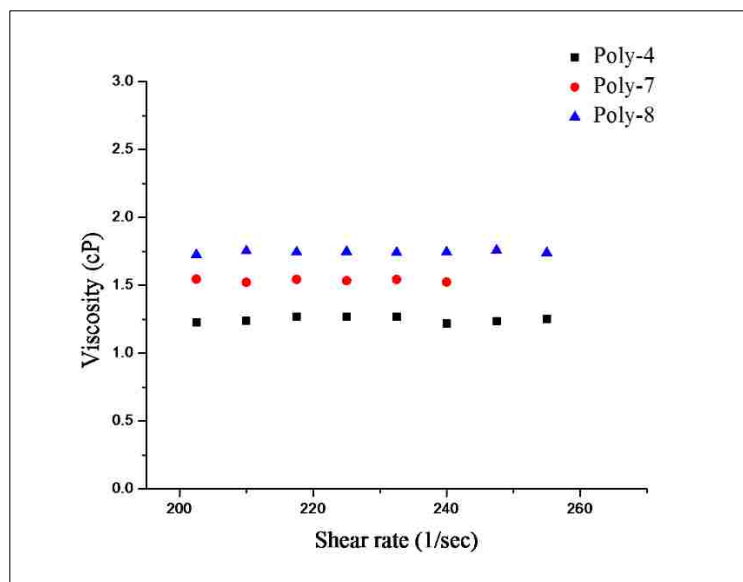


**Fig. 4: Viscosity against shear rate for Poly-4, Poly-7 and Poly-8 at 5.00% solids at 25<sup>o</sup> C**

At higher concentrations the CUP solutions begin to show non-Newtonian viscosity behavior. A representative plot of viscosity against shear rate for Poly-8 at 15% solids by weight was shown in Figure 5. The viscosity decreased with increasing shear rate or shear stress which indicated shear thinning behavior. The effect of molecular weight on the viscosity was evaluated by conducting viscosity measurements on the samples at the same concentration of 5.00% solids by weight. The viscosity values at 25<sup>o</sup>C and 5.00% solids were listed in Table 5. The viscosity of CUP solutions increased with increasing molecular weight of polymers which was attributed to the increased charge density on the surface of CUP particle with increasing molecular weight of the polymer.

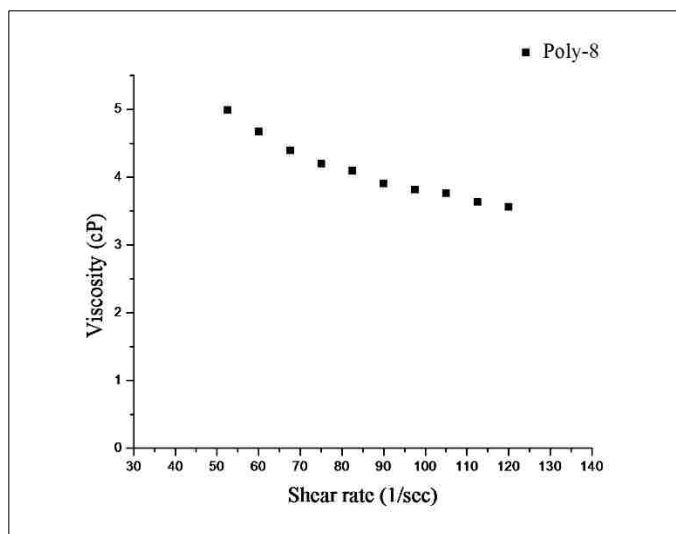


**Fig. 5: Viscosity against shear rate for Poly-8 at 15% solids at 25<sup>0</sup> C**

**Table 5.** Viscosity measurements at 25<sup>0</sup> C for CUP solutions at 5.00% solids by weight

Polymer samples	Viscosity (cP)
Poly-1	0.99
Poly-2	1.03
Poly-3	1.21
Poly-4	1.26
Poly-5	1.29
Poly-6	1.31
Poly-7	1.48
Poly-8	1.71
Poly-9	1.88

For acrylic latexes, viscosity is independent of molecular weight of the resin and depends primarily on the particle size.<sup>15</sup> For water-borne urethane dispersions, the viscosity is independent of molecular weight in the dilute regime.

There is no long range charge interaction which depends only on the particle size as governed by the Einstein's theory of viscosity for dispersions of non-charged particles.<sup>16,17</sup> But as the concentration crosses into the semi-dilute regime, the viscosity builds up due to charge interaction and could be explained by fitting various viscosity models, one of them being the Ruiz-Reina's model.<sup>18</sup>

In the case of CUPs, the viscosity depends on both the molecular weight and particle size. The viscosity of CUP solution increased with increasing molecular weight of the copolymer due to increasing surface charge. For all the three types of resins, the viscosity of the solution increased with decreasing particle size at constant particle surface charge density.<sup>11</sup> Lower the particle size, higher the surface area which leads to higher amount of surface water and an apparent increase in viscosity.<sup>19,20</sup> As the particle size decreases, the maximum possible solid content before gelation also decreases.

Latexes with particle size in the range of 100nm gel at about 65% solids.<sup>21,22</sup> Water-borne urethane dispersion resins, on the other hand, have smaller particle size in the range of about 25nm with a higher ratio of surface water as compared to latexes. So, as the concentration is increased, the viscosity builds up faster than in case of latexes. The maximum percent resin solids for water-reducible resins is lowered to about 45-50% at which they gel. The CUPs gel at a lower concentration because they have the lowest particle size compared to latexes and water-reducible resins. Hence, the maximum possible resin solids is about 30%, after which it gels.

CUPs offer significant advantage in terms of its volatile organic content (VOC). In case of the water reducible resins, the amount of solvent required to dilute the resin increases with increasing molecular weight of the resin which gives a high VOC for high molecular weight water reducible resins.<sup>23,24</sup> But for CUPs, all the organic solvent is

removed during the CUP formation process irrespective of the molecular weight of the polymer.

Also, surfactants are needed for latexes but not for CUPs since CUPs are self-stabilized. CUPs are smaller than latex particles because of which they can have higher CPVC compared to latex, thus potentially giving better hide at lower film thickness. When used as the primary resin with melamine or aziridine crosslinkers, all of the functional groups of CUPs are on the surface making it more readily available for crosslinking. But in a latex, majority of functional groups lie on the inside of the latex particle making it difficult for crosslinking reactions.

### ***Particle size analysis***

To show that the CUP particles were unimolecular, information from two techniques was compared. The absolute molecular weight (Mn) from GPC was used to calculate an average theoretical diameter of collapsed polymer chain and Dynamic Light Scattering (DLS) was used to measure the experimental particle size of the CUP particles. Table 6 shows the comparison of the theoretical and experimental particle size of CUPs. There was good agreement between the experimental particle size of the CUPs and the calculated particle size for all of the polymer samples except for polymers below 13K.

The CUPs based on polymer sample Poly-1 had a number average molecular weight of 3.5K. There was considerable deviation in the experimental particle size as measured using DLS compared to the theoretical particle size which indicated aggregation of individual polymer chains during collapse.

**Table 6.** Comparison of Theoretical and Experimental Particle Size of the CUPs

Polymer synthesized	Particle size (nm)	
	Theoretical	Experimental
Poly-1	2.1	4.6
Poly-2	2.3	4.4
Poly-3	2.9	3.2
Poly-4	3.4	3.3
Poly-5	3.6	3.6
Poly-6	3.9	3.9
Poly-7	5.8	5.8
Poly-8	6.2	5.9
Poly-9	7.4	7.8

Stockmayer, has shown that for random free radical copolymerization, the monomers are distributed statistically along the polymer chain. The MMA-MAA copolymers therefore had a statistical distribution of methacrylic acid monomers along the polymer chain.<sup>14</sup> Also, as the number average molecular weight of the polymer decreases, the average number of acid-groups on an individual polymer chain from the methacrylic acid monomer also decreases. For Poly-2 which had a number average molecular weight of 4.5K, a slight amount of aggregation was noted but it was less than that for Poly-1. All the polymers with molecular weight above 13K water-reduced to CUPs with the expected particle size. The polymers were synthesized based on a 9:1 molar ratio of acrylate group: acid group. So, statistically there was one unit of acid for every ten units in a polymer chain or a molecular weight of 986 Da. For the Poly-1 sample, the average weight of polymer chain was 3500 and hence it had about four carboxylic groups on an average.



But the molecular weight was a normal distribution and some polymer chains had a MW higher than the average and some polymer chains had a MW that was lower than average. So, some polymer chains had less than four carboxylic acid groups while some have more than four acid groups based on the molecular weight distribution and the random incorporation of acid groups.

When the polymer chains collapsed, chains with different molecular weight collapsed to give CUP particles with different particle size and a particle size distribution for CUPs. Figure 6 to 14 represents the particle size distribution for the CUP particles for the various polymers synthesized with molecular weight ranging from 3.5K to 153K.

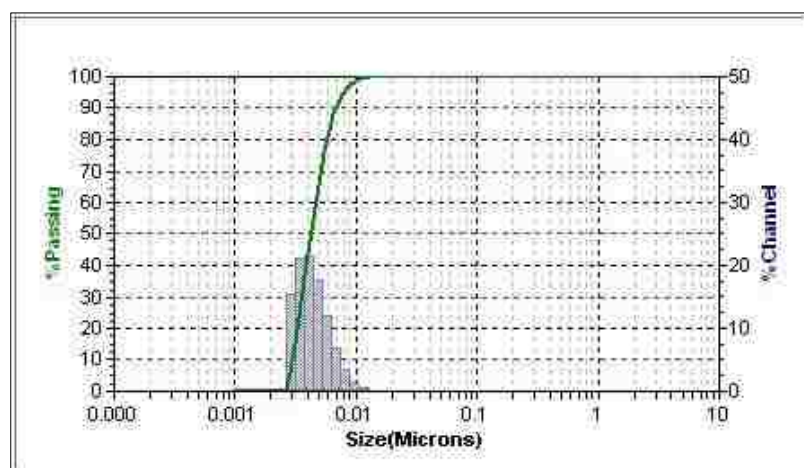


**Fig. 6: Particle size distribution of Poly-1 after filtering**

The Poly-1 sample had a molecular weight distribution and MMA incorporation that resulted in the number of hydrophilic (carboxylate) groups on the polymer chain to vary from anywhere between zero to about five depending upon the molecular weight of

polymer chains. The polymer chains which do not have any hydrophilic (carboxylate) group will be highly unstable when exposed to water. So the chains precipitated out of the solution which was evident in Figure 3. The CUP solutions were filtered using a 0.45 micron filter, to get a clear, transparent solution. The filtered clear CUP solution of poly-1 was analyzed for particle size.

The particle size distribution curve was shown Figure 6. No peaks were observed for particle size near the theoretical value of about 2.1 nm. The particle size was in the range of 3-10nm with an average value of 4.6 nm which indicated polymer aggregation. A percent solids test was done on the CUP solution before and after filtering to determine the percent of the polymer that aggregated and precipitated out of the solution. The percent solids in CUP for Poly-1 before filtering was 19.5% and after filtering it dropped to 12.5% which indicated that about 36% of the polymer chains were larger than 450nm.

In the case of polymeric micelles, the hydrophobic core is protected from the aqueous environment by the hydrophilic corona and if the hydrophobic core is exposed to water, the stability of micelle system is lost. The micelle loses its integrity and the polymer precipitates out.<sup>25</sup> In the CUP system, for the very low molecular weight polymer sample Poly-1, with an average molecular weight of 3.5K, the hydrophilic groups were insufficient to prevent the contact of water with the hydrophobic polymer backbone chain, which caused precipitation of the polymer.

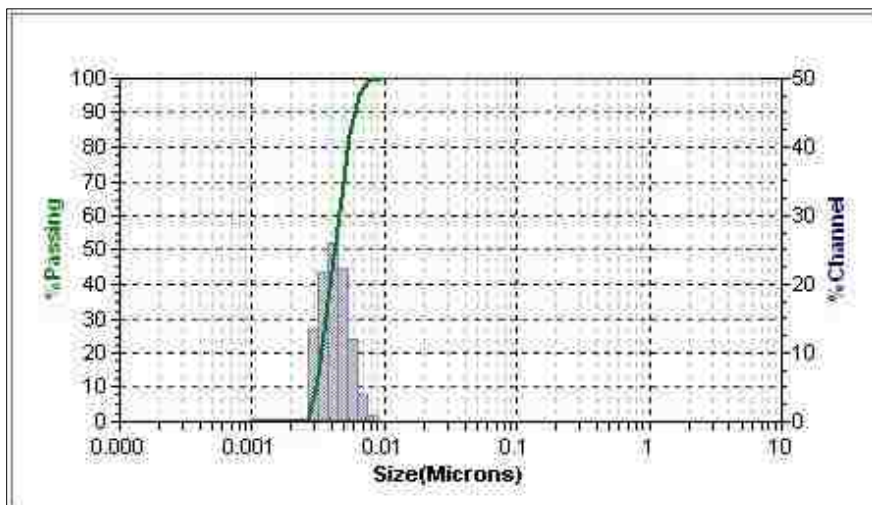


**Fig. 7: Particle size distribution of Poly-2**

From Figure 7, which shows the particle size distribution of CUP solution for Poly-2, the particle size was in the range of 3-9 nm. The average particle size was about 4.4 nm which was higher than the calculated value of 2.3 nm. Though the DLS instrument was capable of detecting particles as low as 0.8 nm, none were observed below 3 nm in the particle size distribution curve for Poly-2 sample. The Poly-2 sample had a molecular weight distribution with an average molecular weight of about 4.5K. Since the methacrylic acid incorporation was statistical, some of the polymer chains would not have sufficient acid groups to stabilize the particle. Unlike Poly-1, the Poly-2 chains did have a better ability to form stable dispersions which were obviously multi-chain particles.

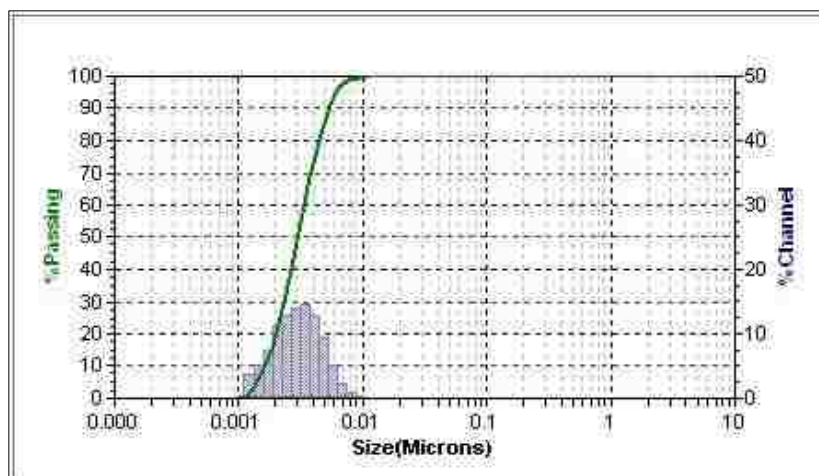


**Fig. 8: Particle size distribution of Poly-3**

Figure 8 shows the particle size distribution for Poly-3 sample (MW = 8.5K). The polymer chains had about eight carboxylate groups on an average with some chains having more and some less. The distribution of particle size was broad with some aggregate formation. The experimental particle size (3.2 nm) was therefore slightly greater than the theoretical value (2.9 nm) which could be possibly due to the aggregation of polymer chains on the lower end of molecular weight distribution or carboxylate content. It should be noted that many of the chains did produce particles consistent with CUP formation.

CUPs based on samples Poly-2 and Poly-3, with average molecular weight of 4.5K and 8.5K respectively had more hydrophilic groups than Poly-1 sample, but still not sufficient to completely prevent contact of water with the hydrophobic backbone. The CUP particles gain stability by aggregating and therefore, a higher particle size than the theoretical value was observed. Figures 9, 10 and 11 show the particle size distribution curve for CUPs prepared from Poly-4 (MW=13K), Poly-5 (MW=15K) and Poly-6 (MW=20K) respectively. The experimental particle size was in good agreement with the

theoretical value. The particle size distributions were broad which was possibly due to a small amount of polymer which collapsed to form particles with larger diameter. Size distribution for Poly-6 indicated a bit of tail towards higher particle size which was mainly due to multiple polymer chain incorporation into the particle during the collapse.

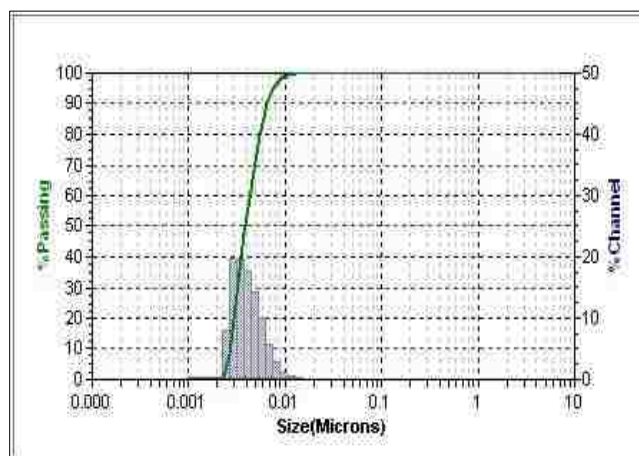


**Fig. 9: Particle size distribution of Poly-4**

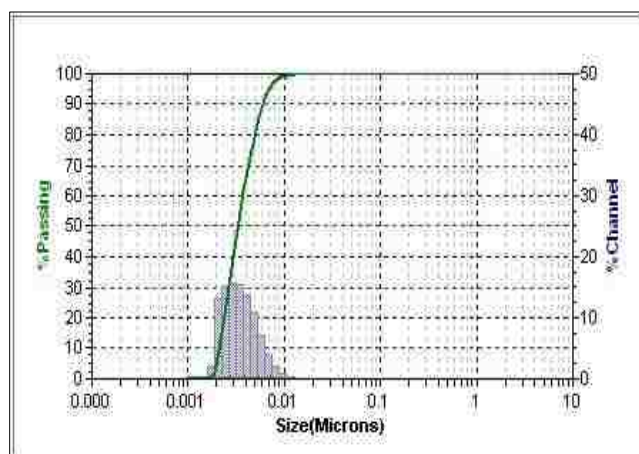


**Fig. 10: Particle size distribution of Poly-5**

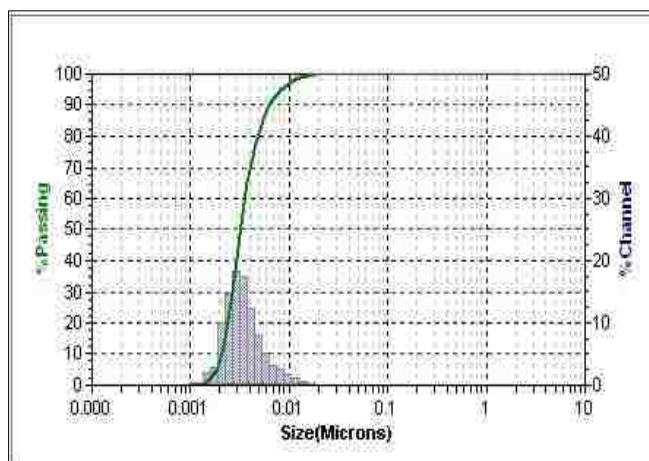


**Fig. 11: Particle size distribution of Poly-6**

The particle size distribution of CUPs prepared from high molecular weight polymers. Poly-7 (MW=72K), Poly-8 (MW=90K) and Poly-9 (MW=153K) were shown in Figures 12, 13 and 14 respectively.

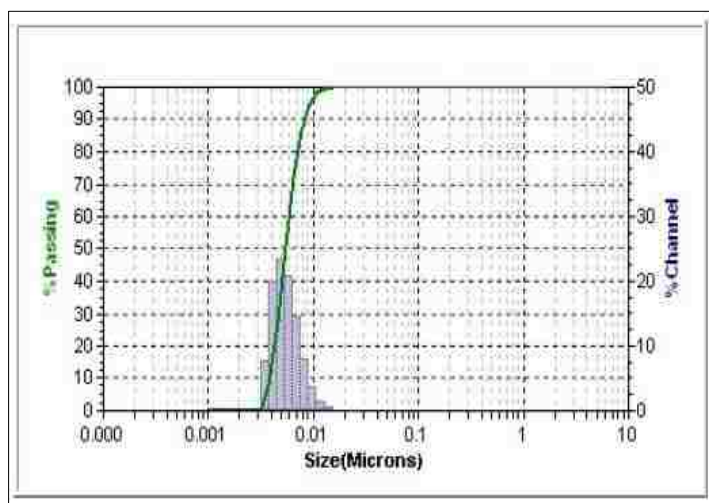


**Fig. 12: Particle size distribution of Poly-7**

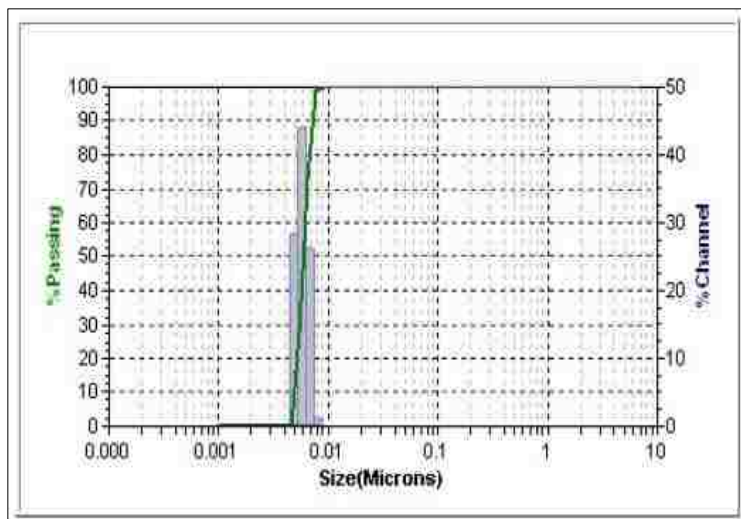


**Fig. 13: Particle size distribution of Poly-8**

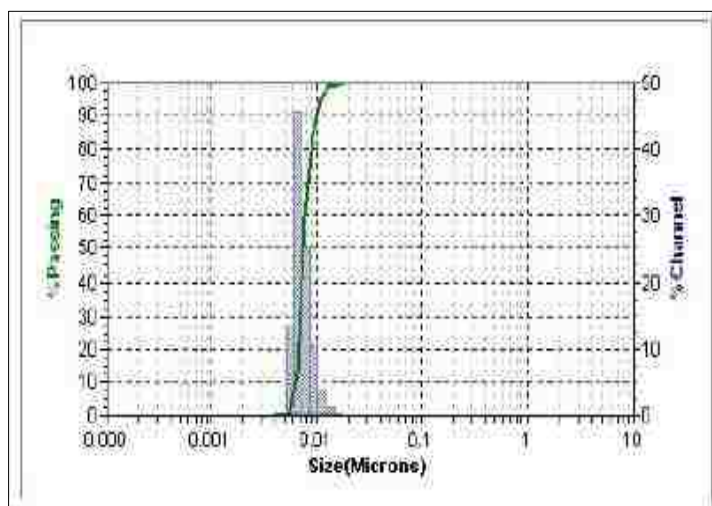


**Fig. 14: Particle size distribution of Poly-9**

## CONCLUSIONS

Colloidal unimolecular polymer particles were successfully synthesized from random copolymers of MMA and MAA. Transition from random coil conformation to

solid spherical particles occurred as the solvent environment was changed from a good solvent to a poor solvent for the polymer backbone giving rise to true nano-scale polymer particles with average particle size less than 10 nm. The particle size measurements using DLS demonstrate that for copolymers with molecular weight below 13000, the unimolecular collapse of polymer chains was not favored because of insufficient stability from electrostatic repulsion and led to the aggregation of polymer chains at the collapse

The polymers with a molecular weight of 13000 and above form CUPs with stable particle size which was consistent with the theoretical particle size. CUPs were formed with stable particle size and uniform size distribution even for molecular weights as high as 150k, but, at lower initial concentration. The size of individual polymer chains restricts the range of viable polymer concentration during the collapse to form colloidal unimolecular polymer particles.

Once the CUP solutions are prepared they can be further concentrated to about 25-30% solids above which they reversibly gel. Unlike conventional water reducible resins, CUP solutions contain no surfactant and are VOC free, except for the amine, making them a very good candidate for future coatings applications, even as a lacquer. CUP solutions have been shown to be stable for over three years.

## **ACKNOWLEDGEMENTS**

The authors would like to acknowledge the Coatings Institute and the Department of Chemistry of Missouri S&T for the financial support and resources and thank Jigar Mistry for help in GPC.



## REFERENCES

1. Kabanov AV, Batrakova EV, Melik-Nubarov NS, Fedoseev NA, Dorodnich TY, Alakhov VY, Chekhonin VP, Nazarova IR and Kabanov VA, "A new class of drug carriers: micelles of poly(ethylene)-poly(propylene) block copolymers as microcontainers for targeting drugs from blood to brain", *J. Control. Rel.*, **22** 141-157 (1992)
2. Kataoka K, Kwon G, Yokoyama M, Okano T and Sakurai Y, "Block copolymer micelles as vehicles for drug delivery", *J. Control. Rel.*, **24** 119-132 (1993)
3. Guo J, Farrell S and Uhrich KE, "Interactions Between Unimolecular Micelles and Liposomes", *Mat. Res. Soc. Symp. Proc.*, **550** 89-94 (1999)
4. Liu H, Jiang A, Guo J and Uhrich KE, "Unimolecular Micelles: Synthesis and Characterization of Amphiphilic Polymer Systems", *J. Polym. Sci.: Part A: Polymer Chemistry*, **37** 703-711 (1999)
5. Guo J, Farrell S and Uhrich KE, "Drug release characteristics of unimolecular polymeric micelles", *J. Control. Rel.*, **68** 167-174 (2000)
6. Morishima Y, Nomura S, Ikeda T, Seki M and Kamachi M, "Characterization of unimolecular micelles of random copolymers of sodium 2-acrylamido-2-methylpropane sulfonate and methacrylamides bearing bulky hydrophobic substituents", *Macromolecules*, **28** 2874-2881 (1995)
7. Noda T, Hashidzume A and Morishima Y, "Micelle formation of random copolymers of sodium-2-acrylamido-2-methylpropanesulfonate and a nonionic surfactant macromonomer in water as studied by fluorescence and dynamic light scattering", *Macromolecules*, **33** 3694-3704 (2000)
8. Chen M and Van De Mark MR, "Rheology studies on colloidal unimolecular polymer (CUP) particles in absence and presence of NaCl", *Polymer Preprints*, **52** 336-337 (2011)
9. Kan CS, "Role of Particle Size on Latex Deformation During Film Formation", *Journal of Coatings Technology*, **71** 89-97 (1999)
10. Riddles CJ, Zhoa W, Hu H-J and Van De Mark MR, "Colloid unimolecular polymers (CUPs) synthesized by random copolymerization of MMA/MAA", *Polymer Preprints*, **52** 232-233 (2011)
11. Chen M, Riddles CJ, Van De Mark MR, *Colloid Polym. Sci.* 291 (2013) 2893-2901
12. Vidulich GA, Evans DF, Kay RL, "The dielectric constant of water and heavy water between 0 and 40.degree.", *J. Phys. Chem.*, **71** (3) 656-662 (1967)
13. Simha R, Branson H, "Theory of Chain Copolymerization Reactions." *J. Chem. Phys.*, **12** 253-267 (1944)
14. Stockmayer WH, "Distribution of Chain Lengths and Compositions in Copolymers." *J. Chem. Phys.*, **13**, 199-207, (1945)

15. Amaral MD, Roos A, Asua JM and Creton C, "Assessing the Effect of Latex Particle size and distribution on the Rheological and Adhesive Properties of Model Waterborne Acrylic Pressure-Sensitive adhesives Films." *J. Colloid Interf. Sci.*, **281** 325-338 (2005)
16. Wicks ZW Jr., Jones FN, Pappas SP and Wicks DA, *Organic Coatings Science and Technology*. Wiley Interscience (2007)
17. Hiemenz PC, Rajagopalan R, *Principles of Colloid and Surface Chemistry*. Marcel Dekker (1997)
18. Ruiz-Reina, E and Carrique F, "Electroviscous Effects of Concentrated Colloidal Suspensions in Salt-free Suspension." *J. Phys. Chem. C*, **111** 141-148 (2007)
19. Ogawa A, Yamada H, Matsuda S, Okajima K and Doi M, "Viscosity Equation for Concentrated Suspensions of Charged Colloidal Particles." *J. Rheol.*, **41** 769-785 (1997)
20. Hernandez FJR, Carrique F and Ruiz-Reina E, "The Primary Electroviscous Effect in Colloidal Suspensions." *Adv. Colloid and Interface Sci.*, **107** 51-60 (2004)
21. Hales TC, "A proof of the Kepler Conjecture." *Annals of Mathematics*, **162** 1065-1185 (2005)
22. Pishvaei M , Gaillat C, McKenna TF, Cassagnau P, "Rheological Behavior of Polystyrene Latex Near the Maximum Packing Fraction of Particles." *Polymer*, **46** 1235-1244 (2005)
23. Brinkman E and Loos F, "New Developments in Water-borne Resins for Industrial Coatings." *Surf. Coat. Int.*, **3** 143-145 (1988)
24. Wilson AD, Nicholson JW and Prosser HJ, *Waterborne Coatings-Surface Coatings-3*. Elsevier Science Publishing Co. Inc. , (1990)
25. Owen SC, Chan DPY and Shoichet MS, "Polymeric micelle stability", *Nano Today*, **7** 53-65 (2012)

## II. SYNTHESIS AND CHARACTERIZATION OF AN ACID CATALYST FOR ACRYLIC-MELAMINE RESIN SYSTEMS BASED ON COLLOIDAL UNIMOLECULAR POLYMER (CUP) PARTICLES OF MMA-AMPS

*Ameya M. Natu and Michael R. Van De Mark<sup>1</sup>*

*Department of Chemistry, Coatings Institute, Missouri University of Science & Technology, Rolla, MO 65409, USA*

### ABSTRACT

Colloidal unimolecular polymer particles (CUPs) based on poly(methyl methacrylate-co-2-acrylamido-2-methylpropane sulfonic acid) were synthesized and characterized and its potential for use as a blocked acid catalyst for curing of acrylic-melamine based resin systems was evaluated. CUPs were synthesized by the process of water reduction of acrylic copolymers and had zero volatile organic content (VOC). The curing performance of CUPs was evaluated by pencil hardness, micro-indentation hardness and solvent resistance measurements. The sulfonic acid containing CUPs catalyzed the curing of acrylic-melamine resin systems effectively and were found to provide final resin properties comparable to the commercially used blocked acid catalysts. On a molar equivalent basis, the amount of CUP catalyst required for the final cured film properties was lower than the commercial blocked acid catalyst. NMR analysis confirmed that the commercial acid catalyst leached out of the cured film when exposed to water for twenty-four hours while the CUP catalyzed coating did not.

### Keywords

Unimolecular, acid catalyst, copolymers, water reduction, volatile organic content

---

<sup>1</sup>Corresponding author, Tel: +1 5733414882.

Email address: mvandema@mst.edu

## 1. INTRODUCTION

There has been a growing interest in hydrophobic polymers bearing hydrophilic groups which show self-organization behavior when placed in a poor solvent such as water. This potential is mainly because of its biological significance and also because of its applications in the field of coatings, polymers and drug delivery [1-6]. Numerous methods have been reported for water-reduction of polymers to provide resins for the coatings industry which have a low volatile organic content (VOC).

Moroshima et al., in his study of self-organization of copolymers, reported that unimolecular micelles with diameter  $< 20$  nm were formed because of hydrophobic interactions (aggregation) when the copolymer was added to water [7]. Liu et al. have reported that amphiphilic copolymers dispersed in water formed unimolecular micelles with a core-shell structure; the hydrophobic part forming the core and hydrophilic groups oriented in the aqueous phase forming the shell [8]. Selb and Gallot reported unimolecular micelles prepared from graft copolymers of styrene and 4-vinyl-N-ethylpyridinium bromide in methanol/water mixtures [9]. The unimolecular micelle systems are often referred to as single chain nanoparticles.

In the present study, we report the synthesis of acrylic copolymers, which, by the process of water reduction followed by solvent removal, gave colloidal unimolecular polymer particles (CUPs). CUP solutions are a two-phase colloidal system composed of solid spherical unimolecular polymer particles as the dispersed phase suspended in the continuous aqueous phase. CUPs are typically prepared from polymers containing hydrophilic groups such as carboxylic acid salts or sulfonic acid salts on a hydrophobic polymer backbone [10].

Polymers with molecular weights ranging from 13,000 to 130,000 have been successfully water-reduced to form CUPs. Polymers with molecular weight lower than 13000 may form CUPs but they have some aggregation due to an insufficient number of stabilizing groups [11]. This research paper explores the synthesis and characterization of CUPs based on copolymers of methyl methacrylate (MMA) and 2-acrylamido-2-methylpropane sulfonic acid (AMPS) monomers and the potential use of the sulfonate based CUPs as an acid catalyst for curing of acrylic-melamine resin systems.

Acrylic resins crosslinked with amino resins are widely used OEM as (original equipment manufacturer) coatings. The acrylic-melamine systems offer excellent chemical and weathering resistance together with good adhesion and color retention. Because of the excellent performance in outdoor exposure acrylic-melamine systems are also widely used in automobile finishes. Acid catalysts are often required for curing of the acrylic-melamine resin systems. Hydroxyl groups and carboxylic acid groups on the acrylic resin react with the amino resin by means of etherification, esterification and amidation reactions [12]. The reactions are promoted by the addition of an acid catalyst. Para-toluene sulfonic acid (p-TSA) based catalyst systems have been widely used for curing the acrylic-melamine resins which reduce the curing temperature and the time required for complete cure [13]. The amount of acid catalyst affects many properties of the coating film including mechanical, weathering and optical properties.

A major drawback of the strong acid catalysts is that they can initiate crosslinking even at room temperature causing storage problems. This means that the catalyst cannot be added to the coating formulation and then stored for future use. Also, the formulations need to be applied immediately after the addition of acid catalyst to prevent crosslinking during storage. To prevent in-can reactions, blocked catalysts, which are usually the tertiary amine

or ammonium salts of the acid are employed [14]. There have been continuous developments in the catalysts used for ambient temperature cure, catalytic activity, lower volatile organic content (VOC), gloss improvement and influence on mechanical properties of the final cured coating [15].

Catalyst systems based on Colloidal Unimolecular Polymer particles (CUPs) provide a new class of polymer catalysts for curing of resins with many advantages over curing systems currently employed. CUPs are true nano-scale polymers with particle diameter in the range of 3-9 nm which provides a high surface availability. CUPs do not contain any coalescent aid, freeze-thaw agent or a surfactant and have a zero volatile organic content (VOC). The process of making CUPs is very simple and materials required are commonly available which make the CUPs very cost effective [16]. CUPs with active sulfonic-acid groups on the surface could be effective in catalyzing the curing of acrylic-melamine resin systems. The CUP catalyst could also get incorporated in the acrylic-melamine resin via the trans-esterification reaction with the melamine component and then become immobile and not leach to the surface [17, 18], as shown in Figure 1. Incorporation of the acid catalyst could be beneficial from the point of view of mechanical properties as well as non-leaching from the crosslinked coating film. Both are beneficial to the overall performance of the coating. This is a significant advantage over the commercial acid catalyst which does not get incorporated into the film.

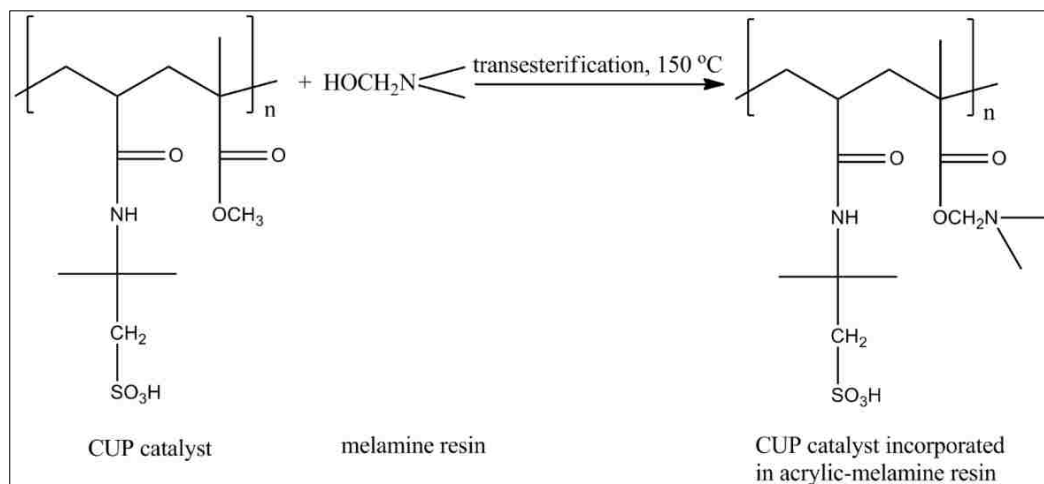


**Figure 1. Incorporation of CUP catalyst in the acrylic-melamine resin via transesterification**

The efficacy of the CUP catalyst in crosslinking of the acrylic-melamine resin system was evaluated and compared with the performance of commercially used blocked para-toluene sulfonic acid catalyst. Three resin systems were evaluated with the new CUP catalyst: a conventional hydroxyl functional acrylic latex (Joncryl 540) (denoted as OH-latex); a conventional carboxyl functional acrylic latex (Neocryl A6037) (denoted as  $\text{CO}_2\text{H}$ -latex); and a carboxyl functional CUP (denoted as  $\text{CO}_2\text{H}$ -CUP) prepared from a polymer based on ethyl-methacrylate (EMA), n-butylmethacrylate (n-BMA) and methacrylic acid (MAA). All three acrylic resins were crosslinked with a melamine resin crosslinker (Cymel 373). The acid value, particle diameter, molecular weight ( $M_n$ ) and glass transition temperature ( $T_g$ ) of the acrylic resins and the CUP catalyst were listed in Table 1.

**Table 1.** Important physical properties of the acrylic resins

Resin Characteristics	CO <sub>2</sub> H-latex	CO <sub>2</sub> H-CUP	OH-latex	CUP-catalyst
Acid value <sup>a</sup>	52	49	-	48.1
Particle diameter <sup>b</sup> (nm)	95	4.5	75.3	5.9
M <sub>n</sub>	65,000	50,000	78,000	80,000
Measured T <sub>g</sub> (°C) <sup>c</sup>	44	75	40	123

a) mg of KOH/ g polymer, b) average diameter measured by DLS, c) mid-point of T<sub>g</sub> transition range.

## 2. MATERIALS AND METHODS

2-Acrylamido-2-methylpropane sulfonic acid (AMPS) was supplied by Lubrizol and used as received. Methyl methacrylate (MMA), 2,2'-azobis(2-methylpropionitrile) (AIBN), and n-butanethiol were obtained from Aldrich. Inhibitors from the monomer MMA were removed by washing with 10% aqueous solution of sodium bicarbonate (NaHCO<sub>3</sub>), distilled water and brine solution respectively, then dried over anhydrous magnesium sulfate and further purified by distillation. AIBN was re-crystallized from methanol prior to use. Absolute anhydrous ethanol was obtained from PHARMCO-AAPER and used as supplied. The hydroxyl functional acrylic latex (Joncryl 540) was obtained from BASF. The carboxyl functional acrylic latex (Neocryl A 6037) was obtained from DSM. The melamine-formaldehyde resin (Cymel 373) was supplied by Cytec Industries. The commercial blocked acid catalyst (NACURE 2547) was obtained from King Industries.



## 2.1. Characterization of Commercial Acrylic Resins

As the molecular weight of the OH-latex and CO<sub>2</sub>H-latex was proprietary information, evaluation of the absolute molecular weight was done by using a gel permeation chromatograph by Viscotek model 305 manufactured by Malvern Corp. Flow rate of THF was 0.5ml/min, and the injection volume was 100 $\mu$ l. The GPC was equipped with refractive index detector, low and right angle light scattering detector and intrinsic viscosity detector, thus yielding absolute molecular weight.

The sample preparation for both latexes was done in the following manner: the latex was first dried in vacuum and then dissolved in THF. The polymer was then precipitated in cold water under shear and then completely dried in-vacuo. The dry polymer was re-dissolved in THF and re-precipitated in cold water under shear. The process ensured that most of the water-soluble additives used in the synthesis of the latexes such as thickeners and surfactants which could give erroneous polymer molecular weight were removed. The double-precipitated dry polymer was then used for molecular weight determination using GPC and the results were listed in Table 1.

## 2.2. Synthesis of Random Copolymer of MMA and AMPS

Copolymer of MMA and AMPS was prepared in a 3-neck flask equipped with a thermometer, a nitrogen inlet and a condenser fitted with a bubble tower. MMA (0.81moles, 81.3 gram) and AMPS (0.09 moles, 18.7 gram) monomers were charged into the flask in a molar ratio of 9:1 along with the solvent absolute ethanol (250 gram) and n-butanethiol (0.0012 moles, 0.11 gram) as a chain transfer agent. AIBN (0.00073 moles, 0.12 gram) was used as the free radical initiator and the polymerization reaction was carried out under refluxing conditions for 24 hrs. The polymer solution was then cooled to room

temperature and precipitated in cold de-ionized water under high shear and then filtered, which removed the unreacted AMPS monomer as it was water-soluble. The traces of unreacted MMA and ethanol were removed in-vacuum. The polymer was further dried using a freeze-drier (Yield=71%).

### **2.3. Water-Reduction of MMA-AMPS Based Copolymer To Form CUPs**

Ten grams of the purified and dry acrylic copolymer was dissolved in ninety grams of methanol, a low boiling and water miscible solvent, to make a 10% w/w solution and was stirred overnight for complete dissolution of the polymer chains. Aqueous ammonium hydroxide solution (28% w/w) was added to neutralize all the acid groups based on the acid number of the copolymer. Then 190 g of deionized water modified to a pH of 8~9 using 28% aqueous  $\text{NH}_4\text{OH}$  solution was added to the polymer solution by a peristaltic pump at a rate of 1.24g/minute. The pH of solution was maintained at 8-9 throughout the process of water reduction. Methanol was stripped off under vacuum to give an aqueous 5.0% w/w CUP solution of poly (MMA-co-AMPS) with zero VOC. The CUP solutions were then filtered through 0.45 $\mu\text{m}$  Millipore membrane to remove any impurities. Further water removal to over 25% solids can be accomplished before a semi-solid gel state is formed. The gel can be simply diluted and reforms a fluid system.

### **2.4. $\text{CO}_2\text{H}$ -CUP Synthesis**

The  $\text{CO}_2\text{H}$ -CUP was based on a polymer of EMA-BMA-MAA. The resin synthesis and water-reduction process for EMA-BMA-MAA polymers has been discussed elsewhere [19]. CUPs were prepared by water-reduction in a manner similar to the CUPs based on MMA-AMPS.

## 2.5. Characterization of Synthesized MMA-AMPS Copolymer

Acid number (AN) (reported in mg of KOH per gram of polymer) for the sulfonic acid copolymer was measured by the titration method found in ASTM D 974; modified by using potassium hydrogen phthalate (KHP) in place of hydrochloric acid and phenolphthalein in place of methyl orange. The density of AMPS polymer was measured using Micromeritics AccuPyc II 1340, a gas displacement pycnometer. A weighed amount of sample was introduced in the sample chamber. Equilibrium flow rate of helium gas was 0.005 pounds per square inch gauge (psig)/min and temperature maintained at  $22.78 \pm 0.04$  °C. Fifty readings were made for the polymer sample and the results were reported by its average and standard deviation.

## 2.6. Characterization of CUPs

The viscosity of CUP solutions were measured using a Brookfield Programmable Rheometer (Model DV-III) at two different temperatures. One milliliter of CUP solution was transferred to the well of the Brookfield LV DVIII by Eppendorf pipet. The well's temperature was controlled by a circulating constant temperature water bath. Shearing viscosities of CUP at varying shear rates were measured. The shear rates were programmed to increase at a set speed and the viscosities were recorded at each speed after one minute of continuous shearing. Particle size and the size distribution of CUPs was measured using a dynamic light scattering (DLS) method by a particle size analyzer from Microtrac (model Nanotracer 250). The DLS instrument was equipped with a laser diode of 780 nm, at a measuring angle of 180°. For measuring the particle size of CUPs, the viscosity of CUPs at two different temperatures was measured and utilized instead of the viscosity of solvent water.

Thermogravimetric analysis (TGA) was performed on a TA Instruments model Hi-Res-TGA Q50 analyzer. The thermal stability of the MMA-AMPS based CUP was determined under nitrogen by measuring weight loss while heating at a rate of  $10\text{ }^{\circ}\text{C min}^{-1}$ . Glass transition temperature was determined by Modulated Differential Scanning Calorimetry (MDSC) conducted under nitrogen with a TA Instruments Differential Scanning Calorimeter Model Q2000 at a heating rate of  $10\text{ }^{\circ}\text{C min}^{-1}$  in the modulated T4P mode, using 40 seconds as the modulation period and  $0.318\text{ }^{\circ}\text{C}$  as the modulation amplitude. The rate of heating and cooling can affect the measured glass transition temperature and therefore the standard heating rate as reported in literature was utilized for the present measurements.

## **2.7. Coating Formulations and Testing**

The MMA-AMPS based CUP dispersion was evaluated as a blocked acid catalyst for curing of three different types of resin systems; OH-latex,  $\text{CO}_2\text{H}$ -latex and  $\text{CO}_2\text{H}$ -CUP. Melamine resin was used as the crosslinker. Formulations for the OH-latex,  $\text{CO}_2\text{H}$ -latex and  $\text{CO}_2\text{H}$ -CUP are shown in Table 2, 3 and 4 respectively. Three formulations were prepared for OH-latex system: Standard: OH-latex crosslinked with melamine resin system without any acid catalyst. System 1: OH-latex crosslinked with a melamine crosslinker in presence of MMA-AMPS CUP as the blocked acid catalyst. System 2: OH-latex crosslinked with melamine in presence of the commercially available blocked-p-TSA as the curing catalyst.

**Table 2.** Formulations for OH-latex cured with melamine

Formulation	Acrylic <sup>a</sup> : melamine <sup>b</sup> (wt./wt. solids)	% Catalyst <sup>c</sup>
Standard	75:25	0
System 1	75:25	0.5 <sup>d</sup>
System 2	75:25	0.5 <sup>e</sup>

a- 45% solids by weight, b-85% solids by weight, c - based on resin solids by wt., d - CUP catalyst (5% wt./wt.), e- commercial catalyst (25% wt./wt.)

Similarly, four formulations were prepared for CO<sub>2</sub>H-latex labeled as A, B, C and D and four formulations for CO<sub>2</sub>H-CUP labeled as E, F, G and H, to determine the effect of particle size of a latex and a CUP resin on the final cured film properties.

**Table 3.** Formulations for CO<sub>2</sub>H-latex cured with melamine

Formulation	Acrylic <sup>a</sup> (% wt.)	Melamine (% wt.)	Catalyst type	% Catalyst <sup>b</sup>
A	100	-	-	0
B	75	25	-	0
C	75	25	Commercial	0.5
D	75	25	CUP	0.5

a - 49% solids by wt., b - based on resin solids by weight, A - CO<sub>2</sub>H-latex, B - CO<sub>2</sub>H-latex + melamine, C-CO<sub>2</sub>H-latex + melamine + blocked p-TSA, D - CO<sub>2</sub>H-latex + melamine + CUP catalyst.

**Table 4.** Formulations for CO<sub>2</sub>H-CUP cured with melamine

Formulation	Acrylic (% wt.)	Melamine (% wt.)	Catalyst type	% Catalyst <sup>a</sup>
E	100	0	-	0
F	75	25	-	0
G	75	25	Commercial	0.5
H	75	25	CUP catalyst	0.5

a - based on resin solids by weight, E- CO<sub>2</sub>H-CUP, F- CO<sub>2</sub>H-CUP + melamine, G- CO<sub>2</sub>H-CUP + melamine+ blocked p-TSA, H- CO<sub>2</sub>H-CUP + melamine+ CUP catalyst

The acrylic resin (hydroxyl or carboxyl functional), the melamine resin and the blocked acid catalyst were mixed. The films were cast on aluminum panels A-36 mill finish from Q-panel, using a standard number 30 wire drawdown bar and placed in the oven after 10 min of flash off time. The panels were then cured at 150 °C. The curing time was varied from 10 min to 30 min to observe the effectiveness of acid catalysts. The curing of acrylic-melamine resin system was evaluated by measuring the pencil hardness on the coated aluminum panels according to the method found in ASTM D3363. The hardness of coating films can be evaluated by various methods such as Knoop hardness, Pencil hardness, Taber abrasion, Tukon hardness [20]. Pencil hardness test was chosen because of its easy interpretation, convenience and wide usage in the paint industry. Pencils of varying hardness in the range of 6B-6H were tested and an average of three readings was reported. A quantitative evaluation of hardness was performed using a micro indentation technique Fisherscope HM2000 S instrument. The micro-indenter had a Vickers diamond indenter. The indenter had a pyramid shape with a square base (vertex angle equal to 136°). Two

types of testing methods were performed using the microindenter. In the first method, called the Standard method (SM), load was applied incrementally up to a maximum of 9 mN over a period of 20 seconds and followed by the unloading cycle. The maximum load was determined experimentally as the load above which the substrate starts interfering with the hardness measurement. The creep time after loading and after unloading cycles was chosen as 30 seconds which is the maximum. A typical load-depth curve for the standard method is shown in Figure 2.

In the second method, known as Enhanced Stiffness Procedure (ESP), each load increment was followed by creep time, unloading and creep time, and then the next cycle followed, till the maximum load of 9 mN was reached. The instrument had a load resolution of  $\pm 40$  nN and a distance resolution of 0.1 nm. A typical load-depth curve for ESP method is shown in Figure 3. The Standard method gives hardness at the maximum load while ESP method gives hardness value at each incremental load thus giving a depth profile of hardness of the coating.

In both the methods, force and depth were measured and recorded continuously, both during loading and unloading cycle. The instrument automatically calculates hardness (H) defined as applied normal force (F) divided by projected area (A) on the original surface at a given point in the experiment using the Oliver-Pharr method from the resultant load vs indentation depth curve (loading/unloading cycles). The average of five measurements was reported. The instrument was calibrated using an acrylic plate to ensure that the results were within the normal range of reproducibility [21].

$$H = \frac{F}{A} \quad (1)$$

MEK double rub test was performed on coated aluminum panels which provides a measure of the solvent resistance of a coating and an estimate of the crosslink density. A lint-free cloth was employed and the test was carried out as per ASTM method D-4752. The average of two readings was reported. Gloss was measured on aluminum panels by a Byk-Gardener micro-gloss meter and the average of five readings with standard deviation less than one were recorded.

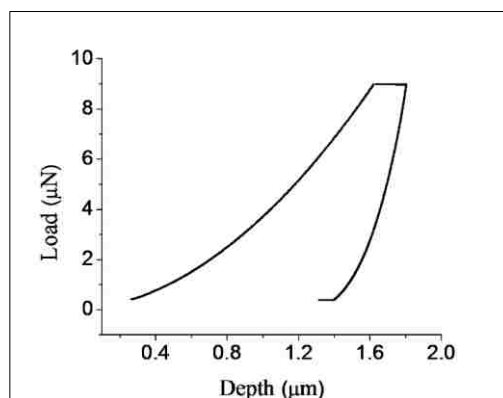


**Figure 2. Load-depth curve using standard method for indentation of System 1**

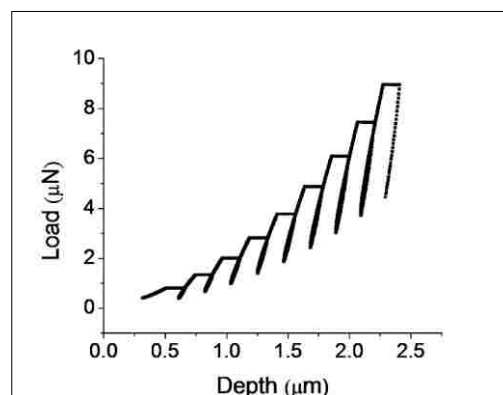


**Figure 3. Load-depth curve using ESP method for indentation testing of System 1**



### 3. RESULTS AND DISCUSSION

The free radical polymerization of MMA and AMPS gave a random copolymer with a yield of 71%. The reactivity ratio of the two monomers reported in the literature indicated that the copolymerization was approximately random in nature. The density of the dry polymer (CUP-catalyst) was measured to be 1.2396 g/cc. The experimental value of acid number was 48.1 (mg KOH/g of polymer). The acid number was slightly greater than the theoretical value of 46.8 (mg KOH/g polymer) which can be explained by the loss of some of MMA monomer through evaporation while purging with nitrogen during the polymerization. The density of the dry OH-latex, CO<sub>2</sub>H-latex and melamine resin was 1.0958, 1.1195 and 1.3206 g/cc, respectively.

#### 3.1. Process of Water-reduction

Figure 4 shows the water-reduction process of MMA-AMPS copolymer which leads to the formation of CUP particles with sulfonate groups on the surface. The copolymer with hydrophobic polymer backbone (MMA: 9 parts) and the sulfonic acid side-chain (AMPS: 1 part) when dissolved in MeOH exists as an extended random coil. When base i.e. ammonium hydroxide was added to the solution, the sulfonic acid groups on the polymer chain formed SO<sub>3</sub><sup>-</sup> and NH<sub>4</sub><sup>+</sup> ions. Bases like NaOH and KOH were not used for neutralization as they do not leave the film during drying and remain as a salt and the CUP particles would not act as acid catalyst.

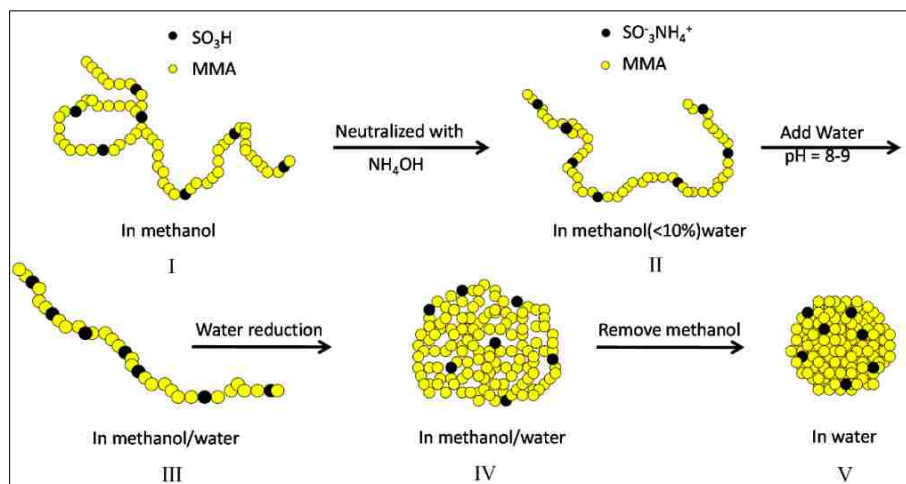


**Figure 4. Process of formation of CUPs from copoly(MMA-AMPS)**

Ammonia serves the dual purpose of stabilization of CUP particles through ionic repulsion and acting as a blocking group for the acid catalyst. The ion pairs are almost completely solvated in methanol. When pH-modified water (pH = 8-9) was added using peristaltic pump, there could be a slight increase in the solvation since water has a dielectric of 78.54 [22] while methanol has a dielectric of 35.74 at 25°C [23]. Negatively charged sulfonate groups repel each other due to the increasing dielectric caused by the added water and the polymer chain becomes more rod-like causing an increase in the viscosity.

With continuous addition of water, at a certain critical point, the amphiphilic polymer chains collapse. The sulfonate groups being hydrophilic orient into the water phase, organizing to produce maximum separation of charge and the hydrophobic polymer chain collapsed to form the interior of the spheroidal CUP particle. In the last step, methanol was stripped off in-vacuo to give zero VOC CUP particles, free of solvent, ammonia and water being the only volatile components. The solvent that was stripped off could be recycled, thus providing an environment friendly resin system.

The unimolecular collapse was also dependent on the concentration of amphiphilic polymer in MeOH and MeOH/water mixture. At a higher concentration, the polymer chains overlap and if overlapped polymer chains come in contact with each other at the critical point, non-unimolecular collapse occurs forming larger particle size or coagulum.

The process of water reduction is analogous to the process of micelle formation. As water was added to the polymer solution in MeOH, the solvent organizes around the hydrophobic units of MMA in the polymer chain. Entropy drives the collapse of polymer chains into CUP particles by the release of the organized water to the bulk even though the polymer chains and charges must become more organized. The collapsed CUP particles approximate a sphere due to the sulfonate group's repulsive nature to each other. The CUP particles are small enough so that the Brownian motion keeps the particles suspended and thermodynamically stable unlike the larger latex particles which settle with time.

### **3.2. Rheological Behavior**

The rheological behavior of a 5% CUP based on poly(MMA-co-AMPS) was shown in Figure 5 as a plot of shear stress against shear rate at 25<sup>0</sup> C and 29<sup>0</sup> C. The CUP solution is a colloidal suspension with charged polymer particles as the dispersed phase in the continuous aqueous phase. In an earlier report, it was shown that the primary and tertiary electroviscous effects dominated the rheology behavior of carboxylate functional CUPs [24]. The rheological behavior of the CUP solution is a function of the concentration of the polymer particles in the solution according to the electrokinetic theory of viscosity of charged colloids [25]. At higher concentration, the electroviscous effects cause deviation of the colloidal solution from Newtonian behavior, but at fairly dilute concentrations (< 10% wt/wt), the CUP solutions have been known to exhibit Newtonian behavior [26].

In the present case, the viscosity measurements were done at a fairly low concentration of 5.0% of polymer particles wt/wt. At both the temperatures, the shear stress on CUP solution increased linearly with increasing shear rate and the yield stress was zero which indicated that the CUPs behave as a Newtonian fluid at a concentration of 5.0% wt/wt. The viscosity values were further used for particle size analysis of CUPs.

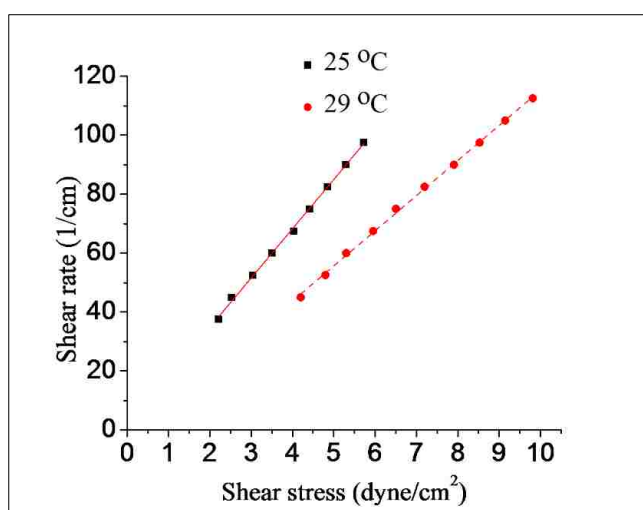


**Figure 5. Shear stress against shear rate for CUP catalyst solution at 5% solids at 1) 25<sup>o</sup> C and 2) 29<sup>o</sup> C**

### 3.3. Role of Solvent and Divalent Cations

Methanol was selected as the primary good solvent due to its excellent solubility towards the MMA-AMPS copolymer, its miscibility with water and a low boiling point allowing it to be easily stripped off without loss of significant amounts of water. The purity of water required for water-reduction was also evaluated with respect to presence of polyvalent cations such as calcium.

For CUPs based on MMA-MAA polymer, it was observed that the presence of divalent cations such as calcium or magnesium in the water caused precipitation of polymer during or after the water-reduction process [27]. The calcium or magnesium ions bind to the carboxylic acid groups of MAA on the CUP particles forming insoluble salts which cause the polymer to precipitate. However, the sulfonate groups are bound weakly to the divalent ions and remain soluble [28, 29].

McCormick et al., based on potentiometric titrations, have indicated that the large dissociation constant for sulfonate as compared to carboxylate in presence of divalent ions, was responsible for the stability of sulfonate polymers [30]. Sabbagh et al. demonstrated that for sulfonate polymers, precipitation occurs only for counterions with a valency of three or more, while carboxylate polymers precipitate in presence of any multivalent counterion [31].

The hypothesis that the presence of low levels of the divalent cations in the water used for reduction should not hinder the formation of CUP particles based on sulfonic acid containing polymers was evaluated by carrying out the water reduction of MMA-AMPS copolymers with water containing 50 ppm of dissolved calcium chloride. No visible haziness was observed and the copolymer water-reduced without any precipitation or coagulation. The particle size was measured by DLS and it was found to be 5.9 nm which was the same as for the CUPs water-reduced in absence of the calcium salt. This indicated that there was no aggregation due to calcium ions.

Figure 6 shows a comparison of CO<sub>2</sub>H-functional and SO<sub>3</sub>H-functional CUP solutions prepared by water-reduction of polymers in presence of 50 ppm of calcium.



**Figure 6. Water reduction in presence of 50 ppm calcium for 1) CO<sub>2</sub>H-copolymer 2) SO<sub>3</sub>H-copolymer**

### **3.4. Particle Size Analysis Using DLS**

The CUP solution was filtered through a 0.45 $\mu$ m Millipore membrane before performing the particle size analysis. The filtration process ensured removal of any foreign material which was typically measured to be less than 0.05% by weight. Figure 7 and Figure 8 show the particle size distribution for SO<sub>3</sub>H-functional CUPs prepared in water with and without the added calcium salt respectively. CUPs are formed by the unimolecular collapse of polymer chains and the particle diameter depends upon the molecular weight of polymer and its density.

The polymer chains have a broad molecular weight distribution unless the polymer is made by living free radical polymerization techniques which give a very narrow molecular weight distribution. The molecular weight distribution leads to a particle size distribution for the CUPs. DLS measurement of the CUP solution indicated an average particle size of 5.9 nm. The theoretical and experimental particle size was in good correlation.

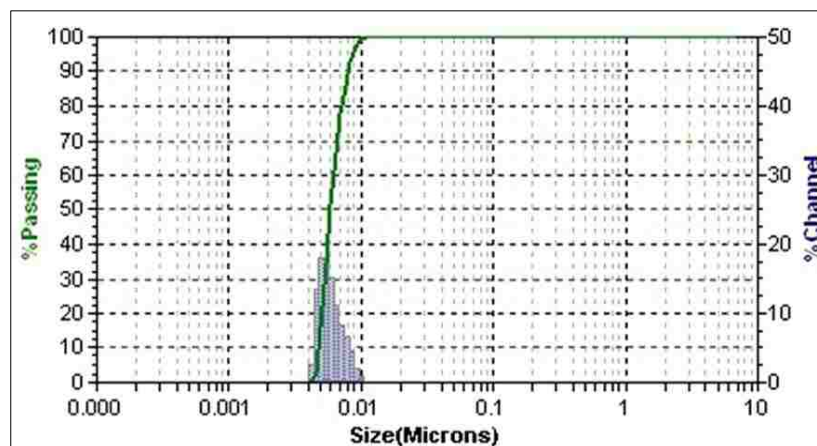


Figure 7. Particle size distribution of SO<sub>3</sub>H-CUPs in presence of 50 ppm of CaCl<sub>2</sub>

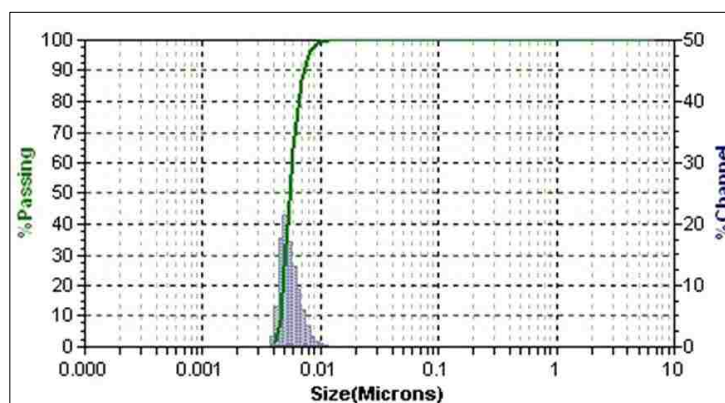


Figure 8. Particle size distribution of SO<sub>3</sub>H-CUPs of poly(MMA-co-AMPS) without CaCl<sub>2</sub>

### 3.5. Thermogravimetric Analysis and Differential Scanning Calorimetry (DSC)

Thermogravimetric analysis (TGA) was performed on the three acrylic resins to determine the thermal stability, and modulated DSC was used to determine the glass transition temperature. Sample preparation involved drying the CUP catalyst, the OH-latex and the CO<sub>2</sub>H-latex in a drying pistol under vacuum to complete dryness. Figure 9 shows the TGA plot for the three acrylic resins. The small mass loss observed for OH-

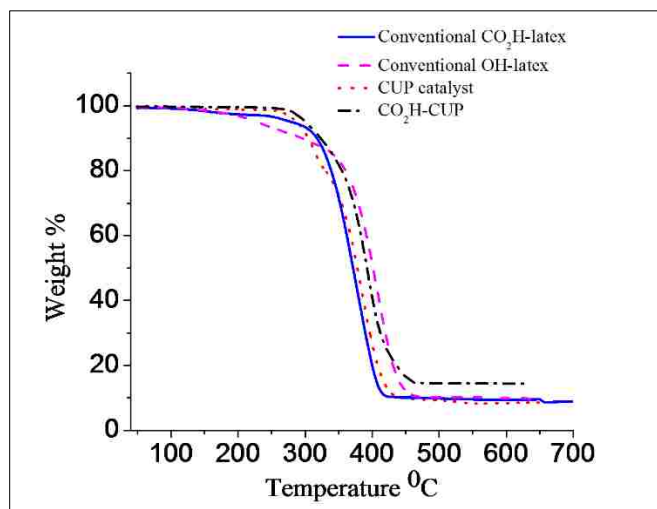
latex between 125-350 °C was possibly due to degradation via cis-elimination, producing alkene and carboxylic acid as degradation products [32]. The onset temperature at which 10% mass loss occurred was above 250 °C for all the three resins and the CUP-catalyst.

Figure 10 shows the DSC thermograms for the CUP catalyst, the OH-latex, the CO<sub>2</sub>H-latex and the CO<sub>2</sub>H-CUP. The DSC thermograms indicate a broad T<sub>g</sub> around 123 °C, 44 °C, 40 °C and 65 °C for the CUP catalyst, CO<sub>2</sub>H-latex, OH-latex and CO<sub>2</sub>H-CUP respectively. The curing reaction needs to be carried out above the T<sub>g</sub> because the polymer chains become mobile above the glass transition temperature.

Vanderhoff et al. have indicated that during the final part of latex film formation, interdiffusion of polymer chains occurs which provides the latex film with its mechanical strength [33]. Hahn et al. have studied the interdiffusion process in detail and reported that the diffusion of polymer particles decreased with increasing molecular weight of the polymer and increased with increasing temperature [34]. Steward et al., in his work on latex film formation demonstrated that smaller latex particles had faster film formation compared to larger particles, which was attributed to the shorter distance required to travel, for entanglement of polymer chains [35]. It was further reported that the diffusion process was restricted below the T<sub>g</sub> of the polymer [35].

Therefore, the CUP catalyst will be mobile and effective towards the crosslinking reaction when the temperature of the reaction is maintained above its T<sub>g</sub> but below the temperature for onset of degradation.





**Figure 9. TGA thermograms of CUP catalyst, OH-latex, CO<sub>2</sub>H-latex and CO<sub>2</sub>H-CUP**

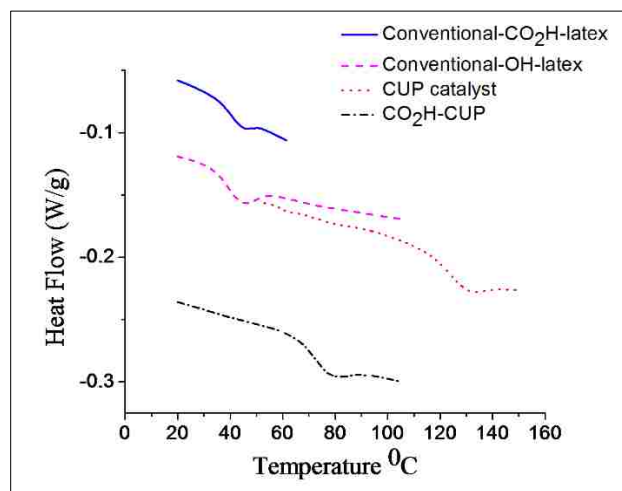


**Figure 10. Modulated DSC thermogram of CUP catalyst, OH-latex, CO<sub>2</sub>H-latex and CO<sub>2</sub>H-CUP**

### 3.6. Effectiveness of CUP Catalyst In Curing OH-latex With Melamine Resin

The amount of crosslinking resin (melamine derivative) usually varies from 5% to 30% by weight of the total resin. The amount of acid catalyst used typically varies from

0.25-1% by weight based on total resin solids for curing at normal curing temperature of about 125 - 150 °C [36]. In the present study, the acrylic: melamine ratio was chosen as 75:25 by weight of resin solids and the amount of catalyst was 0.5% wt./ wt. on total resin solids at a curing temperature of 150 °C. The catalyst amount was similar to the amount of catalyst reported in the literature for acrylic latex-melamine resin systems which was between 0.25-0.5% based on resin solids [37, 38].

The formation of crosslinks during the curing process is dependent upon the curing temperature, the curing time, the mobility of the polymer chains and the availability of the reactive groups. The pencil and the indentation hardness and the solvent resistance give an indication of the crosslinking of the acrylic OH-latex-melamine resin systems. All the acrylic-melamine resin systems gave clear, transparent films without any optical haze which indicated that the two resin systems were compatible with each other and the acid catalysts.

Pencil and indentation hardness gives a measure of the hardness of the coating. Table 5 shows a comparison of pencil and indentation hardness values for the OH-latex crosslinked with melamine resin at different cure times and also the gloss measurements at 60° measuring angle. The normal curing schedule for hydroxyl functional acrylic resins cured with melamine crosslinker with a medium degree of methylation is 30 minutes at 150 °C in presence of an acid catalyst [39]. The addition of acid catalyst to the acrylic-amine resin system improved the curing reaction of the resins which was evident by the hardness values.

**Table 5.** Hardness and gloss values at 60° for the OH-latex system at different cure times (Curing Temperature: 150 °C)

Cure time (min)	Pencil / Indentation hardness (MPa)			Gloss at 60°		
	Standard	System 1	System 2	Standard	System 1	System 2
10	B / 104.9	HB / 140.0	HB / 139.7	98.1	98.1	97.8
15	B / 107.5	F / 143.2	F / 145.8	97.7	97.8	97.0
20	B / 109.1	F / 147.6	F / 150.5	97.5	97.8	97.5
30	B / 110.7	F / 149.4	H / 153.1	98.5	98.0	97.4

The standard resin system was placed in an oven at 50 °C and tested for hardness value to establish a zero-point (hardness at zero or negligible crosslinking) for comparison. The acrylic and melamine resin were dried in-vacuo and dissolved in THF. Films were then casted on aluminum panels, placed in an oven at 50 °C until constant weight was reached (~ 60 min) and then tested for hardness and MEK rubs. The pencil and indentation hardness was 5B and 15.2 MPa respectively, while the MEK rubs was 1 which indicated zero crosslinking. After curing at 150 °C for 30 min, the Standard system showed increased hardness (110.7 MPa) due to moderate degree of crosslinking.

Two major types of reactions occur during the curing process. First is the crosslinking reaction between hydroxyl functional groups of acrylic resin and the methylol groups of melamine resin. Secondly, the melamine resins also undergo self-condensation reaction via the methylol groups. Both the reactions are accelerated by the acid catalysts [40, 41, 42]. The explanation proposed further helps to clarify the effect of these reactions on the mechanical properties of the acrylic coating.

The standard, without any catalyst, did not show any change in the pencil hardness values while the indentation hardness increased slightly as the cure time was varied from 10 minutes to 30 minutes. With the addition of acid catalyst, the pencil hardness values gradually increased from HB to H as the cure time increased from 10 min to 30 min for System 1 and System 2. With acid catalyst, both systems 1 and 2 showed much harder films than without catalyst. At 30 min curing time, the indentation hardness was significantly higher for the catalyzed reaction, both commercial (153.1 MPa) and CUP catalyst (149.4 MPa), which indicated crosslinking of acrylic resin with melamine resin.

The resin system which had the sulfonate-CUP catalyst and the one which had commercial blocked acid catalyst, both gave similar pencil and indentation hardness values which were significantly higher than that of the Standard. The increase in indentation hardness values is consistent with the findings of Larché et al. [43] and Radičević et al. [44], who reported that indentation hardness of acrylic-melamine resin systems increased with increased crosslinking.

Crosslinking reduces the molecular mobility of polymer chains between the crosslinked junctions and also increases the modulus of polymer network due to increased covalent bonding. Hence, the number of possible conformations of the polymer is reduced making the polymer more resistant to penetration [45]. The hardness values indicate that the catalyst based on CUPs of poly(MMA-co-AMPS) effectively catalyzed the curing of acrylic-melamine resins system.

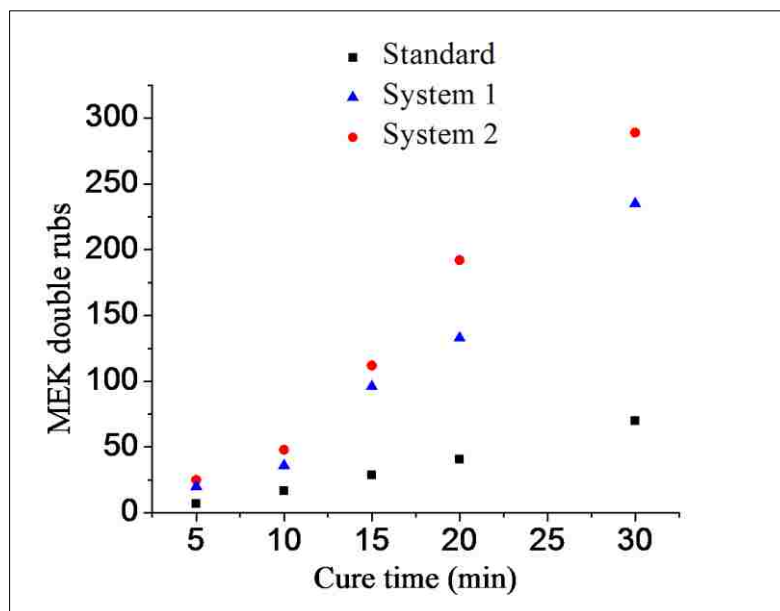


**Figure 11. MEK double rubs as a function of cure time for OH-latex cured with melamine resin at 150 °C**

MEK double-rub test gives a measure of the extent of crosslinking of the films. Figure 11 shows the effect of cure time on the MEK double rub tests for the three systems at 150 °C. The MEK solvent resistance of the coatings increased for all the three systems as the cure time was increased. An increase in the MEK double rubs for the standard indicated that the crosslinking reactions or self-condensation reactions occur to a small extent, but was significantly low compared to the MEK-rubs for the blocked acid catalyzed resin systems. At 30 minutes of cure time, the MEK double rubs exceeded 200 for both the commercial catalyst and the CUP catalyst based resin systems which indicated that both were effective catalysts.

There are two factors at play in the case of the CUP catalyst viz. the diffusion of the catalyst and the catalyst surface activity. Polymers, because of the high molecular weight, have slow diffusion rates compared to small organic molecules [46]. Winnik et al.

have shown that in simple linear polymers,  $D \propto M^{-2}$ , where  $D$  is the diffusion coefficient and  $M$  is the molecular weight [47]. The CUP catalyst, which was prepared from a copolymer of MMA and AMPS, would diffuse slower than the commercial blocked catalyst through the film. But at the same time, the CUP particles are nano-sized and all the active groups i.e. sulfonate groups are present on the surface of CUP particles which enhances the availability of CUPs towards the curing reaction. The commercial catalyst on the other hand, was based on para-toluene sulfonic acid, a low molecular weight compound which should diffuse rapidly. It should be noted that it is the proton that does the catalysis and the sulfonate is the counter ion. The separation of charges in the media is the critical factor limiting catalysis [48].

Figure 11 shows that initially, both the commercial and CUP catalyst have similar MEK double rubs. The surface availability of polymer catalyst dominates the chemistry and diffusion is still rapid enough for the CUP. At higher cure time, the diffusion effect becomes more pronounced and the MEK double rubs for CUP catalyst system was lower than the commercial catalyst system.

As seen in Figure 11, there was an onset time for the initiation of crosslinking process and development of any appreciable film properties. The CUP catalyst used was an ammonium hydroxide blocked acid catalyst. It takes time for the ammonia to volatilize and form the active sulfonic acid groups on the surface of CUP particles. The commercial acid catalyst was also a blocked catalyst and showed an onset time for crosslinking. The loss of water and achieving the temperature needed was also an early component of the delay.

### 3.7. Efficiency of CUP Catalyst In Curing OH-latex With Melamine Resin

The efficiency of the CUP catalyst in curing of the acrylic-melamine resin system was evaluated by comparing the number of molar equivalents of acid on CUP catalyst to the number of mole equivalents of acid from the commercial blocked catalyst required to provide similar mechanical properties to the final cured coating. The number of mole equivalent of acid on the CUP catalyst was  $4.16 \times 10^{-6}$  per gram of resin solids. Similarly, the number of mole equivalent of acid on the commercial blocked catalyst was  $2.91 \times 10^{-5}$  per gram of resin solids. Therefore the amount of commercial blocked-p-TSA catalyst used was seven times more than the amount of CUP catalyst. The measurements performed in this case were based on a weight by weight ratio which was chosen based on the values reported in literature.

To give a direct comparison, OH-functional acrylic resin was crosslinked with melamine resin using  $1.04 \times 10^{-5}$  number of mole equivalent of commercial acid catalyst, at 150 °C for 30 minutes and the pencil hardness and MEK double rubs were evaluated. The resulting film had a pencil hardness of B and MEK double rubs value was 20. When the same molar equivalents of CUP catalyst was used instead, the pencil hardness was H and MEK double rubs value was 225. The difference in hardness and solvent resistance indicated that the surface availability of the sulfonate groups on the CUP catalyst greatly enhance the catalytic activity toward acrylic-melamine crosslinking reaction or at least exhibited a high degree of efficacy which could be due to the sulfonic acid being in the interstitial areas which has a higher dielectric allowing greater separation of proton and sulfonate group.

### 3.8. Effectiveness of CUP Catalyst In Curing CO<sub>2</sub>H -latex and CO<sub>2</sub>H-CUP resin With Melamine Resin

The effectiveness of MMA-AMPS based CUP catalyst was compared with that of commercial blocked acid catalyst in enhancing the curing reactions of CO<sub>2</sub>H-latex and CO<sub>2</sub>H-CUP with melamine resin systems. Figure 12 shows a model for the steps involved in the crosslinking of acrylic-melamine resin. Stage I represents the acrylic-melamine resin just applied to the panel. In Stage II, water evaporated and the acrylic particles come in contact with melamine in between. Stage III represents diffusion of melamine in the latex particle and the beginning of inter-diffusion of the latex particles after which crosslinking occurs to give uniform crosslinked film as Stage IV.

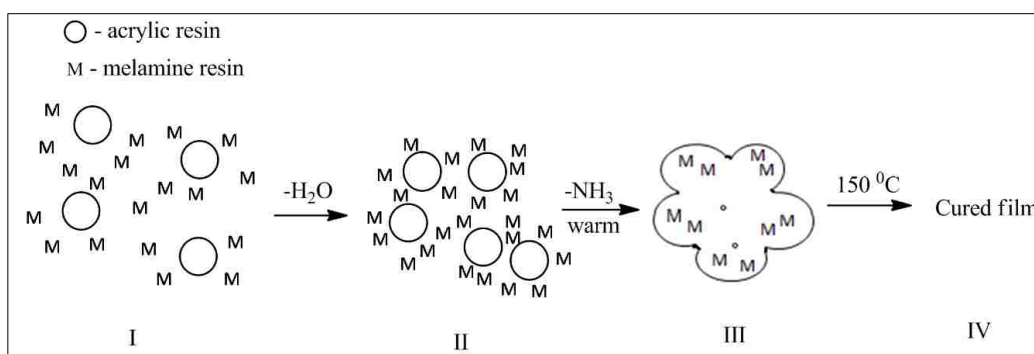


**Figure 12. A model for the stages involved in crosslinking of acrylic-melamine**

If melamine diffusion is faster than the crosslinking reaction then stage III would precede Stage IV which would give a uniform increase in hardness values because of uniform crosslinking. If crosslinking reaction occurs faster than the diffusion of melamine, then, the melamine resin would crosslink only with the surface groups of latex or CUP particle, resulting in an initial increase in the hardness value and then levelling out. For



CO<sub>2</sub>H-CUPs (4.5 nm) with all the acid groups on the surface, diffusion of melamine into the particle would not be a requirement.

The acrylic resin, the melamine resin and the blocked acid catalyst were mixed and films casted on aluminum panels. The panels were cured at 150 °C for different cure times viz. 10, 15, 20 and 30 minutes respectively. Four controls were prepared which included: A) CO<sub>2</sub>H-latex B) CO<sub>2</sub>H-latex mixed with melamine crosslinker without acid catalyst, E) CO<sub>2</sub>H-CUP and F) CO<sub>2</sub>H-CUP mixed with melamine crosslinker without catalyst. The effectiveness of acid catalysts was evaluated by measuring the pencil and indentation hardness and MEK double rub test as shown in Table 6.

**Table 6.** Pencil / Indentation hardness values for CO<sub>2</sub>H-latex and CO<sub>2</sub>H-CUP cured with melamine resin

Resin system	Pencil / Indentation (MPa) hardness values at different cure time			
	10(min)	15(min)	20(min)	30(min)
A	3B / 75.73	3B / 77.36	3B / 80.7	2B / 81.3
B	2B / 94.05	2B / 97.47	B / 98.41	B / 102.24
C	2B / 98.09	2B / 99.97	B / 101.41	HB / 104.29
D	2B / 103.92	2B / 104.20	B / 105.38	HB / 106.32
E	3B / 97.66	2B / 98.09	B / 98.35	B / 100.87
F	2B / 104.57	B / 105.62	HB / 106.30	F / 111.89
G	HB / 123.78	F / 124.34	F / 125.38	H / 126.42
H	B / 125.55	HB / 126.75	F / 127.14	H / 128.81

A- CO<sub>2</sub>H-latex, B- CO<sub>2</sub>H-latex +melamine, C- CO<sub>2</sub>H-latex + melamine+ blocked p-TSA, D- CO<sub>2</sub>H-latex +melamine+ CUP catalyst, E- CO<sub>2</sub>H-CUP, F- CO<sub>2</sub>H-CUP + melamine, G- CO<sub>2</sub>H-CUP + melamine+ blocked p-TSA, H- CO<sub>2</sub>H-CUP + melamine+ CUP catalyst

The zero-point i.e. hardness value at zero or negligible crosslinking for CO<sub>2</sub>H-latex and CO<sub>2</sub>H-CUP was determined. The acrylic and melamine resin were dried in-vacuo and dissolved in THF, films were casted on aluminum panel and placed in an oven at 50 °C until constant weight was reached (~ 60 min). The pencil and indentation hardness for CO<sub>2</sub>H-latex was 3B and 41.3 MPa and for CO<sub>2</sub>H-CUP it was 3B and 43.4 MPa respectively. For both systems, the MEK rubs were 2 which indicated negligible crosslinking. The CO<sub>2</sub>H-CUP had slightly higher hardness due to a higher T<sub>g</sub>.

Measurements at 50 °C represent hardness of control systems i.e. acrylic-melamine films that were still uncrosslinked for comparing with measurements made at 150 °C. As shown in Table 6, when curing was carried out at 150 °C for 30 min, the CO<sub>2</sub>H-latex+melamine and CO<sub>2</sub>H-CUP+melamine systems showed increased hardness of 102.24 (system B) and 111.89 MPa (system F) respectively, which was possibly due to some crosslinking reaction catalyzed by the carboxylic acid on the acrylic resin. It should also be noted that the melamine resin also plays the role of a reactive diluent or a plasticizer for the acrylic resins [20].

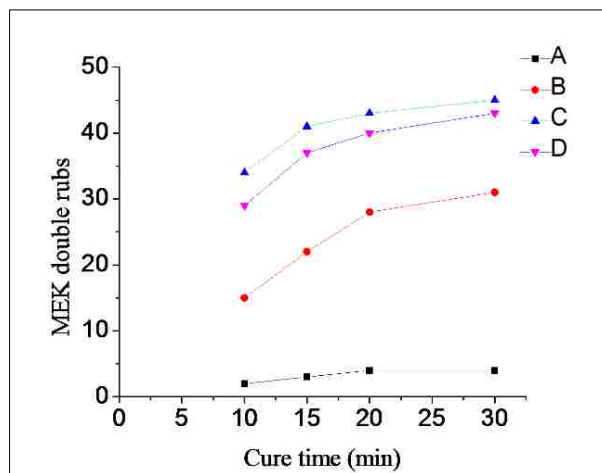
Table 6 also indicated that the CO<sub>2</sub>H-latex without crosslinker had low pencil and indentation hardness (system A). The addition of the melamine crosslinker (system B) improved the hardness as the carboxyl groups of CO<sub>2</sub>H-latex reacted with the methoxy groups on the melamine resin to give crosslinked films. The addition of the blocked acid catalyst further improved the pencil hardness slightly (systems C and D). The pencil hardness values obtained for the system with sulfonate-CUP catalyst were slightly better than that of commercial blocked p-TSA catalyst indicating that sulfonate-CUP-catalyst could be as effective as the commercial blocked p-TSA catalyst. The indentation hardness values corroborate the observed behavior.

The difference in the indentation hardness value of the un-catalyzed and catalyzed system (both commercial catalyst and CUP-catalyst) at each cure time was similar for both CO<sub>2</sub>H-latex and CO<sub>2</sub>H-CUP. For example: At 30 min. cure time, the difference in indentation hardness of CO<sub>2</sub>H-latex systems 'A' & 'D' was 25 MPa and for CO<sub>2</sub>H-CUP systems 'E' & 'F' it was 28 MPa. The similar change of hardness values indicated that crosslinking between acid groups and melamine resin occurred after the melamine resin diffused in to the acrylic resin particles which showed that the melamine resin was compatible with the acrylic resins and its diffusion was rapid.

For identical curing temperature and curing time, the indentation hardness value of all formulations based on CO<sub>2</sub>H -CUP resins was higher as compared to CO<sub>2</sub>H -latex (system: E v/s A, F v/s B, G v/s C and H v/s D). The higher hardness was mainly attributed to the higher T<sub>g</sub> of the CO<sub>2</sub>H-CUP because, the higher the T<sub>g</sub>, the harder the polymer [49]. The molecular weight of the resin could also have contributed slightly to the observed hardness values. Typically, other properties being identical, the higher the molecular weight of polymer below its T<sub>g</sub>, the higher is its hardness [50]. Bas et al. also indicated that smaller particle size of latex resin results in well integrated film and therefore, better crosslinking and hardness properties [51].

The CO<sub>2</sub>H-latex had higher molecular weight (78,000) than CO<sub>2</sub>H-CUP (50,000) but a very large particle size (95 nm) as compared to smaller particle size of the CUP resin (4.5 nm) and the two effects possibly cancelled out. So, the CO<sub>2</sub>H-CUP resin gave higher pencil and indentation hardness than CO<sub>2</sub>H-latex when crosslinked with melamine resin. Though the acid groups on the acrylic resin act as a catalyst for the crosslinking reactions, the addition of the commercial blocked acid catalysts as well as the CUP catalyst enhanced the coating performance. The effect of the particle size of the acrylic resin and the addition

of an external blocked acid catalyst on the mechanical properties of crosslinked coatings was also corroborated by the MEK double rub tests.



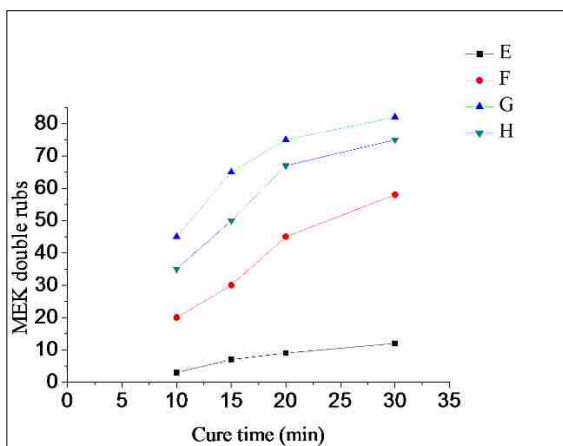
**Figure 13. MEK double rubs against cure time for CO<sub>2</sub>H-latex cured with melamine resin**

Figure 13 and Figure 14 show the MEK double rubs for the CO<sub>2</sub>H-latex and CO<sub>2</sub>H-CUP cured with melamine, respectively. The solvent resistance of the acrylic latex crosslinked with melamine resin was very low. The addition of blocked acid catalysts increased the solvent resistance slightly as compared to the acrylic latex-melamine resin with no catalyst. The solvent resistance of the CO<sub>2</sub>H-CUP cured with melamine was better than that of the CO<sub>2</sub>H-latex -melamine resin system. A small value of the MEK double rub test for the CO<sub>2</sub>H-latex -melamine resin system indicated that the acrylic latex did not crosslink with the melamine to any significant extent.

The CO<sub>2</sub>H-CUP resin crosslinked with melamine gave excellent solvent resistance which was a result of the better availability of the reactive groups on the surface of the

CO<sub>2</sub>H-CUP resin as compared to CO<sub>2</sub>H-latex where only a fraction of the reactive groups are on the surface. Also, CO<sub>2</sub>H-latex had a higher molecular weight (65,000), while CO<sub>2</sub>H-CUP was based on a lower molecular weight of 49,000. For linear polymers, the (diffusion coefficient)  $D \propto M^{-2}$  (molecular weight of polymer) [47] and hence, the diffusion was possibly better in the case of CUPs as compared to latex resins which increased the crosslink efficacy.

The solvent resistance improved with addition of commercial blocked acid catalysts as well as the CUP catalyst based on MMA-AMPS copolymer. Compared to the CO<sub>2</sub>H-latex, the OH-latex (Figure 11) showed much better solvent resistance and pencil and indentation hardness when crosslinked with melamine resin. The result was in agreement with a study reported by Teng et al., where the carboxylic acid groups acted as a barrier to polymer chains due to electrostatic repulsion, thus limiting the extent of polymer chain interdiffusion and lowering the mechanical properties [52].



**Figure 14. MEK double rubs against cure time for CO<sub>2</sub>H-CUP cured with melamine**

Indentation using the ESP (Enhanced Stiffness Procedure) method was performed to determine the depth profile of the hardness and the elastic modulus of the OH-latex, CO<sub>2</sub>H-latex and CO<sub>2</sub>H-CUP resin systems. The depth profile for all the three resin systems was similar and representative plots of elastic modulus and hardness for OH-latex system are indicated in Figures 15 and 16 respectively.

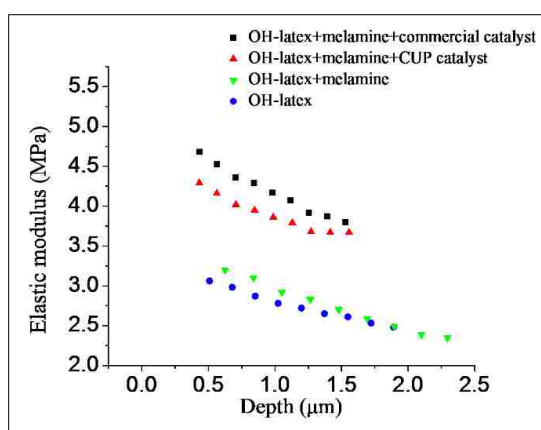


**Figure 15. Elastic modulus vs indentation depth for formulations based on OH-latex**

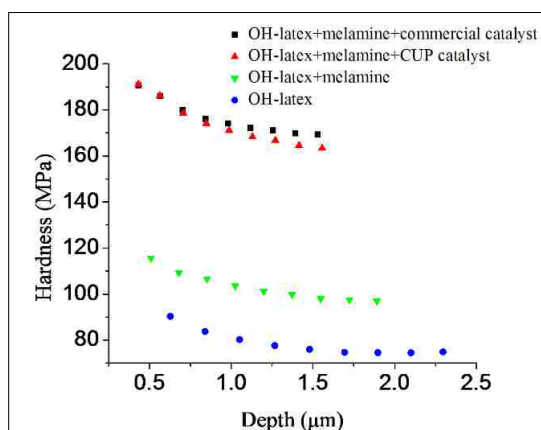


**Figure 16. Indentation Hardness vs indentation depth for formulations based on OH-latex**

ESP method shows that the hardness and elastic modulus increased with addition of acid catalyst which indicated higher crosslinking [53- 55]. Elastic modulus and hardness for the formulations of all three resin systems decreased with increasing contact depth. For the coated aluminum test panel placed in the oven, the temperature is maximum at the surface of the film and at the film-panel interface, since the panel is in contact with the oven. For blocked commercial catalyst and the blocked CUP catalyst to become active, the blocking agent ammonia, has to be removed from the film.

The loss of ammonia occurs from the film's surface, therefore the catalyst at the surface is activated first and the crosslinking chemistry starts at the surface. The diffusion of reactants is reduced which slows down the removal of ammonia. At the film-panel interface, though the temperature is high enough to volatilize the ammonia, the catalyst remains inactive until the ammonia is diffused to the surface and removed. Hence, the hardness and modulus are maximum at the surface and decrease with the indentation depth.

The low molecular weight, commercial acid catalyst based resin system displayed slightly higher hardness value because it would have higher mobility than the high molecular weight polymeric CUP catalyst. Even at maximum indentation depth, the addition of acid catalyst (commercial or CUP catalyst) to acrylic-melamine system considerably increased the hardness and modulus values as compared to non-catalyzed systems which is due to the crosslinking of the acrylic-melamine resin system.

### **3.9. Leaching Experiment**

It was hypothesized that the commercial blocked acid catalyst, being water-soluble, would leach out in water from the cured acrylic-melamine film while the CUP catalyst being water-insoluble and likely covalently linked would not. In order to evaluate the

hypothesis, OH-latex acrylic-melamine films were coated on two aluminum foils and cured at 150 °C for 30 min; one with commercial blocked p-TSA catalyst and the other with the CUP catalyst. The two foils were put in Soxhlet extractors containing water and leached for 24 hrs. All the solvent (water) was removed in-vacuo and the residue was characterized using NMR. In case of commercial blocked acid catalyst, 0.0320 g leached out of 0.9172 g of polymer and for CUP catalyst system, 0.0214 g leached out of 0.9368 g of polymer film.

Figure 17 shows the NMR spectra of the acrylic latex, melamine resin, commercial p-TSA catalyst, CUP catalyst, residue of commercial acid catalyzed film and residue of CUP catalyzed film. The commercial catalyst, OH-latex and melamine being proprietary compounds, not all of the absorption peaks could be accurately identified.

For the commercial acid catalyst, peak at 2.4 ppm was assigned to  $-\text{CH}_3$  (methyl) group and peaks at 7.2 ppm and 7.7 ppm were assigned to hydrogen atoms on the aromatic ring. For the melamine resin, the peak at 2.1 ppm corresponded to methylol hydrogen, the peak at 3.4 ppm corresponded to  $(-\text{OCH}_3)$  methoxy group and the peak at 5.1 ppm corresponded to  $(-\text{CH}_2)$  methylene proton adjacent to nitrogen of melamine resin. The peaks in the NMR spectrum of the residue of acrylic-melamine resin cured with the commercial catalyst could be related to the NMR spectra of the acrylic latex, melamine resin and commercial catalyst and corresponded to the water-soluble components (peaks at 2.1 ppm, 2.4 ppm, 2.9 ppm, 7.2 ppm and 7.7 ppm). The two peaks at 7.2 ppm and 7.7 ppm were characteristic of p-TSA of the commercial acid catalyzed film and indicated that the commercial acid catalyst leached out during the Soxhlet extraction process.

In the NMR spectra of the CUP catalyst, the peaks between 0.8 and 1.5 ppm were assigned to  $(-\text{CH}_3)$ ,  $(-\text{CH}_2)$  and  $(-\text{CH})$  groups on the MMA-AMPS copolymer backbone,



the peak at 2.0 ppm was assigned to the methylene group closest to sulfonic acid and the peak at 3.6 ppm was assigned to hydrogen on the (-OCH<sub>3</sub>) methoxy group. The peak at 2.1 ppm corresponded to the peak observed in melamine resin which was water-soluble. Absence of any peak at 3.6 ppm in the NMR of residue from the CUP catalyzed film indicated that the CUP catalyst was incorporated in the acrylic-melamine film possibly due to some of the ester groups on the polymeric catalyst reacting with melamine resin and hence did not leach out of the film.

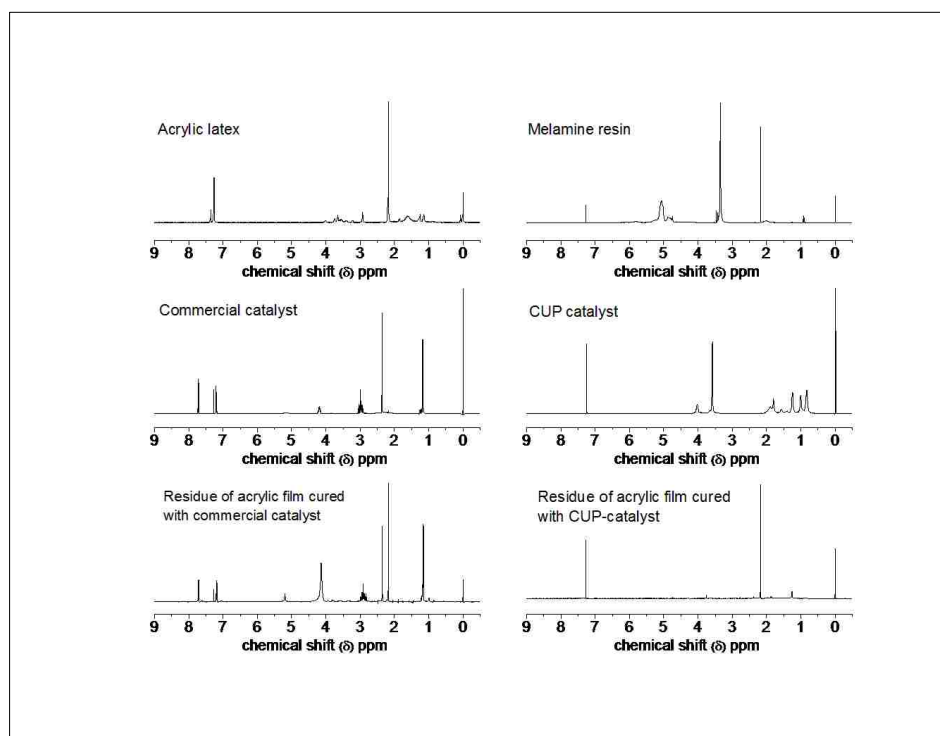


**Figure 17. NMR spectra of acrylic latex, melamine resin, blocked p-TSA, CUP catalyst, residue of acrylic film cured with blocked p-TSA and residue of acrylic film crosslinked with CUP catalyst**

#### 4. CONCLUSIONS

Colloidal unimolecular polymer particles (CUPs) based on poly (MMA-co-AMPS) were successfully prepared by the process of water-reduction and subsequent solvent removal. Dynamic light scattering analysis confirmed the true-nano size of the CUPs with a mean particle diameter of 5.9 nm. Unlike CUPs based on methacrylic acid monomer, the CUPs based on sulfonic acid functional monomer are able to undergo water-reduction process without any visible coagulum or polymer precipitation in the presence of 50 ppm of calcium ions. The CUPs with sulfonate groups on the surface prove to be effective as acid catalysts for curing of acrylic-melamine resin systems and promote the curing reactions for both the hydroxyl functional as well as carboxyl functional acrylic resins with melamine resin. DSC and TGA thermograms indicated that the curing temperature was higher than the glass temperature for all the acrylic resins which improved the mobility and the diffusion of polymer acid catalyst to the crosslinking site. CUP catalyst was more efficient than the p-TSA blocked catalyst based on the actual mole equivalents required, providing excellent properties to the final cured films. The CO<sub>2</sub>H -CUPs displayed better film properties compared to CO<sub>2</sub>H -latex because of the smaller particle size which resulted in better availability of reactive groups and better coalescence. Unlike conventional water reducible resins, CUP solutions are free of surfactant and are zero-VOC, offering a potentially high performance technology option for future OEM coatings applications.

## 5. ACKNOWLEDGEMENTS

The authors would like to acknowledge the Coatings Institute and the Department of Chemistry of Missouri S&T for the financial support and resources. We thank Dr. Nicholas Leventis of Missouri S&T University and his student Dhairyashil Mohite for measuring the density of the dry copolymer and thank our fellow researchers: Cynthia Riddles, Minghang Chen, Jigar Mistry, Sagar Gade, and Catherine Hancock for their help.

## 6. REFERENCES

- [1] G. Riess, *Prog. Polym. Sci.* 28 (2003) 1107-1170.
- [2] A.V. Kabanov, E.V. Batrakova, N.S. Melik-Nubarov, N.A. Fedoseev, T.Y. Dorodnich, V.Y. Alakhov, V.P. Chekhonin, I.R. Nazarova and V.A. Kabanov, *J. Control. Rel.*, 22 (1992) 141-157
- [3] K. Kataoka, G. Kwon, M. Yokoyama, T. Okano and Y. Sakurai, *J. Control. Rel.*, 24 (1993) 119-132
- [4] J. Guo, S. Farrell and K.E. Uhrich, *Mat. Res. Soc. Symp. Proc.*, 550 (1999) 89-94
- [5] H. Liu, A. Jiang, J. Guo and K.E. Uhrich, *J. Polym. Sci. A Poly. Chem.*, 37 (1999) 703-711
- [6] Y. Morishima, S. Nomura, T. Ikeda, M. Seki and M. Kamachi, *Macromolecules* 28 (1995) 2874-2881.
- [7] H. Liu, A. Jiang, J. Guo and K. E. Uhrich, *J. Polym. Sci., Part A: Polym. Chem.*, 37 (1999) 703-711.
- [8] J. Selb and Y. Gallot, *Die Makromolekulare Chemie*, 181 (1980) 809-822.
- [9] C. J. Riddles, W. Zhao, H. Hu, M. Chen and M. R. Van De Mark.; *Polymer*, 55 (2014) 48-57.
- [10] M. R. Van De Mark, A. M. Natu, S. V. Gade, M. Chen, C. Hancock and C. J. Riddles, *J. Coat. Technol. Res.*, 11 (2) (2014) 111-122.
- [11] J. O. Santer, *Prog. Org. Coat.* 12 (1984) 309-320.
- [12] B. Müller and U. Poth, *Coatings Formulation: An International Textbook*, 2<sup>nd</sup> revised edition, Vincentz Network, GmbH and Co., Germany (2011).

- [13] Z. W. Wicks, Jr., F. J. Jones and S. P. Pappas, *Organic Coatings: Science and Technology*, Vol 1, Wiley-Interscience, New York (1992).
- [14] D. Bauer, *Prog. Org. Coat.*, 14 (1986) 193-218.
- [15] M. Chen and M. R. Van De Mark, *Polym. Prepr. (Am. Chem. Soc., Div. Polym. Chem.)*, 52 (2011) 336-337.
- [16] Z. W. Wicks and B. W. Kostyk, *J. Coat. Technol.*, 49 (634) (1977) 77-84.
- [17] G. Tillet, B. Boutevin and B. Ameduri, *Prog. Polym. Sci.*, 36 (2011) 191-217.
- [18] J. K. Mistry, A. M. Natu and M. R. Van De Mark, *J. Appl. Polym. Sci.*, 131 (2014) 40916 doi:10.1002/app.40916.
- [19] J. V. Koleske, *Paint and Coating Testing Manual: 14<sup>th</sup> Edition of the Gardner Sward Handbook* (1995) Chapter 48 555-584.
- [20] W. C. Oliver and G. M. Pharr, *J. Mater. Res.*, 7 (1992) 1564-1583.
- [21] A. A. Maryott and E. R. Smith, *Table of Dielectric Constants of Pure Liquids*, NBS Circular 514 (1951)
- [22] M. Mohsen-Nia, H. Amiri and B. Jazi, *J. Solution. Chem.*, 39 (2010) 701-708.
- [23] M. Chen, C. J. Riddles and M. R. Van De Mark, *Langmuir*, 29 (2013) 14034-14043.
- [24] R. Hidalgo-Álvarez, A. Martín, A. Fernández, D. Bastos, F. Martínez and F. J. de las Nieves, *Adv. Colloid Interf. Sci.*, 67 (1996) 1-118.
- [25] P. C. Hiemenz and R. Rajagopalan, *Principles of Colloid and Surface Chemistry*, 3<sup>rd</sup> edition, Marcel Dekker, New York, (1997).
- [26] M. Chen, C. J. Riddles and M. R. Van De Mark, *Colloid Polym. Sci.*, 291 (2013) 2893-2901.
- [27] J. Goodwin, *Colloids and Interfaces with Surfactants and Polymers*, 2<sup>nd</sup> edition, John Wiley & Sons Ltd., (2009).
- [28] H-F. Eicke and G. D. Parfitt, *Interfacial Phenomena in Apolar Media*, Surfactant science series; 21, Marcel Dekker Inc. 1987.
- [29] C. L. McCormick and D. L. Elliot, *Macromolecules*, 19 (1986) 542-547.
- [30] I. Sabbagh and M. Delsanti, *Eur. Phys. J. E* 1 (2000)75-86.
- [31] R. C. Wilson and W. F. Pfohl, *Vib. Spectrosc.* 23 (2000) 13-22.
- [32] J. W. Vanderhoff, E. B. Bradford and W. K. Carrington, *J. Polym. Sci.: Symp. No.* 41, (1973) 155.
- [33] K. Hahn, G. Ley and R. Oberthur, *Colloid and Polym. Sci.*, 266 (1988) 631-639.
- [34] P. A. Steward, J. Hearn and M. C. Wilkinson, *Adv. Colloid Interf. Sci.*, 86 (2000) 195-267.
- [35] W. Funke, 'Surface Coatings Vol. I Raw Materials and Their Usage', Oil and Color Chemist's Association, Chapman and Hall, 1983.
- [36] F. N. Jones, G. Chu and U. Samaraweera, *Prog. Org. Coat.*, 24 (1994) 189-208.

- [37] D. A. Borovicka Sr., United States Patent: 4608410 (1986).
- [38] P. K. T. Oldring and G. Hayward, Resins for Surface Coatings, Vol II, SITA Technology Ltd, London, England, 1987.
- [39] D. R. Bauer, Prog. Org. Coat., 14 (1986) 193-218.
- [40] J. O. Santer, Prog. Org. Coat., 12 (1984) 309-320.
- [41] J. N. Koral and J. C. Petropoulos, Journal of Paint Technology 28 (1966) 600-609.
- [42] J. F. Larché, P. O. Bussière, P. Wong-Wah-Chung and J. L. Gardette, Eur. Polym. J., 48 (2012) 172-182.
- [43] R. Ž. Radičević and J. K. Budinski-Simendić, J. Serb. Chem. Soc., 70 (2005) 593-599.
- [44] F. Li and R. Larock, J. Polym. Sci. B Polym. Phys., 39 (2001) 60-77.
- [45] M. A. Winnik, Journal of Coatings Technology, 74 (2002) 49-63.
- [46] M. A. Winnik, A. Pinenq, C. Kruger, J. Zhang and P. V. Yaneff, Journal of Coatings Technology, 71 (1997) 47-60.
- [47] F. H. Westheimer, H. Frank and A. W. Jones, J. Amer. Chem. Soc., 63 (1941) 3283-3286.
- [48] S. Fakirov, F. J. Baltá Calleja and M. Krumova, J. Polym. Sci. B, Poly. Phys., 37 (1999) 1413-1419.
- [49] J. P. Harrington, Spe/Antec Proceedings, CRC Press 1<sup>st</sup> Edition 1997.
- [50] S. Bas and M. D. Soucek, React. Funct. Polym., 73 (2013) 291-302.
- [51] G. Teng, M. D. Soucek, X. F. Yang and D. E. Tallman, J. Appl. Polym. Sci., 88 (2003)245-257.
- [52] E. Wornyo, K. Gall, F. Yang and W. King, Polymer, 48 (2007) 3213-3225.
- [53] T. H. Fang and W. J. Chang, Microelectronic Journal 35 (2004) 595-599.
- [54] W. Shen, J. Sun, Z. Liu, W. Mao, J. D. Nordstorm, P. D. Ziemer and F. N. Jones, J Coat. Technol. Res., 1 (2004) 117-125.

### III. SYNTHESIS AND CHARACTERIZATION OF CATIONIC COLLOIDAL UNIMOLECULAR POLYMER PARTICLES (CUPS)

Ameya M. Natu, Marcus Wiggins and Michael R. Van De Mark\*

Department of Chemistry, Missouri S&T Coatings Institute,  
Missouri University of Science & Technology, Rolla, MO 65409

#### ABSTRACT

Due to the limitation of experimental techniques, the preparation of stable, surfactant free cationic colloidal dispersions with true nano-scale particle diameter (3-9 nm) has been a major challenge. By using low concentration of the cationic functional copolymers during water-reduction, it should be possible to achieve unimolecular collapse of a polymer chain to a spherical particle with charged quaternary ammonium groups on the surface providing stability via electrostatic repulsion. Water-reduction was carried out at dilute polymer concentration in methanol (10% by weight) to obtain colloidal unimolecular polymer particles (CUPs). The cationic CUP systems were evaluated for the basic physical properties such as rheology and static and dynamic surface tension using a capillary viscometer and maximum bubble pressure surface tensiometer, respectively. True nano-scale (diameter 3-9 nm), zero-volatile organic content (VOC), spheroidal CUP particles with cationic groups on the surface were obtained. The experimental viscosity, which was influenced by the electroviscous effects arising from the surface charge and the associated surface water layer, increased with the increasing concentration and molecular weight (MW) of CUPs. The density of surface water was 1.6% greater than the bulk water density which was possibly due to the structuring of water around charged quaternary ammonium groups. The equilibrium surface tension values decreased linearly with increasing concentration and surface charge density of CUP particles due to a greater

reduction in surface energy. The rate of surface tension reduction decreased with increasing molecular weight of the CUP due to diffusion effects.

### **Keywords**

Cationic, colloidal, nanoparticle, water-reduction, rheology, surface tension, surface-water.

## **1. INTRODUCTION**

Cationic colloids have received considerable attention because of the applications such as flocculants in mining, water-filtration, and sewage treatment, as antimicrobial agents and in drug delivery systems [1-5]. Researchers have devoted their time and efforts to study the physical and chemical properties of cationic polyelectrolytes because of the potential to shed light on the fundamental properties of proteins, nucleic acids etc. [6]

However, most studies have focused on nanoparticle synthesis via self-aggregation of well-defined amphiphilic block copolymers [7]. Synthesis of particles with true nano-scale size (<10 nm) has been a challenge due to the aggregation of the hydrophobic part of multiple polymer chains [8]. Ramos et al. [9] reported an excellent review on aqueous cationic polymer nanoparticles, but the particle size was greater than 25 nm due to aggregation and it was difficult to determine the effect of surface water associated with the charged particles due to presence of additives like emulsifiers, surfactants and rheology modifiers in the system. Sun et al. [10] demonstrated that quaternary ammonium functional oligomers in water self-assembled via hydrophobic aggregation to form spherical vesicles with an average size of 50 nm and displayed surface activity. The present study describes

a facile route to achieve stable, cationic aqueous polymer dispersions with controllable particle size in the true nano-scale region (3-9 nm) and free of any additive, prepared via water-reduction of amphiphilic acrylic random copolymers synthesized using simple free radical polymerization technique.

By the process of water-reduction of anionic carboxylate-functional copolymers; aqueous, surfactant free, nano-particle dispersions with negative charge on the spherical particles have been developed and termed as Colloidal Unimolecular Polymer particles (CUPs) [11, 12]. CUPs are formed as a result of hydrophobic/hydrophilic interactions of the polymer with a change in solvent environment. The collapse of individual polymer chains to form CUPs is driven by the polymer-polymer interactions being greater than polymer-solvent interactions and entropically favored by the release of water on the surface of polymer chain. Methacrylic acid based copolymers with molecular weight (MW) in the range of 13,000 to 155,000 have been successfully reduced to form CUPs and polymers with MW less than 13,000 gave some aggregation due to an insufficient number of stabilizing groups [13].

The cationic copolymer used for CUP synthesis was composed of hydrophobic methyl methacrylate and cationic [2-(methacryloyloxy)ethyl] trimethylammonium chloride (QUAT) monomers. Figure 1 shows the structure of the two monomers utilized for the copolymer synthesis. Figure 2 shows the process of CUP particle formation with the hydrophilic quaternary ammonium groups on the surface of the CUP particle and the hydrophobic groups forming the core of the spheroidal particle.



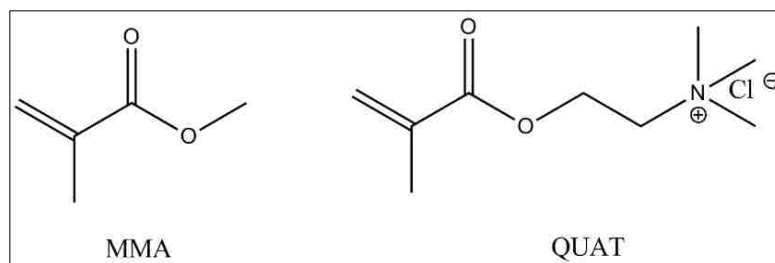


**Figure 1. Monomer structure**

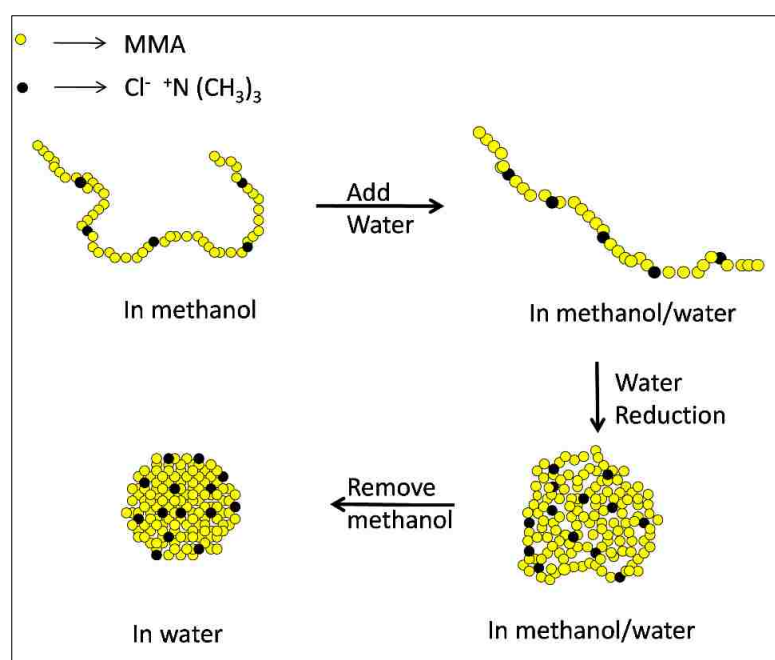


**Figure 2. CUP formation process**

The CUP suspension is an excellent model material to study the behavior of biomacromolecules like proteins and viruses. CUPs offer distinct advantages over typical polyelectrolytes which includes thermodynamic stability, easy preparation and cost-effectiveness. Because of the potential applications ranging from flocculants to drug delivery, it is necessary to study and understand the important physical properties such as

rheology and surface tension of CUPs. As CUP solutions are free of any additive, the observed rheology behavior of CUPs can be directly correlated with the electroviscous effects, the effective surface charges, the associated water fraction and the surface water thickness.

In a previous report, the rheological behavior of carboxylate ( $\text{CO}_2^-$ ) functional CUPs in the dilute region (volume fraction  $< 0.10$ ) was shown to be dominated by the tertiary electroviscous effects [14]. The thickness of surface water layer was significant as compared to the diameter of CUP particles [15]. In the present study, the rheology and surface tension behavior of cationic quaternary ammonium functional CUPs in relation to the anionic carboxylate functional CUPs and the effect of surface charge density and concentration of CUP particles on its equilibrium and dynamic surface tension were determined. The associated water fraction and the thickness of the surface water layer were determined based on their relationship with the intrinsic viscosity of the system. The intrinsic viscosity was further determined from the relation of relative viscosity with the volume fraction.

Equilibrium surface tension measurement indicate the effectiveness of CUPs in lowering the surface tension of air-water interface at equilibrium condition and is governed by the thermodynamics of the CUP at the interface. Dynamic surface tension (DST) is controlled by the diffusion / kinetics of CUP to the interface and is important because it gives information on the rate of movement of CUP particles to the air-water interface providing insights on the adsorption mechanism. DST gives better correlation to actual applications because many processes such as spraying, printing, foaming or coating occur under dynamic conditions [16].

## 2. THEORETICAL BASIS FOR RHEOLOGY BEHAVIOR

For a dilute suspension of non-charged spherical particles, the specific viscosity of the suspension can be expressed by Einstein's model [17], equation 1.

$$\eta_{sp} = 2.5 * \phi \quad (1)$$

Where,  $\eta_{sp}$  is the specific viscosity of suspension and  $\phi$  is the volume fraction of particles in the solution. For charged particles, the electroviscous effects must be considered.

### 2.1. Primary Electroviscous Effect

The primary electroviscous effect results from the distortion of a fluid stream near charged spheres. The contribution of primary electroviscous effect to the suspension rheology decreases with increasing concentration of the charged particles in the system which is attributed to the effect of counter-ion condensation [18].

### 2.2. Secondary Electroviscous Effect

When the particle concentration is low, the primary electroviscous effect dominates because very little to no secondary electroviscous effect is present. At some concentration, depending on the solvent and surface charge of the particle, the electrical double layers will feel each other, making the suspension structured, which leads to an increase in viscosity and is known as the secondary electroviscous effect. The contribution of the secondary electroviscous effect to the viscosity of the suspension is proportional to the square of the volume fraction and is negligible until the interparticle distance approaches the effective collision diameter of CUP particles [19].

### 2.3. Tertiary Electroviscous Effect

Typically, the expansion or contraction of particles due to the change in conformation, especially of polyelectrolytes, gives rise to the tertiary electroviscous effect [20, 21]. For rigid spheres, the change of radius will be possibly due to adsorption of surfactant or polyelectrolyte to its surface, or a structured water layer. For the CUP suspension, which is free of surfactant and added electrolyte, the tertiary electroviscous effect could only arise from a structured water layer on the surface of the particle. Assuming that water forms homogeneous layer with thickness  $\delta$  on the surface of the CUP particle, the effective volume fraction  $\Phi_{eff}$  can be calculated as equation 2.

$$\Phi_{eff} = \phi \left( 1 + \left( \frac{\delta}{R_S} \right) \right)^3 \quad (2)$$

### 2.4. Determination of Intrinsic Viscosity of CUPs

The associated water layer on the surface of cationic CUPs can significantly enhance the viscosity which would have implications on the use of cationic CUPs as rheology modifiers. Therefore, it was important to determine the bound water fraction and surface water thickness of the cationic CUPs. Oncley [22] has shown that the bound water fraction and the thickness of water layer on the surface of protein could be determined from the intrinsic viscosity of the suspension, and the same method was used for CUPs.

The intrinsic viscosity of uncharged polymer is typically determined by extrapolating the reduced viscosity to infinite dilution. But there is no general method to determine the intrinsic viscosity of polyelectrolyte solution without added electrolyte. In many cases, the reduced viscosity of polyelectrolytes does not approach a set value when the concentration is dilute. Many methods have been attempted to determine the value of

intrinsic viscosity. One of them was derived from the relationship of the relative viscosity ( $\eta_{rel}$ ) with the volume fraction ( $\phi$ ) at dilute concentration and expressed as equation 3 [23].

$$\ln(\eta_{rel}) = [\eta]_{\phi}\phi \quad (3)$$

Where,  $[\eta]_{\phi}$  is the intrinsic viscosity in terms of volume fraction.

### 3. MATERIALS AND METHODS

#### 3.1. Materials

[2-(methacryloyloxy)ethyl]trimethylammonium chloride (QUAT), methyl methacrylate (MMA), 2,2'-azobis (2-methylpropionitrile) (AIBN), methanol and 1-butanethiol were purchased from Aldrich. Absolute anhydrous ethanol was purchased from PHARMCO-AAPER and used as supplied. Inhibitors in MMA were removed by washing with 10% aqueous solution of sodium bicarbonate ( $\text{NaHCO}_3$ ), distilled water and brine solution respectively, then dried over anhydrous magnesium sulfate and further purified by distillation. QUAT was purified twice by precipitation into acetone. The purified monomer was dried in a vacuum oven at 45 °C until a constant weight was obtained and then stored in a desiccator at 5 °C. AIBN was re-crystallized from methanol prior to use and n-butanethiol was used as received.

#### 3.2. Polymer Synthesis and Characterization

Copolymers of MMA and QUAT were prepared in a 3-neck flask equipped with a thermometer, a nitrogen inlet and a condenser fitted with a bubble tower to maintain a positive pressure in the system. MMA (0.81 moles, 81.3 g) and QUAT (0.09 moles, 18.7

g) monomers were charged into the flask in a molar ratio of 9:1 along with the solvent absolute ethanol (250 gram) and n-butanethiol (amount determined by the target molecular weight of the polymer) as the chain transfer agent. AIBN (0.00073 moles, 0.12 gram) was used as the free radical initiator and the polymerization reaction was carried out under refluxing conditions for 24 hrs. The polymerization process was similar to that reported in the literature for MMA-QUAT solution copolymerization [24].

The polymer solution was then cooled to room temperature and precipitated in cold de-ionized water under high shear and then filtered. For further purification, the polymer was re-dissolved in ethanol and precipitated in cold deionized water under high shear to remove the unreacted QUAT monomer as it was water-soluble. The traces of un-reacted MMA and ethanol were removed in-vacuum. The polymers were thoroughly dried using a freeze-drier. Polymers with different molecular weights were synthesized by controlling the amount of chain transfer agent n-butanethiol (0.20, 0.14 and 0.10 g for poly-1, poly-2 and poly-3 respectively).

The  $^1\text{H-NMR}$  spectra was recorded on a 400 MHz Varian FT/NMR spectrometer. The density of the dry polymer was measured by a gas displacement pycnometer: Micromeritics AccuPycII 1340. Volume of sample can be calculated as equation 4.

$$V_s = V_c + V_r / \left(1 - \frac{P_1}{P_2}\right) \quad (4)$$

Where,  $V_s$  is the sample volume,  $V_c$  is the volume of the empty sample chamber,  $V_r$  is the volume of the reference volume,  $P_1$  is the first pressure (i.e. in the sample chamber only) and  $P_2$  is the second (lower) pressure after expansion of the gas into the combined volumes of sample chamber and reference chamber. Equilibrium flow rate of Helium gas was

0.005psig/min, temperature was controlled at  $25.89\pm 0.04$  °C. Twenty five readings were made for each sample, and the results were reported by its average and standard deviation.

### **3.3. Water-reduction**

The purified and dry acrylic copolymers were dissolved in dry and distilled methanol, a low boiling and water miscible solvent. The polymer was stirred overnight for complete dissolution of polymer chains. Deionized water was then added to the polymer solution by a peristaltic pump at a rate of about 1.24g/minute. Methanol was then stripped off under vacuum to give CUPs in VOC free aqueous solution. The CUP solutions were then filtered through 0.45 $\mu$ m Millipore membrane to remove any impurities. Water reduction process-Poly-1 (MW=36K): 10 g of poly (MMA-co-QUAT) was dissolved in 90g of methanol to prepare a 10% w/w solution. Then 190 gram of deionized water was added by means of a peristaltic pump. The methanol was then completely stripped off in-vacuum and the sample was further concentrated by stripping off water to give a 10% w/w CUP solution of poly (MMA-co-QUAT) in water.

### **3.4. Particle Size and Distribution of CUPs**

Particle size of CUPs was measured by a dynamic light scattering technique, using the Microtrac Nanotrac 250. The DLS works on the principle of Brownian diffusion, where the scattered light is Doppler shifted corresponding to the diffusion of suspended particles. The viscosity of the solution was used instead of water to account for the change in diffusion coefficient due to the viscosity increase caused by the charged groups on the surface of CUP particles [12].

### 3.5. Absolute Viscosity of CUPs

The CUP solutions were tested for shear rate dependency of the viscosity on a Brookfield LV DVIII viscometer, using 1ml of sample for each run. After each run, the CUP sample was diluted with Milli-Q ultrapure water to the next concentration. The solutions were run from 10 to 1% and also at 0.5%.

The absolute viscosity of CUP suspension was measured using an Ubbelohde capillary viscometer maintained at  $25.0 \pm 0.1$  °C using a constant temperature water bath. The suspensions were equilibrated for 30 minutes. Evaporation and CO<sub>2</sub> contamination was avoided by covering the viscometer with a plastic wrap. A stop watch with 0.01 second precision was used to monitor the elution time. The estimated standard error was within 0.5%. Absolute viscosity was calculated by equation 5.

$$\eta = t * d * c \quad (5)$$

Where, t, d, and c were elution time, density of solution and Ubbelohde viscometer constant with units of second, g/ml and cP/second respectively. The relative viscosity of solution was calculated as:

$$\eta_r = \eta / \eta_0 \quad (6)$$

Where,  $\eta_0$  is the viscosity of water (0.89 cP at 25 °C).

### 3.6. Surface Tension

The maximum bubble pressure method (MBPM) was used to measure the static and dynamic surface tension of CUPs. As compared to Du Noüy ring method [25], oscillating jet method [26] and pendant drop method [27], the MBPM offers distinct advantages such as: negligible effect of humidity, air turbulence, and contamination of carbon dioxide and ease of operation and cleaning after testing. Sensadyne PC-500 LV was



used to measure the surface tension of CUP suspensions. Suspensions were equilibrated in a constant temperature water bath at  $25 \pm 0.1$  °C before measurement. An inert gas (nitrogen) was bubbled through two probes of different radii immersed in the solution at same level. A broad range of gas bubble rates were used for measuring the dynamic surface tension. The maximum and minimum bubble rate were determined as the rate beyond which the surface tension did not further increase or decrease. The bubbling of nitrogen through the probes produced a differential pressure signal which was directly related to surface tension. The tensiometer was calibrated with analytical reagent 100% ethanol and Milli-Q ultrapure water for each polymer system. Flow rate of nitrogen gas was 40ml/minute and flow pressure was maintained at 25 psi.

## **4. RESULTS AND DISCUSSION**

### **4.1. Characterization of Polymer and CUPs**

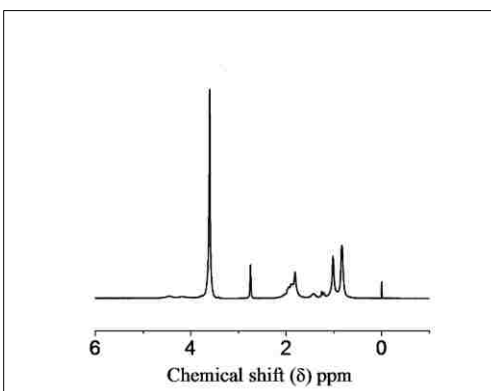
Table 1 shows the density data along with the DLS particle size and the molecular weight of the three copolymers. The densities of the dry CUP increased with increasing molecular weight as expected, since the weight fraction of end groups decreased with increasing molecular weight [28]. The particle size was measured using DLS nanotracer based on the Brownian diffusion principle. The scattered light was Doppler shifted based on the diffusion of particles. The molecular weight of the copolymers was calculated using the relation typically used for globular proteins where the molecular weight is related to the protein size and its density.

**Table 1.** % Yield, density, diameter and molecular weight of the three QUAT-CUPs

Sample ID	% Yield	$\rho_p^a$	Particle diameter (nm)	MW <sup>b</sup>
Polymer 1	70	1.1715±0.0014	4.3	36,000
Polymer 2	79	1.1751±0.0012	5.6	55,000
Polymer 3	76	1.1866±0.0005	6.3	94,000

a-density of dry CUP (g/cc), b- $MW = \frac{\pi d^3 \rho_p N_A}{6}$ ,  $N_A$ = Avogadro's Number

The NMR spectra of all the three polymers were similar and a representative NMR spectrum of 36K polymer is shown in Figure 3. The chemical shifts between 0.8-1.1 ppm were assigned to the protons of  $-\text{CH}_3$  group on the MMA and QUAT backbone, 1.1-1.5 ppm was assigned to protons of  $-\text{CH}_2$  group of QUAT, 1.9 ppm was assigned to the  $-\text{CH}_2$  of MMA in the polymer backbone and 3.3-3.5 ppm were assigned to the protons of  $-\text{N}^+(\text{CH}_3)_3$  group of the QUAT and the  $-\text{OCH}_3$  group of MMA. The observed chemical shifts are consistent with the values reported in literature [10, 24].

**Figure 3.** NMR of polymer 1 (MW=36K)

## 4.2. Water-reduction Process

Figure 2 shows the process of water-reduction to form CUP particles with quaternary ammonium groups on the surface which prevents the particles from aggregating through electrostatic repulsion. The polymer had a hydrophobic backbone of methyl methacrylate and water-compatible quaternary ammonium groups in a molar ratio of 9:1. When dissolved in methanol, the polymer chain exists as an extended random coil and the ion pairs were almost completely solvated in methanol. On addition of deionized water using peristaltic pump, there could be a slight increase in the solvation since water has a dielectric of 78.54 [29] while methanol has a dielectric of 35.74 at 25 °C [30]. Positively charged quaternary ammonium groups then repelled each other due to the increasing dielectric caused by the added water and the polymer chain became more rod-like increasing the viscosity of suspension.

At a certain critical point during the addition of water, the amphiphilic polymer chains collapsed with the quaternary ammonium groups oriented into the water phase, organizing to produce maximum separation of charge. The hydrophobic polymer backbone formed the interior of the spheroidal CUP particle. In the last step, methanol was stripped off in-vacuo to give zero-VOC CUP particles. The solvent that was stripped off could be recycled, thus providing an environment friendly resin system. Further water removal up to 20% solids can be achieved before a semi-solid gel state was formed. The formed gel can be simply diluted again to return to a fluid system. This behavior is unlike typical latex particles which gel up irreversibly.

The unimolecular collapse was also dependent on the concentration of the amphiphilic polymer in methanol and methanol/water mixture. If the concentration was high, the polymer chains overlap and if overlapped polymer chains come in contact with

each other at the critical point, non-unimolecular collapse occurred forming larger particle size or coagulum.

The process of water reduction is similar to the process of micelle formation. The solvent organizes around the hydrophobic units of MMA in the polymer chain with the addition of water to the polymer solution in methanol. The collapse of polymer chains into CUP particles is favored by an increase in the entropy through the release of the organized water to the bulk even though the polymer chains and the charges become more organized. The collapsed CUP particles approximate a sphere due to the quaternary ammonium group's electrostatic repulsion. Brownian motion keeps the small CUP particles suspended in water and thus they are thermodynamically stable unlike the larger latex particles which settle with time.

### **4.3. Rheological Behavior**

The rheological behavior of a 5% QUAT-CUP-55K is shown in Figure 4 as a plot of shear stress against shear rate at two different temperatures of 25 °C and 29 °C. The CUP solution is a colloidal suspension with charged polymer particles as the dispersed phase in the continuous aqueous phase. At both the temperatures, the shear stress on the CUP solution increased almost linearly with increasing shear rate and the yield stress was zero which indicated that the CUPs behaved basically as a Newtonian fluid at a concentration of 5.0% wt/wt. The viscosity values were further used for particle size analysis of CUPs instead of the viscosity of the solvent to compensate for the change in diffusion of charged particles.

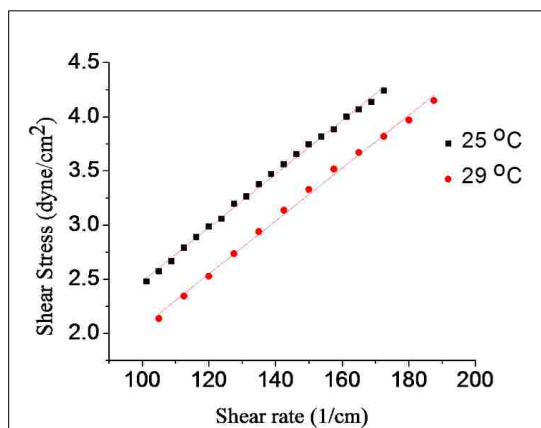


**Figure 4. Plot of shear stress vs shear rate for QUAT-CUP-55K at 25 °C and 29 °C**

#### **4.4. Particle Size Analysis Using DLS**

The CUP solution was filtered through a 0.45  $\mu\text{m}$  Millipore membrane before performing the particle size analysis which ensured removal of any foreign material which was typically measured to be less than 0.05% by weight. Figure 5 shows the particle size distribution graphs for the three QUAT-CUPs. CUPs are formed by the unimolecular collapse of polymer chains and the particle diameter depends upon the molecular weight of polymer and its density. The polymer chains have a broad molecular weight distribution unless the polymer is made by living free radical polymerization techniques which give a very narrow molecular weight distribution. The molecular weight distribution leads to a particle size distribution for the CUPs.

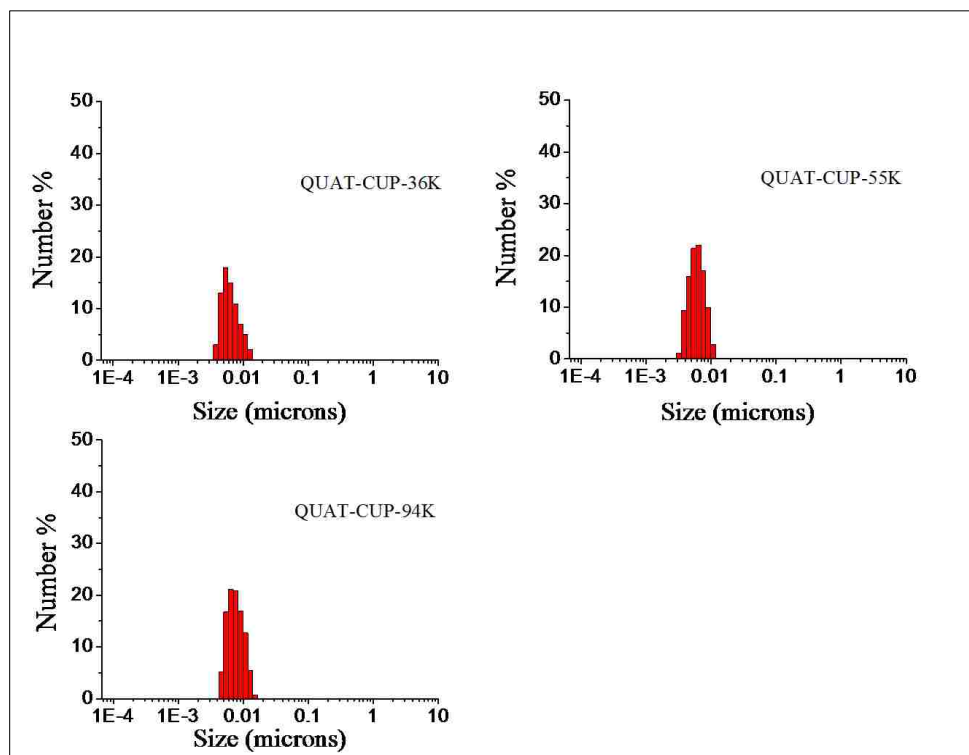


**Figure 5. Particle size distribution graphs using DLS for the three QUAT-CUPs**

#### 4.5. Specific Viscosity Comparison

The specific viscosities of the CUP suspensions were measured at dilute concentrations ( $\phi < 0.10$ ) and plotted against the volume fractions for the three copolymers as shown in Figure 6. For comparison, the viscosity of carboxylate-functional ( $\text{CO}_2^-$ )-CUP (M.W=36K) and the theoretical viscosity based on the Einstein's model was also shown. The specific viscosity was measured using a Ubbelohde capillary viscometer. The viscosity increased with increasing volume fractions for all the CUP suspensions as explained further.

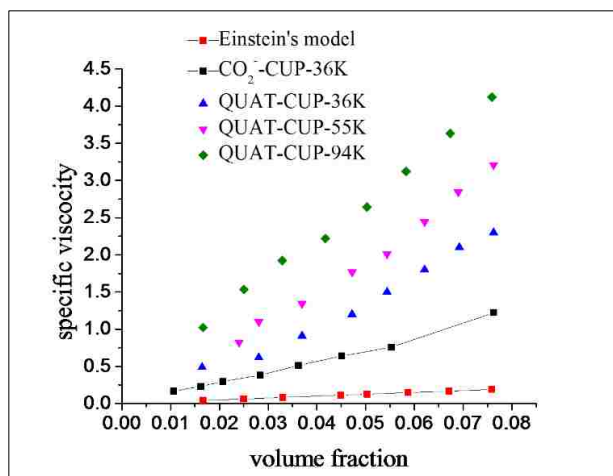


**Figure 6. Plot of specific viscosity of the three quaternary ammonium functional and one carboxylate functional [14] CUP solutions as a function of volume fraction**

The experimental viscosity for all of the samples deviated from Einstein's model in the dilute regime (volume fraction < 0.10). The primary electroviscous effect typically decreases with increasing concentration and the secondary electroviscous effect is negligible in the dilute concentration regime. Therefore, the observed increase in viscosity with concentration was attributed to the tertiary electroviscous effect arising from a higher associated water fraction.

At each volume fraction, the QUAT-CUP-36K displayed a higher viscosity as compared to CO<sub>2</sub><sup>-</sup>-CUP-36K possibly due to greater associated water fraction i.e. a higher tertiary electroviscous effect. Novoselova et al. have indicated that the quaternary ammonium functional hydrogels and polymers displayed higher water-absorption than the carboxylate counterparts [31]. The associated water fraction and the thickness of surface water layer of CUP particles was further calculated from the intrinsic viscosity of the three CUP systems which was determined from the slope of  $\ln(\eta_{rel})$  versus volume fraction plots as shown in Figure 7.

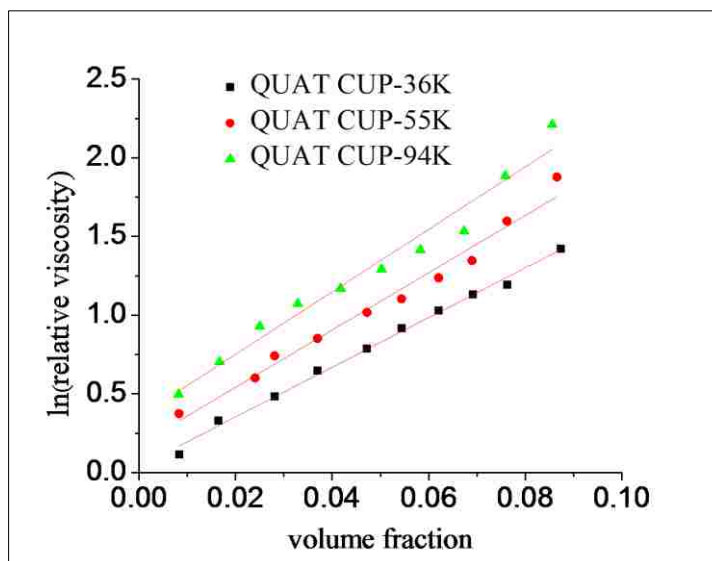


**Figure 7. Plot of  $\ln(\eta_{rel})$  versus volume fraction for quaternary ammonium functional CUPs.**

The associated water fraction,  $\beta$ , defined as the weight ratio of surface water to CUP was calculated by using equation 7 [32], where,  $\rho_1$  is the density of water (0.997 g/cc) and  $\rho_2$  is the density of CUP at 25 °C. Assuming that each particle is spherical and surrounded by a uniform layer of water molecules with thickness  $\delta$ , then  $\delta$  can be expressed as equation 8.

$$\beta = \frac{\rho_1}{\rho_2} \left( \frac{[\eta]}{2.5} - 1 \right) \quad (7)$$

$$\delta = R_s \left[ \left( \frac{\beta \rho_2}{\rho_1} \right)^{\frac{1}{3}} - 1 \right] \quad (8)$$

The  $[\eta]_\phi$ ,  $\beta$  and  $\delta$  values listed in Table 2 indicated that there was significant amount of surface water on the CUP particles. The thickness of water layer increased with increasing molecular weight of the copolymer which resulted in increased viscosity. Assuming that all the quaternary ammonium groups on the CUP particle were dissociated, the bare surface charge density for spherical CUP particles can be estimated by equation 9.



$$\sigma = \left(\frac{MW}{4\pi}\right)^{\frac{1}{3}} \cdot \left(\frac{3}{\rho N_A}\right)^{-\frac{2}{3}} \cdot \frac{e}{m_{MMA}b + m_{QUAT}} \quad (9)$$

Where,  $\rho$  is the density of polymer,  $N_A$  is Avogadro number,  $q$  is the elementary charge,  $m_{MMA}$  is the molecular weight of methyl methacrylate,  $m_{QUAT}$  is the molecular weight of quaternary ammonium functional monomer and  $b$  is the molar ratio of MMA to QUAT.

**Table 2.** Intrinsic viscosity, associated water fraction and surface water thickness for the three QUAT-CUPs

Polymer	$[\eta]_{\phi}$	$\beta^a$	$\delta$ (nm)
QUAT-CUP-36K	15.8	4.5	1.6
QUAT-CUP-55K	17.2	5.0	2.3
QUAT-CUP-94K	20.0	5.9	2.9

a- associated water fraction (gram water / gram CUP)

The density of polymer and the molar ratio were similar for the three polymers from Table 1 and therefore the surface charge density was roughly linear with the cube root of molecular weight of the polymer. The radius of particle can be expressed as  $R_s = \left(\frac{3 \cdot MW}{4\pi\rho N_A}\right)^{1/3}$  which indicated that the radius of particle was also proportional to its molecular weight. The bare surface charge density was proportional to particle size. The bigger the particle was, the higher the surface charge density would be, which corresponded to more quaternary ammonium groups at the surface per unit area. Therefore more counterions, and more associated water molecules will be attracted to the CUP surface to dissipate the charges and forming a thicker surface water layer.

The increase in viscosity with molecular weight could also be partly due to the hydrodynamic effects. The higher the molecular weight of the polymer, the larger the hydrodynamic volume and higher the viscosity of system. But, for spherical charged colloid particles, Rattanakawin et al. [33] have demonstrated that the hydrodynamic effects are negligible as compared to the electroviscous effect.

Chen et al. had indicated that the bound water fraction and the surface water thickness for  $\text{CO}_2^-$ -CUP-36K was 2.4 (g water/g CUP) and 1.0 nm respectively [14]. As seen in Table 2, QUAT-CUP-36K had higher bound water fraction (4.5 g water/g CUP) and surface water thickness (1.6 nm). The contribution of the chloride counter-ion of QUAT-CUPs and sodium counter-ion of  $\text{CO}_2^-$ -CUPs to the corresponding experimental viscosity would be similar because both ions have similar number of associated water molecules ( $\leq 6$ ) in the first hydration shell [34, 35]. Therefore, the higher viscosity for QUAT-CUPs as compared to  $\text{CO}_2^-$ -CUPs was mainly attributed to the higher associated water fraction on the surface of QUAT-group.

Numerous researchers based on various experimental techniques like viscosity, NMR spectroscopy and dielectric relaxation measurements have reported that the quaternary ammonium groups increased the viscosity of aqueous suspension [36-38]. Based on Monte Carlo simulations, Hribar-Lee et al. [39] recently reported that the tetramethyl ammonium (TMA) cation has a minimum of two hydration shells with a further cage-like structuring of water molecules around the TMA ion [40]. García-Tarrés et al. [41], using molecular simulation dynamics reported that the hydration number i.e. number of water molecules in the hydration shell, for tetramethylammonium (TMA) ion was 23. On the other hand, Monte-Carlo simulations [42] and ab-initio calculations [43] assigned a hydration number of 5-7 to the carboxylate ion. Therefore, the higher experimental

viscosity of QUAT-CUPs as compared to carboxylate-CUPs was due to a higher associated water fraction which was in agreement with the reported simulations. Figure 8 shows a pictorial representation of QUAT and  $\text{CO}_2^-$ -CUP surface with the hydration layer.

Novoselova et al. [31] reported that the viscosity of aqueous solutions of quaternary ammonium functional surfactant remained constant ( $\sim 1$  cP) until the critical micelle concentration (CMC,  $\sim 0.01$  mole/L) was reached. Beyond the CMC, the viscosity of surfactant system increased steadily with increasing concentration. The viscosity of QUAT-CUPs increased continuously with increasing concentration even in the dilute concentration regime ( $0.06 \cdot 10^{-3}$  –  $3.6 \cdot 10^{-3}$  mole/L) which was attributed to the unimolecular micelle conformation of the QUAT-CUPs i.e. no CMC.

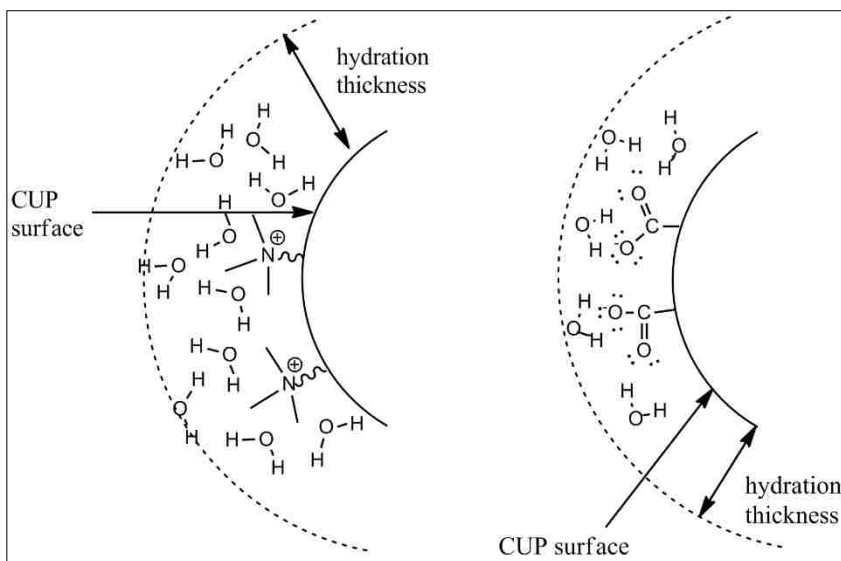


**Figure 8. Representative structure of QUAT and  $\text{CO}_2^-$ -CUP surface with hydration layer**

#### 4.6. Density of Surface Water

It has been reported in literature that the density of bulk water differs from the density of water associated with a latex particle [44]. The effect of surface charged groups has been difficult to quantify mainly due to the large particle size of latex resins [45]. For example, in the case of CUP particles with a 3.3-nm radius, the volume fraction occupied by surface water is ~61 % of the CUP particle volume. On the other hand, for a typical commercial latex resin with particle radius of 100 nm, assuming same thickness of associated water as for CUPs, the ratio of surface water to latex by volume is only 1.72 %. Therefore, it is difficult to probe the associated water density. Recently, Van De Mark et al. reported a simple method to determine the density of surface water on  $\text{CO}_2^-$ -CUPs, based on the relationship between the surface water (S), the bulk water (B), and the particle volume fraction ( $\Phi_p$ ) [15].

A similar analysis for the surface water density on 94K-QUAT-CUPs was performed as follows: For the CUP system composed only of the CUP particles, the associated water and the bulk water, the summation of volume fraction is one [15], as shown in equation 10.

$$\Phi_p + \Phi_{H_2O,S} + \Phi_{H_2O,B} = 1 \quad (10)$$

Also there exists a conservation of mass of the total material [15] as shown in equation 11.

$$m_s = m_p + m_{H_2O,S} + m_{H_2O,B} \quad (11)$$

Where,

$$m_p = \rho_s * f \quad (12)$$

$$m_{H_2O,S} = \rho_{H_2O,S} * \Phi_{H_2O,S} \quad (13)$$

$$m_{H_2O,B} = \rho_{H_2O,B} * \Phi_{H_2O,B} \quad (14)$$

and  $\Phi$  denotes volume fraction,  $m$  denotes mass and  $\rho$  denotes density for each material respectively and  $\rho_s$  denotes density of CUP dispersion.

The relation between volume fraction of CUP particle and surface water [15] can be expressed as equation 15:

$$\Phi_{H_2O,S} = \left[ \left( 1 + \delta/r \right)^3 - 1 \right] * \Phi_p \quad (15)$$

Where,  $r$  denotes radius of CUP particle. Using equation 11 through 15, equation 10 was solved to get,

$$1/\rho_s = af + b \quad (16)$$

Where,

$$b = \frac{1}{\rho_{H_2O,B}} \text{ and } a = \frac{(1+\delta/r)^3}{\rho_p} - \frac{1}{\rho_{H_2O,B}} - \frac{\rho_{H_2O,S}}{\rho_p * \rho_{H_2O,B}} * \left[ \left( 1 + \delta/r \right)^3 - 1 \right] \quad (17)$$

Equation 16 represents a linear fit equation to the plot of  $1/\rho_s$  vs  $f$ , where,  $f$  denotes the weight fraction of CUP particles and  $\rho_s$  denotes the density of CUP dispersion at the corresponding weight fraction. The density of CUP dispersion at various weight fractions was measured using a pycnometer and a graph of  $1/\rho_s$  vs  $f$  was plotted as shown in Figure 9. The graph was fit to a straight line equation and the value of the slope from the straight line corresponded to the value of 'a'. A similar trend was observed for all the three CUP suspensions.

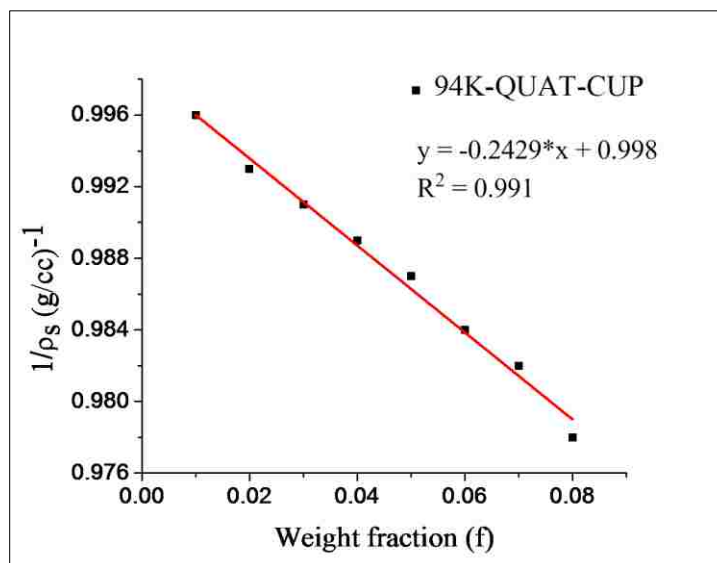


**Figure 9. Effect of weight fraction (f) on  $1/\rho_s$**

Equation 17 was solved for the surface water density ( $\rho_{H_2O,S}$ ) by substituting the slope value obtained from Figure 9 for the value of 'a'. The density of surface water for 94K-QUAT-CUP was 1.0132 g/cc which was 1.6% larger than the density of bulk water which was 0.997 g/cc at 25 °C. Compared to the surface water density (1.0688 g/cc) reported by Van De Mark et al. [15] for 111K-CO<sub>2</sub><sup>-</sup>-CUP, the density of surface water on 94K-QUAT-CUP was lower, which could be attributed to the difference in the structure of water around the functional groups. It is reported in literature that about 3-6 water molecules can directly associate with each negatively charged carboxylate group via hydrogen bonds [46]. While for QUAT-functionality, the water molecules form a cage-like structure around the QUAT-group via weaker dipole-dipole interaction and do not coordinate directly to the cation [42, 47].

#### 4.7. Equilibrium Surface Tension Behavior

The equilibrium surface tension of all the three QUAT-CUP suspensions decreased linearly with increasing concentration of the CUPs as indicated in Figure 10. The surface tension reduction is similar to that observed for typical surfactants i.e. the higher the amount of surface active groups, the greater the surface tension reduction. Increasing the CUP concentration also increased the counter-ion concentration (chloride ions), some of which condensed on the CUP surface reducing its effective charge. The phenomenon known as Manning condensation (counterion condensation) is widely accepted in charge stabilized colloidal suspensions [48].

The counterion condensation causes the effective charge to be lower than the bare surface charge and allows more number of CUP particles with better packing at the air-water interface. At the same time, the total number of charged groups at the air-water interface increases because only a small fraction of the charged groups on the CUP surface undergo Manning condensation. Therefore, the electrostatic repulsion increased at the surface which reduced the surface energy of the system. The overall effect was a reduction in the equilibrium surface tension with increasing concentration of CUPs. The counter-ion condensation occurs for both the carboxylate and QUAT functional CUPs. The counter-ion condensation in case of QUAT functional CUPs was not quantified because of lack of a suitable theoretical program to calculate the theoretical effective surface charge on the QUAT functional CUPs.

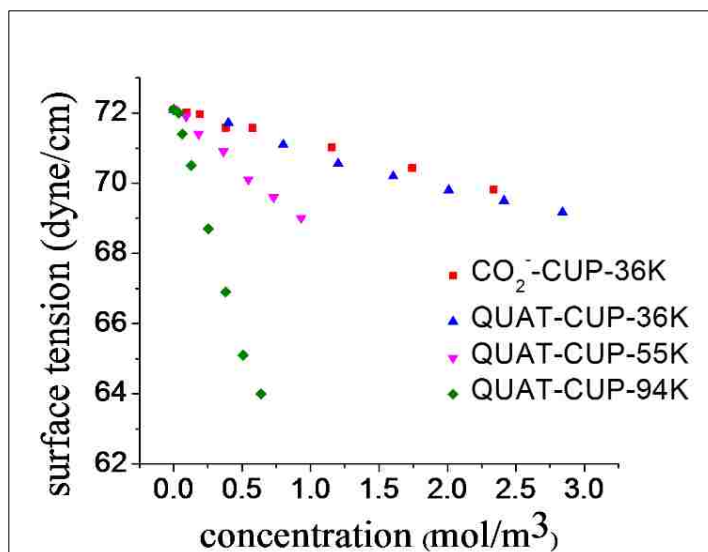


**Figure 10. Surface tension versus concentration for the three QUAT-CUPs and CO<sub>2</sub><sup>-</sup>-CUP-36K**

It is interesting that Okubo appears to be the only author reporting the air-water surface tension of salt-free, spherical, colloidal polymeric suspensions [49]. Okubo reported that the surface activity of methyl polyenimine increased with increasing molecular weight possibly due to the corresponding increase in hydrophobicity of polymer backbone [49].

The equilibrium surface tension of QUAT-CUPs decreased with increasing molecular weight. The decrease in surface tension was attributed to the increase in the number of cationic charged groups on the surface of CUP particle with increasing molecular weight. The individual polymer chain was composed of 9:1 ratio of MMA (M.W. = 100): QUAT (M.W. = 208) on an average. Therefore, there was one quaternary ammonium group for every 1108 Da of polymer and therefore, the polymer with 36K, 55K and 94K molecular weight had on an average, 32, 50 and 85 charged groups respectively, per particle.



Particles arriving at an interface can either have attractive (van der Waals) or repulsive forces (electrostatic) between them which determines the change in the surface energy. Increase in the van der Waals attractive force increases the surface energy which increases the surface tension at the interface since more work is required to distort the surface and the surface tension is lowered by reducing the surface energy [50].

CUP particles with charged quaternary ammonium groups repelled each other when adsorbed at the air-water interface and possibly reduced the surface energy of the system, therefore, lowering the surface tension. CUPs with higher molecular weight had more charged groups per unit area on the surface and therefore had increased electro-repulsion which gave greater reduction in surface tension.

The QUAT-CUP and CO<sub>2</sub><sup>-</sup>-CUP with similar molecular weight (36K) showed similar reduction in surface tension which was possibly due to similar polarities of the hydrophilic quaternary ammonium and carboxylate group which resulted in similar reduction of surface energy via electrostatic repulsion. The surface tension versus concentration was fit to a linear equation expressed as equation 18 and the results listed in Table 3.

$$\gamma - \gamma_w = k * c \quad (18)$$

Where,  $\gamma_w$  is the surface tension of water,  $k$  is the slope (surface activity) and  $c$  is the concentration (mole/m<sup>3</sup>). At infinite dilution, the surface tension of CUPs should approach a value of 72.08 dyne/cm which is the surface tension of pure water at 25 °C. The intercept ( $\gamma_w$ ) for all the three suspensions were found to be close to 72.08 dynes/cm as predicted.

**Table 3.** Surface tension fitting parameters

CUP system	$k$	$\Delta k$	Intercept ( $\gamma_w$ )	$\Delta\gamma_w$	$R^2$
CO <sub>2</sub> <sup>-</sup> -CUP-36K	-0.96	0.03	72.1	0.03	0.993
QUAT-CUP-36K	-1.1	0.05	72.0	0.09	0.990
QUAT-CUP-55K	-3.4	0.11	72.1	0.06	0.994
QUAT-CUP-94K	-13.3	0.39	72.2	0.13	0.994

#### 4.8. Dynamic Surface Tension Behavior

Figure 11 shows the plot of dynamic surface tension against surface age for the three QUAT-CUPs and CO<sub>2</sub><sup>-</sup>-CUP-36K at a concentration of 0.5 mole/m<sup>3</sup>. Surface age is defined as the time interval between the onset of bubble growth and the moment of maximum pressure. Therefore as the surface age was increased, the bubble rate reduced which gave the CUP particles more time to reach the air (bubble)-water interface.

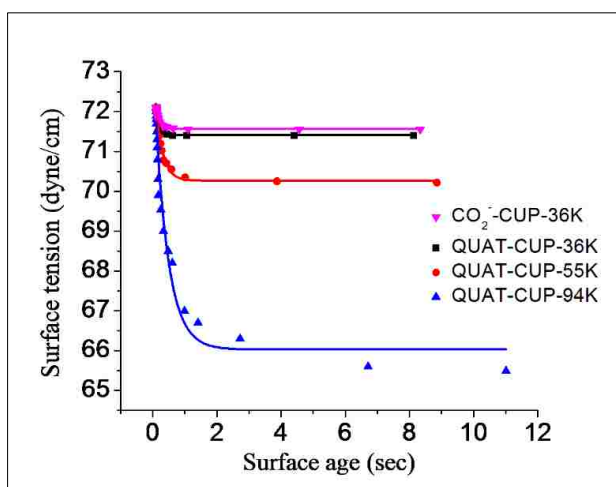


**Figure 11. Surface tension vs surface age for QUAT-CUP and CO<sub>2</sub><sup>-</sup>-CUP-36K at 0.5 mole/m<sup>3</sup>**

The data gave a good exponential fit represented by the equation 19. The fitting parameters were shown in Table 4.

$$\gamma - \gamma_e = A * \exp(-t/\tau_k) \quad (19)$$

Where,  $\gamma_e$  is the equilibrium surface tension; A and  $\tau_k$  (kinetic relaxation time) are the fitting parameters.

Figure 11 indicated that the QUAT-CUP-94K took longer time to reach equilibrium than QUAT-CUP-55K and QUAT-CUP-36K and the equilibrium surface tension decreased with increasing molecular weight. The exponential relaxation of surface tension is consistent with the kinetically limited adsorption (KLA) model reported by Diamant and Andelman [51]. The fitting parameter  $\tau_k$  (kinetic relaxation time or the half-time to reach constant surface tension), according to Andelman et al., is indicative of the electrostatic potential at the surface which gives rise to electrostatic repulsion. The  $\tau_k$  increased with increasing molecular weight as shown in Table 4 and indicated a barrier to surface adsorption via electrostatic repulsion thus slowing down absorption of CUP at the interface.

**Table 4.** Fitting parameters for dynamic surface tension versus surface age at 0.5 mole/m<sup>3</sup>

CUP system	$\gamma_e$ (dyne/cm)	A	$\tau_k$ (sec)	R <sup>2</sup>
CO <sub>2</sub> <sup>-</sup> -CUP-36K	71.6	1.9	0.089	0.993
QUAT-CUP-36K	71.4	2.1	0.069	0.995
QUAT-CUP-55K	70.3	3.6	0.240	0.993
QUAT-CUP-94K	65.0	7.5	0.462	0.975

Van De Mark et al. have shown that for accurate particle size measurement of CUPs using DLS, the viscosity of the solvent was replaced by the viscosity of the solution because of the increasing viscosity due to electroviscous effects [12]. The collective diffusion coefficient ( $D_c$ ) was approximated from the generalized Stokes-Einstein's model for the diffusion of spherical particles expressed as equation 20, relating the collective diffusion coefficient to the radius of particle ( $r$ ) measured by DLS and the viscosity of the solution.

$$D_c = \frac{k_b * T}{6 * \pi * \eta * r} \quad (20)$$

Where,  $k_b$  is the Boltzmann constant and T is the absolute temperature of the solution.

The diffusion coefficients ( $D_c$ ) were calculated to be 0.82, 0.45 and 0.28 ( $10^{-6}$  cm<sup>2</sup>/s) for the 36K, 55K and 94K-QUAT-CUPs (each at a volume fraction of 0.05) respectively. Therefore, the QUAT-CUP-94K taking more time to reach equilibrium surface tension could be explained by a slower diffusion of the higher molecular weight CUP to the air-water interface.

Ferdous et al. [52] have shown that the presence of charged particles at the air-water interface reduced the interfacial tension due to a reduction in the surface energy. In a similar way, the CUP particles also caused reduction in surface tension due to surface charged groups (QUAT and CO<sub>2</sub><sup>-</sup>). The higher molecular weight CUP particle caused greater reduction in surface tension value because higher molecular weight CUP had more surface charged groups per unit area which caused a greater reduction in the surface energy and therefore greater reduction in the surface tension.

Figure 12 shows the effect of concentration on the dynamic surface tension for the three QUAT-CUPs. The dynamic surface tension decreased with increasing concentration which was attributed to greater reduction in surface energy due to higher number of

particles. The dynamic surface tension data shown in Figure 12 for the three MW CUPs at various concentrations was fit to equation 19 and the kinetic relaxation time ( $\tau_k$ ) was shown in Table 5.

With increasing concentration, the viscosity of CUP solution increased, slowing the diffusion of CUP particle to the air-water interface. Increasing the concentration also increased the probability of a CUP particle getting adsorbed at the air-water interface and decreased the distance needed to travel to reach the interface. The overall effect was an increase in the relaxation time to reach equilibrium.

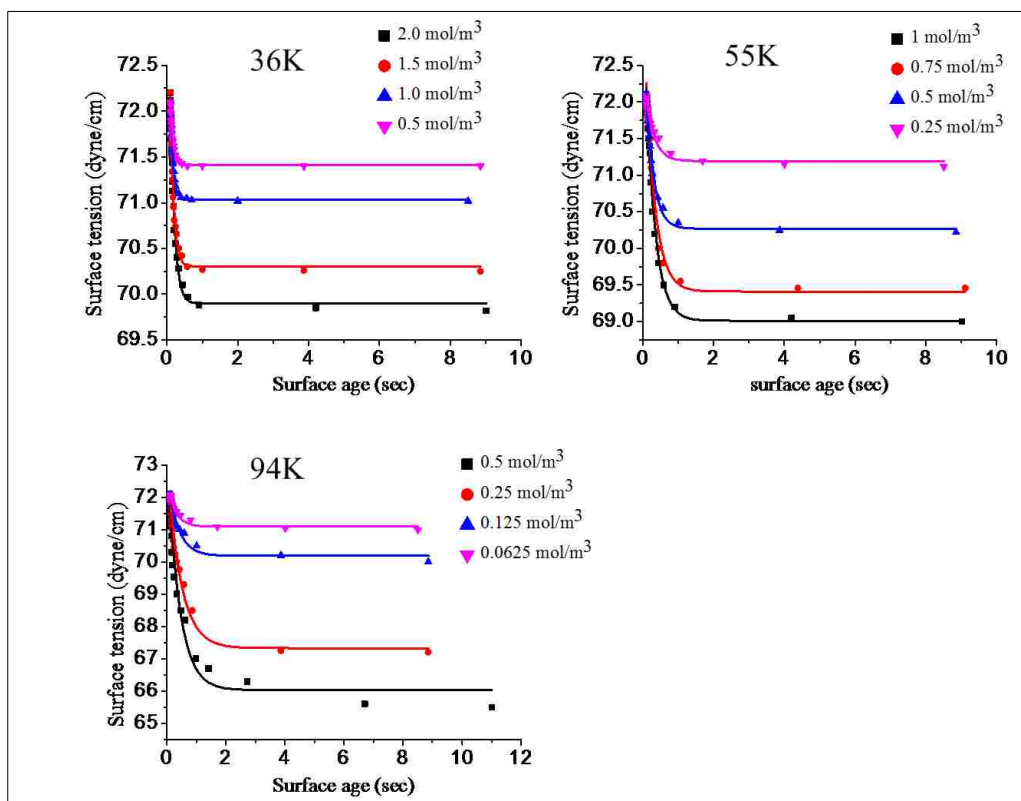


**Figure 12. Dynamic surface tension versus surface age at 4 different concentration for QUAT-CUPs (36K, 55K, 94K)**

**Table 5.** Relaxation time ( $\tau_k$ ) for the three CUPs at various concentrations

QUAT-CUP	Concentration (mole/m <sup>3</sup> )	$\tau_k$ (sec)	R <sup>2</sup>
36K	0.50	0.069	0.995
"	1.01	0.074	0.998
"	1.50	0.092	0.995
"	1.99	0.115	0.996
55K	0.25	0.234	0.972
"	0.50	0.240	0.993
"	0.75	0.276	0.982
"	0.99	0.280	0.994
94K	0.06	0.263	0.957
"	0.13	0.358	0.972
"	0.25	0.459	0.984
"	0.50	0.462	0.975

## 5. CONCLUSIONS

Colloidal unimolecular polymer (CUP) particles with cationic groups on the surface were successfully synthesized by the process of water reduction on MMA-QUAT copolymers. The CUPs had zero volatile organic content (VOC) due to the complete removal of organic solvent and the particle size was in the true nano-scale region (3-9 nm). At similar molecular weight the QUAT-CUPs had a thicker bound or associated water layer as compared to the CO<sub>2</sub><sup>-</sup>-CUPs. Higher bound water fraction for QUAT-CUPs resulted in a greater viscosity as compared to CO<sub>2</sub><sup>-</sup>-CUPs at similar volume fraction.

QUAT-CUPs with higher molecular weight resulted in greater surface tension reduction due to higher charge density which reduced the surface energy. Density measurements using pycnometer revealed that the associated surface water on QUAT-CUP was 1.6% higher than the bulk water. The surface water density was lower as compared to similar molecular weight carboxylate functional CUP which was attributed to weaker dipole-dipole interactions of QUAT groups with surface water, while carboxylate groups had direct hydrogen bonding giving the surface water a more compact structure.

The equilibrium surface tension was similar for the  $\text{CO}_2^-$ -CUP-36K and QUAT-CUP-36K possibly due to similar polarities of the charged groups. Dynamic surface tension studies revealed that the rate of surface tension reduction was possibly a function of the molecular weight of the polymer and the surface charge density of the CUP particle. Higher molecular weight CUPs required more time to reach the equilibrium surface tension due to a slower diffusion, but gave a lower surface tension value due to greater reduction in surface energy arising from a higher number of surface charged groups per unit area.

Further study would be directed towards studying the surface active properties of CUPs with different molecular weight but similar charge density which would elucidate more clearly the impact of diffusion and surface charge on the surface tension of CUPs.

## 6. ACKNOWLEDGEMENTS

The authors would like to acknowledge the Coatings Institute and the Department of Chemistry of Missouri S&T for the financial support and resources. We thank Dr. Nicholas Leventis of Missouri S&T University for measuring the density of the dry CUPs.

## 7. REFERENCES

1. Z. Liu, H. Xiao, N. Wiseman, *J. Appl. Polym. Sci.* 76 (2000) 1129-1140.
2. M.G. Rasteiro, F.A.P. Garcia, P.J. Ferreira, E. Antunes, D. Hunkeler, C. Wandrey, *J. Appl. Polym. Sci.* 116 (2010) 3603-3612.
3. N. Beyth, I. Yuodvin-Farber, R. Bahir, A.J. Domb, E.I. Weiss, *Biomaterials* 27 (2006) 3995-4001.
4. H. Jia, G. Zhu, P. Wang, *Biotechnol. Bioeng.* 84 (2003) 406-414.
5. S. S. Davis, L. Illum, *Biomaterials* 9 (1988) 111-115.
6. S.K. Samal, M. Dash, S.V. Vlierberghe, D.L. Kaplan, E. Chiellini, C.V. Blitterswijk, P. Dubruel, *Chem. Soc. Rev.* 41 (2012) 7147-7194.
7. Q. Liu, Y. Li, Y. Duan, H. Zhou, *Polym. Int.* 61 (2012) 1593-1602.
8. S.C. Liufu, H.N. Xiao, Y.P. Li, *J. Colloid. Interf.* 285 (2005) 33-40.
9. J. Ramos, J. Forcada, R. Hidalgo-Alvarez, *Chem. Rev.* 114 (2013) 367-428.
10. G. Sun, M. Zhang, J. He, P. Ni, *J. Polym. Sci. Pol. Chem.* 47 (2009) 4670-4684.
11. J.K. Mistry, A.M. Natu, M.R. Van De Mark, *J. Appl. Polym. Sci.* 131 (2014) DOI: 10.1002/app.40916.
12. C.J. Riddles, W. Zhao, H.J. Hu, M. Chen, M.R. Van De Mark, *Polymer* 55 (2014) 48-57.
13. M.R. Van De Mark, A.M. Natu, S.V. Gade, M. Chen, C. Hancock, C.J. Riddles, *J. Coat. Technol. Res.* 11 (2014) 111-122.
14. M. Chen, C.J. Riddles, M.R. Van De Mark, *Langmuir* 29 (2013) 14034-14043.
15. M. Chen, C.J. Riddles, M.R. Van De Mark, *Colloid. Polym. Sci.* 291 (2013) 2893-2901.
16. G. Buckton, E.O. Machiste, *J. Pharm. Sci.* 86 (1997) 163-166.
17. A. Einstein, *Annalen der Physik* 323 (1905) 639-641.
18. I.G. Watterson, L.R. White, *J. Chem. Soc. Farad. T. 2.* 77 (1981) 1115-1128.
19. W.B. Russel, *J. Fluid Mech.* 85 (1978) 673-683.
20. K.A. Vaynmerg, N. J. Wagner, *J. Rheol.* 45 (2001) 451-466.
21. L. Jiang, S.B. Chen, *J. Non-Newton. Fluid.* 96 (2001) 445-458.
22. J.L. Oncley, *Ann. NY. Acad. Sci.* 41 (1941) 121-150.
23. I.M. Kreiger, *Ad. Colloid Interfac.* 3 (1972) 111-136.
24. N.A. Fefelova, Z.S. Nurkeeva, G.A. Munn, V.V. Khutoryanskiy, *Int. J. Pharm.* 339 (2007) 25-32.



25. P.L. Du Noüy, *J. Gen. Physiol.* 1 (1919) 521-524.
26. N. Bohr, *Philos. T. R. Soc. Lond.* (1909) 281-317.
27. E. Tornberg, *J. Colloid Interf. Sci.* 60 (1977) 50-53.
28. G.C. East, D. Margerison, E. Pulat, *T. Faraday Soc.* 62 (1966) 1301-1307.
29. A.A. Maryott, E.R. Smith, *Natl. Bureau Stand.* (1951).
30. M. Mohsen-Nia, H. Amiri, B. Jazi, *J. Solution Chem.* 39 (2010) 701-708.
31. N.V. Novoselova, A.A. Bobyleva, E.V. Lukovskaya, E.A. Sumtsova, V.N. Matveenkov, A.V. Anisimov, V.I. Terenin, *Theor. Found. Chem. Eng.* 41 (2007) 649-659.
32. P. Hiemenz, R. Rajagopalan, *Principles of Colloid and Surface Chemistry* 3<sup>rd</sup> Edition, revised and expanded, CRC Press, (1997).
33. C. Rattanakawin, R. Hogg, *Miner. Eng.* 20 (2007) 1033-1038.
34. D.H. Powell, A.C. Barnes, J.E. Enderby, G.W. Neilson, P.S. Salmon, *Faraday Discuss. Chem. Soc.* 85 (1988) 137-146.
35. J. Mähler, I. Persson, *Inorg. Chem.* 51 (2011) 425-438.
36. W.Y. Wen, S. Saito, *J. Phys. Chem.* 68 (1964) 2639-2644.
37. G.H. Haggis, J.B. Hasted, T.J. Buchanan, *J. Chem. Phys.* 20 (1952) 1452-1465.
38. E.R. Nightingale Jr., *J. Phys. Chem.* 60 (1962) 894-897.
39. B. Hribar-Lee, K.A. Dill, V. Vlachy, *J. Phys. Chem. B* 114 (2010) 15085-15091.
40. W.I. Babiaczyk, S. Bonella, L. Guidoni, G. Ciccotti, *J. Phys. Chem. B* 114 (2010) 15018-15028.
41. L. Garcia-Tarres, E. Guardia, *J. Phys. Chem. B* 102 (1998) 7448-7454.
42. W.L. Jorgensen, J. Gao, *J. Phys. Chem.* 90 (1986) 2174-2182.
43. G.D. Markham, C.L. Bock, C.W. Bock, *Structural Chemistry* 8 1997 293-307.
44. Y. Lei, J.R. Child, J.G. Tsavalas, *Colloid and Polym. Sci.* 291 (2013) 143-156.
45. F. Merzel, J.C. Smith, *Proc. Natl. Acad. Sci. USA* 99 (2002) 5378-5383.
46. M.V. Fedotova, S.E. Kruchinin, *J. Mol. Liq.* 164 (2011) 201-206.
47. J.Z. Turner, A.K. Soper, J.L. Finney, *J. Chem. Phys.* 102 (1995) 5438-5443.
48. G.S. Manning, *J. P. Chem.* 79 (1975) 262-265.
49. T. Okubo, *J. Colloid Interf. Sci.* 125 (1988) 386-398.
50. S. Tanvir, L. Qiao, *Nanoscale Res. Lett.* 7 (2012) 1-10.
51. H. Diamant, H. D. Andelman, *J. Phys. Chem.* 100 (1996) 13732-13742.
52. S. Ferdous, M.A. Ioannidis, D.E. Henneke, *J. Nanopart. Res.* 14 (2012) 1-12.

#### **IV. RHEOLOGY AND SURFACE TENSION BEHAVIOR OF SULFONATE FUNCTIONAL COLLOIDAL UNIMOLECULAR POLYMER (CUP)**

Ameya Natu, Marcus Wiggins, Minghang Chen and Michael R. Van De Mark

Department of Chemistry, Missouri S&T Coatings Institute,

Missouri University of Science & Technology, Rolla, MO 65409

##### **ABSTRACT**

Colloidal Unimolecular Polymer (CUP) particles were prepared by water-reduction of copolymers of methyl-methacrylate and 2-acrylamido-2-methylpropane sulfonic acid. Absence of additives like surfactant or emulsifier, easy synthesis and controllable true-nano scale size (diameter 3-9 nm) make the CUP systems an excellent material to study the electro-viscous effects and the effect of surface water on the rheology and surface tension. In the dilute concentration regime (volume fraction  $< 0.10$ ), the tertiary electroviscous effects dominated the rheology behavior and the associated water fraction on the surface of sulfonate ( $\text{SO}_3^-$ )-CUPs increased with increasing molecular weight or surface charge density of the CUP particles. The  $\text{SO}_3^-$ -CUPs had a thicker and a denser surface water layer than the carboxylate ( $\text{CO}_2^-$ ) functional CUPs. Surface activity was higher for the  $\text{SO}_3^-$ -CUPs as compared to  $\text{CO}_2^-$ -CUPs which was related to the surface charge density. Dynamic surface tension study indicated that the rate of surface tension reduction decreased with increasing concentration and the charge density of CUPs.

## 1. INTRODUCTION

Charged colloidal suspensions are used in numerous applications such as paints, coatings, drug-delivery and polymeric flocculants [1-4]. A thorough understanding of the rheology and surface tension behavior of the systems during synthesis, processing and application is of utmost importance because of its impact on the stability and utility of the charged colloidal systems. In the past, researchers have used materials such as surface charged latexes, charged nano-silica, fullerenes etc. to study the effect of surface charge, surface water and molecular weight on the rheology and surface tension behavior [5-7].

This research reports the synthesis of sulfonate functional Colloidal Unimolecular Polymer (CUP) particles which is a new type of a nanoscale (particle diameter  $< 10\text{nm}$ ), two-phase colloidal system with sulfonate groups on the surface of the particle. Solid, spheroidal polymer particles make up the dispersed phase suspended in the continuous aqueous phase. The change in solvent environment from an organic solvent to water forces the polymer chain to collapse on itself due to unfavorable interaction between the polymer and water, producing nanoscale CUPs in the range of 3 to 9 nm [8]. The collapse to a spherical shaped globule is driven by the polymer-polymer interaction being greater than the polymer-solvent interaction and entropically favored by the release of the water similar to micelle formation.

Figure 1 shows the formation of CUP particles with sulfonate groups on the surface, keeping the particles from aggregation. Once formed the colloidal particles are thermodynamically stable. The CUP suspensions contain only the charged particles, water and counterions [9]. The CUP suspensions being colloidal in nature and having ionizable groups on the surface are similar in nature to spherical polyelectrolytes. Polyelectrolytes

have been a subject of great research interest as it offers an insight into the behavior of biomacromolecules like proteins and viruses. Compared to the spherical polyelectrolytes, CUPs as a model material to study proteins offers distinct advantages such as: thermodynamic stability, simple to prepare and cost-effective.

Because of the potential as a resin system, rheology modifier, surfactant or encapsulating agent in applications ranging from paints and coatings to drug delivery, it is necessary to study and understand the important physical properties such as rheology, surface tension etc. As CUPs are free of any additive such as thickener or surfactant, the observed viscosity behavior can be directly related to the electroviscous effects, the effective surface charges and the surface water.

Brader [10] has published a detailed review on the rheology behavior of hard spheres in water, without considering the effect of associated surface water. The presence of surface water greatly affects the effective volume fraction and the rheology of waterborne resins. The surface water effect can be neglected if the size of the resin particle is large, as is the case with most waterborne latex resins. For CUP particles, the surface water can be a dominating factor and the rheology behavior will be quite complicated.

In a previous report, the rheological behavior of  $\text{CO}_2^-$ -functional CUPs in the dilute region (volume fraction  $< 0.10$ ) was shown to be dominated by the tertiary electroviscous effects [11]. The thickness of surface water layer was significant as compared to the size of CUP particles which resulted in the dominant tertiary electroviscous effect. The present research evaluated the rheology and surface tension behavior of  $\text{SO}_3^-$  functional CUPs in relation to  $\text{CO}_2^-$ -functional CUPs.

The associated water fraction and the thickness of the surface water layer were determined based on the relationship of the intrinsic viscosity of the system with the

associated water fraction. Equilibrium surface tension measurements provide information on the effectiveness of CUPs in lowering the surface tension of air-water interface at equilibrium which is governed by the thermodynamics of the CUP particles at the interface. Dynamic surface tension (DST) is important because it gives information on the rate of movement of CUP particles to the air-water interface providing information on the adsorption mechanism and is controlled by the diffusion of CUPs to the interface. DST gives better correlation to actual applications because many important processes like spraying, printing, foaming or coating occur under non-equilibrium / dynamic conditions. The surface tension measurements were performed using the maximum bubble pressure technique.

As shown in Figure 1, the surface charges prevent the CUP particles from aggregating and the charged layer plays an important role in determining the electrophoretic mobility, rheology, and surface tension of CUPs. The present study will first discuss the determination of effective charge based on the theoretical models and then evaluate its effect on the rheology of CUPs. Once the effective charge ( $Q_{eff}$ ), is determined, the effective charge density ( $\sigma$ ), can be expressed as  $\sigma = Q_{eff} / \pi d^2$  where, d is the diameter of CUPs.

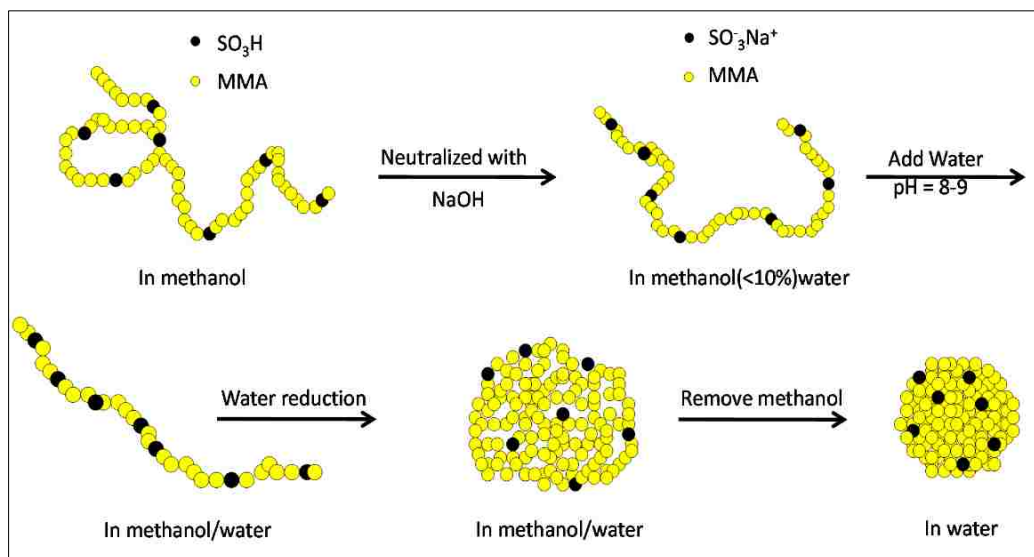


**Figure 1. Process of CUP formation from poly(methyl methacrylate-co-2-acrylamido-2-methyl propane sulfonic acid)**

## 2. THEORETICAL BASIS

### 2.1. Determination of Effective Charge

**2.1.1. Nernst-Einstein model:** The relation between the electrophoretic mobility ( $\mu$ ), the friction coefficient ( $f$ ), and the effective charge ( $Q_{\text{eff}}$ ) expressed as equation 1, is based on the assumption that the counterions surrounding the macroions have no interactions with the macroions [12].

$$\mu = \frac{Q_{\text{eff}}}{f} \quad (1)$$

In case of a spherical particle with radius  $a$ , the friction coefficient ( $f$ ), is related to the diffusion coefficient ( $D$ ), by the Stokes-Einstein theory [12] as equation 2:

$$D = \frac{k_B T}{f} = \frac{k_B T}{6\pi\eta a} \quad (2)$$

Where,  $k_B$  is Boltzman constant,  $T$  is absolute temperature,  $\eta$  is viscosity of solvent. Combining equation 1 and 2, the relation between electrophoretic mobility and effective

charge can be expressed as equation 3 where,  $\mu^\infty$  stands for the electrophoretic mobility at infinite dilution.

$$Q_{eff} = 6\pi\eta a\mu^\infty \quad (3)$$

The advantage of Nernst-Einstein model is its simplicity. As long as the electrophoretic mobility at infinite dilution and particle size is known, the effective charge can be determined. The major disadvantage is that there is no available model to extrapolate the  $\mu^\infty$  for spherical particles.

**2.1.2. Hessinger's model:** If a suspension with low surface pKa is neutralized by a base like sodium hydroxide (NaOH), the conductivity of the suspension and electrophoretic mobility of particle will change correspondingly. When all protons are neutralized, the relationship can be expressed as equation 4 [13].

$$\sigma = ne[Z_{eff}(\mu_p + \mu_{Na^+}) + M(\mu_{OH^-} + \mu_{Na^+})] + \sigma_b \quad (4)$$

Where,  $\sigma$  is the conductivity of suspension,  $n$  is the number density of particles,  $Z_{eff}$  is the effective charge,  $\mu_p$  and  $\mu_{Na^+}$  are the electrophoretic mobility of the particle and sodium ion respectively,  $M$  is the number concentration of small ions per particle defined as  $M=1000*c*N_A/n$  where  $c$  is the concentration of small ions in mol/L and  $\sigma_b$  is the conductivity of the background.

The effective charge can be determined from the dependence of conductivity on the number density of the particles. The method is relatively simple, but it involves measuring the conductivity and electrophoretic mobility, which normally need several instruments.

**2.1.3. Charge renormalization:** The concept of charge renormalization was first raised by Manning [14] and was widely accepted in charge stabilized colloidal suspensions. The basic idea is that some counterions surrounding macro-ions will bind or condense on

the surface of the macro-ion due to minimization of electrostatic repulsion between charges, which causes the effective charge to be smaller than the bare charge of the colloidal particle.

Alexander [15] et al. have done pioneering work on calculating the effective charge for spherical charged particles. The model is based on the assumption that each colloidal particle occupies the center of a spherical Wigner–Seitz (WS) cell [16] with the presence of counterions. Thus, the charge density profile can be readily calculated as well as effective charge.

Alexander's model works well for colloidal particle with known bare charges. For a spherical particle containing weak acid or base groups on the surface, the bare charge is regulated by the dissociation equilibrium at the surface of the particle. Ninham and Parsegian [17] first proposed a model in which the surface of the colloid has ionizable groups which dissociate depending on the counterion atmosphere. The basic idea is that two electro-repulsive surfaces tend to minimize the total free energy.

Based on the free energy concept, Belloni [18] further developed a simple program to calculate the effective charge as long as the particle size, maximum bare charge, pKa, of the ionizable groups, pH of the reservoir solution, and salinity of reservoir are known. It should be noted that even though the sulfonic acid is a strong acid and is completely ionized in water as compared to weaker carboxylic acid, Manning condensation occurs for sulfonate in the presence of sodium counterion, as the concentration of CUP particles increases. The Manning condensation in the case of sulfonate functional particles is usually lower than that for carboxylate functional particles.



## 2.2. Theories Related With Rheology

For dilute suspension with non-charged spheres, which leads to no interaction between particles, the specific viscosity of suspension can be expressed as equation 5:

$$\eta_{sp} = 2.5 * \phi \quad (5)$$

Where,  $\eta_{sp}$  is the specific viscosity of suspension and  $\phi$  is the volume fraction of particles in the solution, according to Einstein's model from the standpoint of Brownian motion [19]. Simha's model can be used to correct Einstein's model when the concentration is high enough to lead to hydrodynamic interactions between particles [20]. The specific viscosity can then be expressed as equation 6:

$$\eta_{sp} = 2.5 * \phi * s(\phi) \quad (6)$$

Where,  $s(\phi)$  is Simha's equation defined as:

$$S(\phi) = 4(1 - \phi^{\frac{7}{3}}) / [4(1 + \phi^{\frac{10}{3}}) - 25\phi(1 + \phi^{\frac{4}{3}}) + 42\phi^{\frac{5}{3}}] \quad (7)$$

For charged particles, the viscosity of suspension gets more complicated due to increased particle interaction and the electroviscous effects need to be considered.

The *primary electroviscous effect* which results from the distortion of a fluid stream near charged spheres has been extensively studied. Hiemenz [21] reports a comprehensive review covering numerous theoretical models right from Smoluchowski's model [22] to Russel's model [23] considering the effect of shearing. Smoluchowski first created the concept of primary electroviscous effect and expressed intrinsic viscosity as:

$$[\eta] = 2.5[1 + 4(\epsilon_r \epsilon_0 \zeta)^2 / k\eta_0 R_s^2] \quad (8)$$

Where,  $\epsilon_r$  is the dielectric constant of solvent,  $\epsilon_0$  is permittivity of vacuum,  $k$  is specific conductivity of the continuous phase,  $\zeta$  is the zeta potential, and  $R_s$  is radius of spheres.

The equation was further modified by replacing the specific conductivity ( $k$ ) of the continuous phase with the Debye length which relates the primary electroviscous effect with the thickness of electrical double layer [24, 25]. In the present study, the most recent analytical expression of primary electroviscous coefficient ( $p$ ), derived by Watterson and White [25] and presented as equation 9 was utilized.

$$p \approx \frac{6\varepsilon_0\varepsilon_r k_B T}{5\eta_0 e^2} \frac{\sum_{i=1}^N n_i^\infty Z_i^2 \lambda_i}{\sum_{i=1}^N n_i^\infty Z_i^2} L(\kappa R_s) \left(\frac{e\zeta}{k_B T}\right)^2 \quad (9)$$

Where,  $\eta_0$  is the viscosity of water,  $Z_i$  is the valence of the ions,  $\lambda_i$  is the drag coefficient of various ions in the solution, expressed as equation 10 with  $\Lambda_i^0$  as the limiting equivalent conductance of each ion.  $L(\kappa R_s)$  is a function of  $\kappa R_s$ , expressed as equation 11.

$$\lambda_i = \frac{N_A e^2}{\Lambda_i^0} \quad (10)$$

$$L(\kappa R_s) = \frac{10\pi}{3} Z(\kappa R_s) (1 + \kappa R_s)^2 \quad (11)$$

Where,

$$Z(\kappa R_s) \approx (200\pi\kappa R_s)^{-1} + \left(\frac{11\kappa R_s}{3200\pi}\right) \text{ for thick double layers, i.e., small } \kappa R_s, \text{ or}$$

$$Z(\kappa R_s) = \left(\frac{3}{2\pi}\right)(\kappa R_s)^{-4} \text{ for thin double layers, i.e., large } \kappa R_s. \quad (12)$$

The zeta potential value was obtained by the relation between effective charge and zeta potential given as:

$$\zeta = \frac{Q_{eff}}{4\pi\varepsilon_0\varepsilon_r R_s (1 + \kappa R_s)} \quad (13)$$

*Secondary electroviscous effect* is typically negligible at low concentration where the primary electroviscous effect dominates. At some concentration, depending on the solvent and surface charge of the particle, the electrical double layer will feel each other, making the suspension structured, which leads to an increase in viscosity. The alignment of the particles due to each other's presence leads to the secondary electroviscous effect.

The contribution of the secondary electroviscous effect to the viscosity of the suspension is proportional to the square of the volume fraction. Russel's rheological model [5], described as equation 14, relates the relative viscosity of suspension to the volume fraction of charged particles and was second order in volume fraction when  $kR_s$  was small and interparticle distance was large.

$$\eta_{rel} = 1 + [\eta]\phi + \frac{2}{5}([\eta]\phi)^2 + \frac{3}{40} \ln\left(\frac{\alpha}{\ln(\alpha)}\right) (\kappa L)^4 \frac{\phi^2}{(\kappa R_s)^5} + B(\phi^3) \quad (14)$$

Where,  $[\eta]$  is the intrinsic viscosity which includes the primary electroviscous effect,  $\alpha$  represent the ratio of electro-repulsion force to Brownian motion (equation 15) and  $L$  is the effective collision diameter (equation 16).

$$\alpha = (4\pi\epsilon_0\epsilon_r\psi_s^2 R_s^2 \kappa) \exp(2\kappa R_s) / k_B T \quad (15)$$

$$L = \kappa^{-1} \ln\left[\frac{\alpha}{\ln(\alpha)}\right] \quad (16)$$

In equation 15,  $\psi_s$  is the surface potential of the charged particle which is calculated using an analytical expression derived by Ohshima [26] shown as equation 17.

$$\psi_s = \frac{k_B T}{ze} \ln\left[\frac{1}{6\phi \ln\left(\frac{1}{\phi}\right)} \left(\frac{ze}{k_B T}\right)^2 \left(\frac{Q_{eff}}{4\pi\epsilon_0\epsilon_r R_s}\right)^2\right] \quad (17)$$

*Tertiary electroviscous effect* is generally applicable to the expansion or contraction of particles due to the change in conformation especially of polyelectrolytes [27, 28]. For rigid spheres, the possible change of radius will be due to adsorption of surfactant or polyelectrolyte to its surface, or a structured water layer. In the CUP suspension, free of electrolyte and surfactant, the only possible tertiary electroviscous effect comes from a structured water layer on the surface of the particle. Assuming that water forms a homogeneous layer with thickness ( $\delta$ ) on surface of particle, the effective volume fraction ( $\Phi_{eff}$ ) can be calculated as:

$$\Phi_{eff} = \phi \left( 1 + \left( \frac{\delta}{R_S} \right) \right)^3 \quad (18)$$

### 2.3. Determination of Intrinsic Viscosity of CUPs

The intrinsic viscosity of uncharged polymer is determined by extrapolating the reduced viscosity to infinite dilution. But there is no general method to determine the intrinsic viscosity of polyelectrolyte solution without added electrolyte. In many cases, the reduced viscosity of polyelectrolytes does not approach a set value when the concentration is dilute. It may increase sharply and sometimes a maximum value was observed [29]. Many methods have been attempted to determine the value of intrinsic viscosity. The method used in the present study was derived from the relation between relative viscosity ( $\eta_{rel}$ ) and volume fraction ( $\phi$ ), in the dilute regime [30] and expressed as equation 19, where  $[\eta]_{\phi}$  is the intrinsic viscosity in terms of volume fraction.

$$\ln(\eta_{rel}) = [\eta]_{\phi} \phi \quad (19)$$

The CUP particles are small, rigid and charged and therefore subject to hydrodynamic interaction and electroviscous effects. In summation of the analysis above, the intrinsic viscosities for each CUP with different molecular weight was determined from the slope of  $\ln(\eta_{rel})$  versus volume fraction. The surface water thickness of CUP particles was estimated using the densities of CUP suspension. The effective charge of CUPs at various volume fractions was determined by using Belloni's [18] program. Based on the effective charge, the Debye-Hückel parameter, zeta potential, primary electroviscous coefficient, and effective collision diameter was calculated. The experimental viscosity was compared with the theoretical viscosity calculated using equation 14. Surface tension measurements were performed for the three CUPs at various volume fractions using the maximum bubble pressure surface tensiometer.

### 3. EXPERIMENTAL

#### 3.1. Materials

Methyl methacrylate (MMA), 2, 2'-azobis (2-methylpropionitrile) (AIBN), n-butanethiol and methanol was purchased from Aldrich. 2-Acrylamido-2-methylpropane sulfonic acid (AMPS) was obtained from Lubrizol and used as received. Absolute anhydrous ethanol was purchased from PHARMCO-AAPER and used as supplied. AIBN was re-crystallized from methanol prior to use. Inhibitor from MMA was removed by washing with 10% aqueous solution of sodium bicarbonate ( $\text{NaHCO}_3$ ), distilled water and brine solution respectively, then dried over anhydrous magnesium sulfate and further purified by distillation. The distillation was carried under copper bromide to prevent polymerization during distillation

#### 3.2. Synthesis and Characterization of Copolymers

Copolymers of MMA and AMPS were prepared in a 3-neck flask equipped with a thermometer, a nitrogen inlet and a condenser fitted with a bubble tower to maintain a positive pressure in the system. MMA (0.81 moles, 81.3 g) and AMPS (0.09 moles, 18.7 g) monomers were charged into the flask in a molar ratio of 9:1 along with the solvent absolute ethanol (250 gram) and n-butane thiol (amount determined by the target molecular weight of the polymer) as the chain transfer agent. AIBN (0.00073 moles, 0.12 gram) was used as the free radical initiator. The reaction was carried out for 24 hours under refluxing conditions.

The polymer solution was then cooled to room temperature and precipitated in cold de-ionized water under high shear and then filtered which removed the unreacted AMPS monomer as it was water-soluble. The traces of un-reacted MMA and solvent (ethanol)

from the polymer were removed in-vacuum. The polymer was then placed into a 50° C vacuum oven for complete drying. Polymers with different molecular weights were synthesized by controlling the amount of chain transfer agent n-butanethiol (0.24, 0.14 and 0.11 g for poly-1, poly-2 and poly-3 respectively). Different molecular weight correspond to different surface charge density.

Acid numbers (AN) were measured by the titration method found in ASTM D 974; modified by using potassium hydrogen phthalate (KHP) in place of hydrochloric acid, and phenolphthalein in place of methyl orange. The titration was performed in methanol as solvent. The density of the dry cup was then measured by a gas displacement pycnometer: Micromeritics AccuPycII 1340. Volume of sample can be calculated as:

$$V_s = V_c + V_r / \left(1 - \frac{P_1}{P_2}\right) \quad (20)$$

Where,  $V_s$  is the sample volume,  $V_c$  is the volume of the empty sample chamber,  $V_r$  is the volume of the reference volume,  $P_1$  is the first pressure (i.e. in the sample chamber only) and  $P_2$  is the second (lower) pressure after expansion of the gas into the combined volumes of sample chamber and reference chamber. Equilibrium flow rate of Helium gas was 0.005psig/min, temperature was controlled at 25.89±0.04 °C. Twenty five readings were made for each sample, and the results were reported by its average and standard deviation. The dry CUP density is important for calculating of theoretical particle size of the CUP particles.

### 3.3. Preparation of CUPs

The purified and dry acrylic copolymers were dissolved in methanol which is a low boiling and water miscible solvent, at a concentration of 10% w/w and stirred overnight

for complete dissolution of the polymer chains. Aqueous sodium hydroxide solution was added to neutralize all the acid groups on the copolymer based on the acid number. Deionized water modified to a pH of 8~9 using 1 molar aqueous NaOH solution was then added to the polymer solution by a peristaltic pump at a rate of 1.24g/minute. The pH of solution was maintained at 8-9 throughout the process of water reduction. Methanol was stripped off under vacuum to give CUPs in VOC free aqueous solution. The CUP solutions were then filtered through 0.45 $\mu$ m Millipore membrane to remove any impurities which were typically less than 0.05%.

Water reduction process: 10 gram of poly (MMA-co-AMPS) was dissolved in 90 gram of methanol to make a 10% w/w solution. The sulfonic acid groups on the CUP particles were neutralized by adding aqueous NaOH solution (1 molar) and 190 gram of deionized water was then added by means of a peristaltic pump. Methanol was then stripped off in vacuum and the sample was further concentrated by stripping off water to give a 10.0 % w/w CUP solution of poly (MMA-co-AMPS) in water. The CUP solution was filtered through a 0.45 micron filter to remove any impurities which were typically found to be less than 0.05% solids. The CUP suspensions were characterized for their shearing and absolute viscosity, particle size and equilibrium and dynamic surface tension as shown below. The viscosity measurements were performed using a capillary viscometer, a programmable rheometer and the surface tension measurements were performed on a bubble surface tensiometer. The surface tensiometer measures the pressure difference between two capillaries of different diameter and the maximum pressure difference corresponds to the surface tension of the liquid in which the capillaries are immersed.

### 3.4. Characterization of CUPs

**3.4.1. Shearing viscosity.** The solutions were tested for shearing viscosity on a Brookfield LV DVIII viscometer, using 1ml of sample for each run. After each run, the sample was diluted with Milli-Q ultrapure water to the next concentration. The solutions were run at each whole percent from the most concentrated to 1%, and at 0.5% CUP.

**3.4.2. Absolute viscosity of CUP solutions.** The absolute viscosity of CUP suspension was measured using the Ubbelohde capillary viscometer which was maintained at  $25.0 \pm 0.1$  °C using a constant temperature water bath. The suspensions were equilibrated for 30 minutes. Evaporation and CO<sub>2</sub> contamination was avoided by covering the viscometer with a plastic wrap. A stop watch with 0.01 second precision was used to monitor the elution time. The estimated standard error was within 0.5%. Absolute viscosity was calculated by equation 21.

$$\eta = t \cdot d \cdot c \quad (21)$$

Where, t, d, and c were elution time, density of the solution and constant of Ubbelohde with units of second, g/ml and cP/second, respectively. The relative viscosity of solution was calculated as:

$$\eta_r = \eta / \eta_0 \quad (22)$$

Where,  $\eta_0$  is the viscosity of water (0.89 cP at 25<sup>0</sup> C).

**3.4.3. Particle size of CUPs.** Particle size of CUPs was measured by dynamic light scattering technique, using the instrument Microtrac Nanotrac 250. The viscosity of suspension was used instead of water because the charged groups on the surface of CUP particles increased the viscosity of the suspension affecting the diffusion coefficient. The details of this observation are reported elsewhere [31].



**3.4.4. Surface tension measurement.** The maximum bubble pressure [32] method was used to measure the surface tension because of its advantages over other methods such as the Du Noüy ring method [33], oscillating jet method [34], drop methods [35]. First, since the measurement was done inside the dispersion, the effect of humidity, air turbulence, and contamination of carbon dioxide were avoided. Secondly the operation and cleaning after testing was easier. Sensadyne PC-500 LV was used to measure the surface tension of CUP suspensions. Suspensions were equilibrated in a constant temperature water bath at  $25 \pm 0.1$  °C. The tensiometer was calibrated with analytical reagent 100 % absolute ethanol and Milli-Q ultrapure water. Flow rate of nitrogen gas was 40ml/minute and flow pressure was maintained at 25 psi. An average of three readings with less than 0.1 dyne/cm difference was reported. For dynamic surface tension, the maximum and minimum bubble rate were determined as the rate beyond which the surface tension did not change.

## 4. RESULTS AND DISCUSSION

### 4.1. Acid Number and Density

The acid number and densities of the copolymers were listed in Table 1. It shows that the composition of the copolymers had similar acid numbers. The densities of the dry CUP increased with increasing molecular weights as expected since the weight fraction of end groups decreased with increasing molecular weight [36]. The last column indicates the molecular weight of the three copolymers. The molecular weight was determined based on its relationship with the particle radius and density as demonstrated in the case of globular proteins.

**Table 1.** % Yield, acid number and density of the copolymers

sample ID	% Yield	Calculated acid value <sup>a</sup>	Measured acid value <sup>a</sup>	$\rho_p$ (g/cc)	MW <sup>b</sup>
Polymer 1	75	46.8	47.1	1.1971±0.0015	28K
Polymer 2	77	46.8	46.9	1.2016±0.0020	56K
Polymer 3	71	46.8	48.1	1.2396±0.0017	80K

a- mg KOH / g polymer, b-  $MW = \frac{\pi d^3 \rho_p N_A}{6}$ ,  $N_A$  = Avogadro's Number

#### 4.2. Particle Size Analysis

The particle size of the CUPs was measured by Microtrac Nanotracer 250 with dynamic light scattering. Table 2 shows the measured particle size for the three CUP suspensions using the DLS. The DLS measured particle size based on the Doppler shift principle where the scattered light is Doppler shifted due to Brownian motion. The viscosity of the sample also affects the diffusion coefficient. The experimental and the theoretical particle size calculated based on the density and the molecular weight of copolymer were in good correlation. This indicated a unimolecular collapse of polymer chains to form CUPs.

**Table 2.** Particle size of CUP measured from Nanotracer 250

sample ID	Measured diameter using DLS(nm)
polymer 1	4.2
polymer 2	5.3
polymer 3	5.9

### 4.3. Specific Viscosity of CUP Suspension

The specific viscosities of CUP suspensions were measured and plotted against volume fractions for the three polymers. Figure 2 shows the specific viscosities of the three polymers at low volume fractions ( $< 0.10$ ). For comparison, the viscosity of a carboxylate functional CUP (M.W=28K) was also shown. The polymer synthesis and water-reduction process for methyl methacrylate-methacrylic acid (MMA-MAA) copolymer has been discussed elsewhere [11].

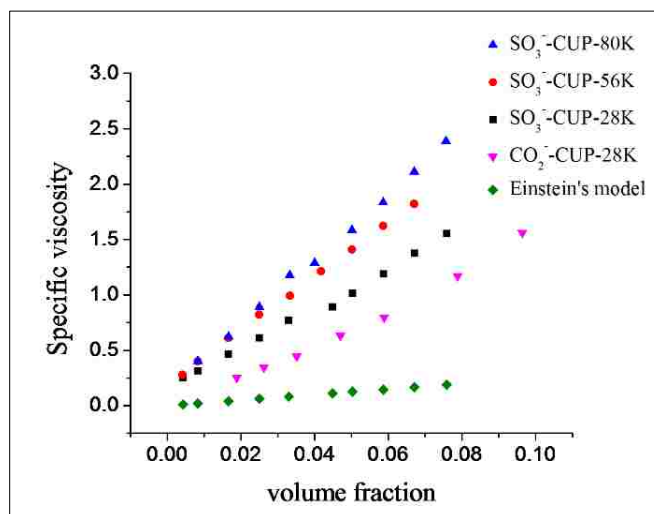


**Figure 2. Plot of specific viscosity of the three sulfonate functional and one carboxylate functional CUP solutions as a function of volume fraction**

The experimental viscosity for all of the samples deviated from Einstein's model even for the dilute regime (volume fraction  $< 0.10$ ). The sulfonate functional CUP had higher viscosity than the carboxylate functional CUP at similar molecular weight (28K) and volume fraction which was attributed to the higher hydrophilic nature of sulfonate group. The sulfonate group has three hydrogen bond acceptors (oxygen atom) compared to

two for carboxylates. The higher hydrogen bonding possibly contributed to a thicker surface water layer and higher associated water fraction on the sulfonate CUPs. It is also reported in literature that sulfonate group is more hydrophilic than carboxylate and the secondary amide group present on the AMPS monomer also interacts strongly with water, thereby increasing the contribution of the tertiary electroviscous effect to the overall CUP solution viscosity [37, 38].

Oncley [39] has shown that the thickness of water layer on the surface of charged particles could be determined from the intrinsic viscosity of the suspension. The intrinsic viscosity could be determined from the slope of a plot of  $\ln(\text{relative viscosity})$  versus volume fraction of CUP particles. This relation is typically used in the case of charged polyelectrolytes. Figure 3 shows the plot of  $\ln(\text{relative viscosity})$  versus volume fraction for the three  $\text{SO}_3^-$ -CUPs and the calculated values of intrinsic viscosity, surface water thickness and bound water fraction were shown in Table 3.

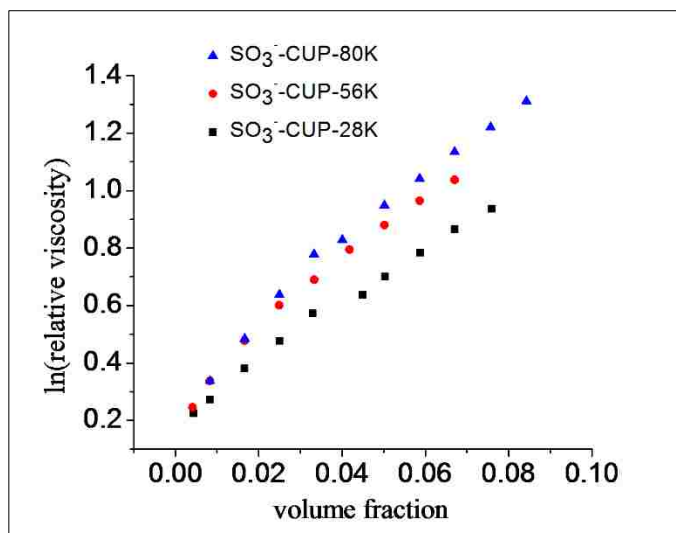


**Figure 3.** Plot of  $\ln(\eta_{\text{rel}})$  versus volume fraction for sulfonate functional CUPs

The associated water fraction,  $\beta$ , defined as the weight ratio of surface water to CUP molecules was calculated by using equation 23 [21] where  $\rho_1$  is the density of water (0.997 g/cc) and  $\rho_2$  is the density of CUP at 25<sup>0</sup> C. Assuming that each particle is spherical and surrounded by a uniform layer of water molecules with thickness  $\delta$ , then  $\delta$  can be expressed as equation 24.

$$\beta = \frac{\rho_1}{\rho_2} \left( \frac{[\eta]}{2.5} - 1 \right) \quad (23)$$

$$\delta = R_s \left[ \left( \frac{\beta \rho_2}{\rho_1} \right)^{\frac{1}{3}} - 1 \right] \quad (24)$$

Table 3 indicated that there was significant amount of water associated with the surface of CUP particles. The surface water can form hydrogen bond with the sulfonate functional groups on the surface of the CUP particles. The thickness of water layer increased with increasing molecular weight of the copolymer. As discussed below, each sulfonate functional group can form six hydrogen bonds using the three oxygen atoms with two lone pair of electrons each, in the sulfonate group. Assuming that all the acid groups on the CUP particle were on the surface, and were completely neutralized and dissociated, the bare surface charge density for spherical CUP particles can be estimated by equation 25.

$$\sigma = \left( \frac{MW}{4\pi} \right)^{\frac{1}{3}} \cdot \left( \frac{3}{\rho N_A} \right)^{-\frac{2}{3}} \cdot \frac{e}{m_{MMA}b + m_{MAMPS}} \quad (25)$$

Where,  $\rho$  is the density of polymer,  $N_A$  is the Avogadro number,  $q$  is the elementary charge,  $m_{MMA}$  is the molecular weight of methyl methacrylate,  $m_{MAMPS}$  is the molecular weight of sulfonic acid functional monomer, and  $b$  is the molar ratio of MMA to AMPS.

**Table 3.** Intrinsic viscosity, associated water fraction and surface water thickness of SO<sub>3</sub><sup>-</sup>-CUPs

CUP	$[\eta]_{\phi}$	$\Delta[\eta]_{\phi}$ <sup>a</sup>	Adj. R <sup>2</sup>	$\beta$ <sup>b</sup>	$\delta$ (nm)
SO <sub>3</sub> <sup>-</sup> -CUP-28K	9.90	0.24	0.992	2.47	0.92
SO <sub>3</sub> <sup>-</sup> -CUP-56K	12.4	0.30	0.983	3.29	1.55
SO <sub>3</sub> <sup>-</sup> -CUP-80K	12.8	0.28	0.984	3.31	1.78

a) Standard error of  $[\eta]_{\phi}$ ; b) associated water fraction (gram water per gram CUP)

The density of polymer and  $b$  was similar for the three polymers from Table 1 and therefore the surface charge density increased linearly with the cube root of the polymer molecular weight. The radius of the particle can be expressed as  $R_s = \left(\frac{3 \cdot MW}{4\pi\rho N_A}\right)^{1/3}$ , which indicated that the radius of CUP particle was also proportional to its molecular weight. Therefore, the bare surface charge density was proportional to the particle size. As the particle size increased, the number of sulfonate groups at the CUP surface per unit area and the counterions also increased. Therefore more water aligned at the surface to dissipate the charges, increasing the associated water fraction. This increased the contribution of the tertiary electroviscous effect to the overall viscosity.

The viscosity increase with molecular weight could also be partly due to the hydrodynamic effects because the higher the molecular weight of the polymer, the larger is the hydrodynamic volume which increases the contribution of hydrodynamic effects to the viscosity. Rattanakawin<sup>2</sup> et al. have demonstrated that the hydrodynamic effects are negligible as compared to the electroviscous effect for spherical charged colloid particles and therefore could be neglected. Chen<sup>11</sup> had indicated that the associated water fraction

for  $\text{CO}_2^-$ -CUP (MW=28K) was 2.3. The sulfonate functional CUP (MW=28K) had a higher associated water fraction as compared to carboxylate functional CUP which was attributed to the higher effective charge and greater hydrogen-bonding capability of the sulfonate functional CUPs. At each volume fraction, the effective charge calculated using Belloni's program for the sulfonate functional CUP was higher than that of the carboxylate functional CUP. Based on molecular dynamic simulations, Yan et al. [40] reported that at similar charge density, the sulfonate group had a larger hydration number (8-14) than the carboxylate (5-7) because of the higher number of oxygen atoms with which the water molecules could hydrogen bond. Figure 4 shows a pictorial representation of the variation in the thickness of the hydration layer on the  $\text{SO}_3^-$  and  $\text{CO}_2^-$ -CUP surface. The thickness of water layer on the sulfonate functional CUPs was thicker than that on the carboxylate functional CUPs.

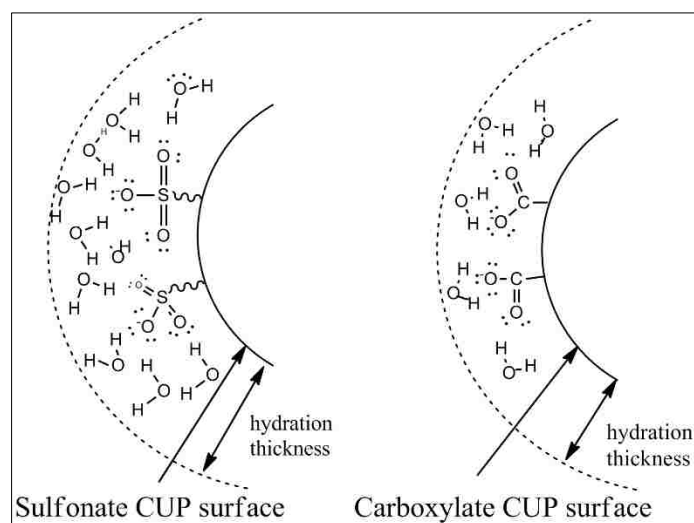


**Figure 4. Representative structure of  $\text{SO}_3^-$  and  $\text{CO}_2^-$ -CUP surface with hydration layer**

#### 4.4. Surface Water Density

Recent studies on the states of water in latex resins report that the density of bulk water differs from the density of water associated with a latex particle [41]. But the contribution of the hydrophilic surface charged groups towards the surface water density has been difficult to quantify due to the large particle size of latex resins [42]. To put it into context, for CUP particles with a 3.3-nm radius, the volume fraction occupied by surface water is about 61 % of the CUP particle volume. But the ratio of surface water to latex by volume is only 1.72 % for a typical commercial latex resin with particle diameter of 100 nm, assuming same thickness of associated water for both CUPs and the latex resin. Therefore, determining the associated water density becomes more difficult. Van De Mark et al. [43] reported a simple method to determine the density of surface water on  $\text{CO}_2^-$ -CUPs, based on the relationship between the surface water (S), the bulk water (B), and the particle volume fraction ( $\Phi_p$ ).

A similar analysis for the surface water density on  $\text{SO}_3^-$ -CUPs was performed in the following manner: The summation of volume fraction for the CUP system composed only of CUP particles, associated water and bulk water is one [43], as shown in equation 26:

$$\Phi_p + \Phi_{H_2O,S} + \Phi_{H_2O,B} = 1 \quad (26)$$

Based on the conservation of mass of the total material [43] equation 27 is obtained:

$$m_s = m_p + m_{H_2O,S} + m_{H_2O,B} \quad (27)$$

Where,

$$m_p = \rho_s * f \quad (28)$$

$$m_{H_2O,S} = \rho_{H_2O,S} * \Phi_{H_2O,S} \quad (29)$$



$$m_{H_2O,B} = \rho_{H_2O,B} * \Phi_{H_2O,B} \quad (30)$$

And,  $\Phi$  denotes the volume fraction,  $m$  denotes the mass and  $\rho$  denotes the density for each material and  $\rho_s$  denotes density of CUP dispersion.

The relation between the volume fraction of CUP particle and the surface water [41] can be expressed as equation 31:

$$\Phi_{H_2O,S} = \left[ \left( 1 + \delta/r \right)^3 - 1 \right] * \Phi_p \quad (31)$$

Where,  $r$  denotes the radius of CUP particle. Based on equation 27 through 31, equation 26 was solved to obtain equation 32:

$$1/\rho_s = af + b \quad (32)$$

Where,

$$b = \frac{1}{\rho_{H_2O,B}} \text{ and } a = \frac{(1+\delta/r)^3}{\rho_p} - \frac{1}{\rho_{H_2O,B}} - \frac{\rho_{H_2O,S}}{\rho_p * \rho_{H_2O,B}} * \left[ \left( 1 + \delta/r \right)^3 - 1 \right] \quad (33)$$

Equation 32 represents the equation of a straight line for the plot of  $1/\rho_s$  vs  $f$ , where,  $f$  denotes the weight fraction of CUP particles and  $\rho_s$  denotes the density of CUP dispersion at the corresponding weight fraction. The density of CUP dispersion at various weight fractions was measured using a pycnometer and a graph of  $1/\rho_s$  vs  $f$  was plotted as shown in Figure 5. The plot gives a linear curve which was fitted with a straight line equation. The slope value from the curve indicated the value of 'a' in the equation 33. Using the value of 'a' the density of surface water could be calculated.

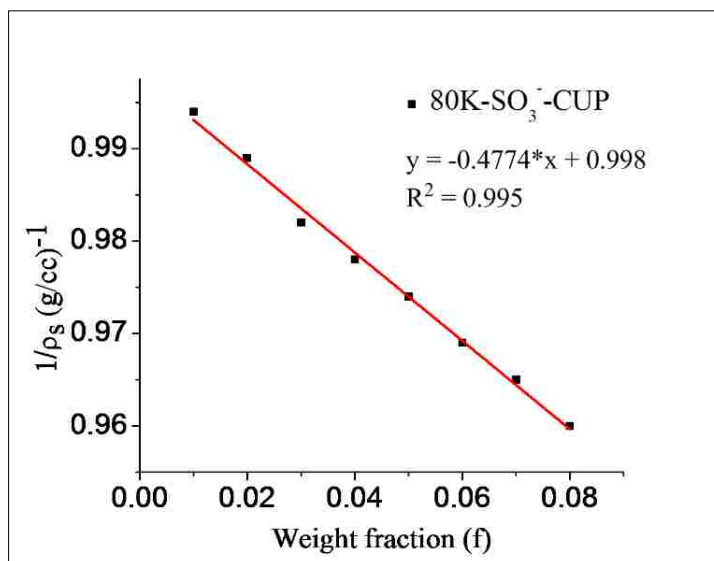


**Figure 5. Effect of weight fraction (f) on  $1/\rho_s$**

Surface water density ( $\rho_{H_2O,S}$ ) was calculated using equation 33 by substituting the slope value obtained from Figure 5 for the value of 'a'. The density of surface water for  $SO_3^-$ -CUP was 1.0971 g/cc which was 10.0% larger than the density of bulk water (0.997 g/cc) at 25 °C. The surface water density reported by Van De Mark et al. [43] for  $CO_2^-$ -CUP was 7.18% larger (1.0688 g/cc) than the bulk water density. The higher density of surface water for sulfonate as compared to carboxylate CUP could be attributed to the difference in the structure of water around the respective functional groups. The sulfonate group has higher hydration number as compared to the carboxylate which could result in a more compact hydration layer and therefore increased surface water density [38].

#### 4.5. Rheological Model Fitting

The experimental viscosity was fit with Russel's model and the theoretical viscosity calculated using equation 14. The effective charge ( $Z_{eff}$ ) was calculated using Belloni's

program and the primary electroviscous coefficient was determined using equation 9. The values of  $\alpha$  and L were calculated using equation 10 and 11 respectively. For  $\alpha$ , it's factor 'A' ranges from 0.6 to 1, so there exist a minimum and a maximum value of  $\alpha$  and therefore a minimum and maximum value for the theoretical expected viscosity. The Debye-Hückel parameter (k) was calculated using equation 34 where, pH is the pH value of the solution. Table 4 lists the values for some of the intermediate calculated parameters.

$$\kappa^2 = \frac{e^2}{\epsilon_0 \epsilon_r k_B T} (nZ_{eff} + 2000N_A \cdot 10^{pH-14}) \quad (34)$$

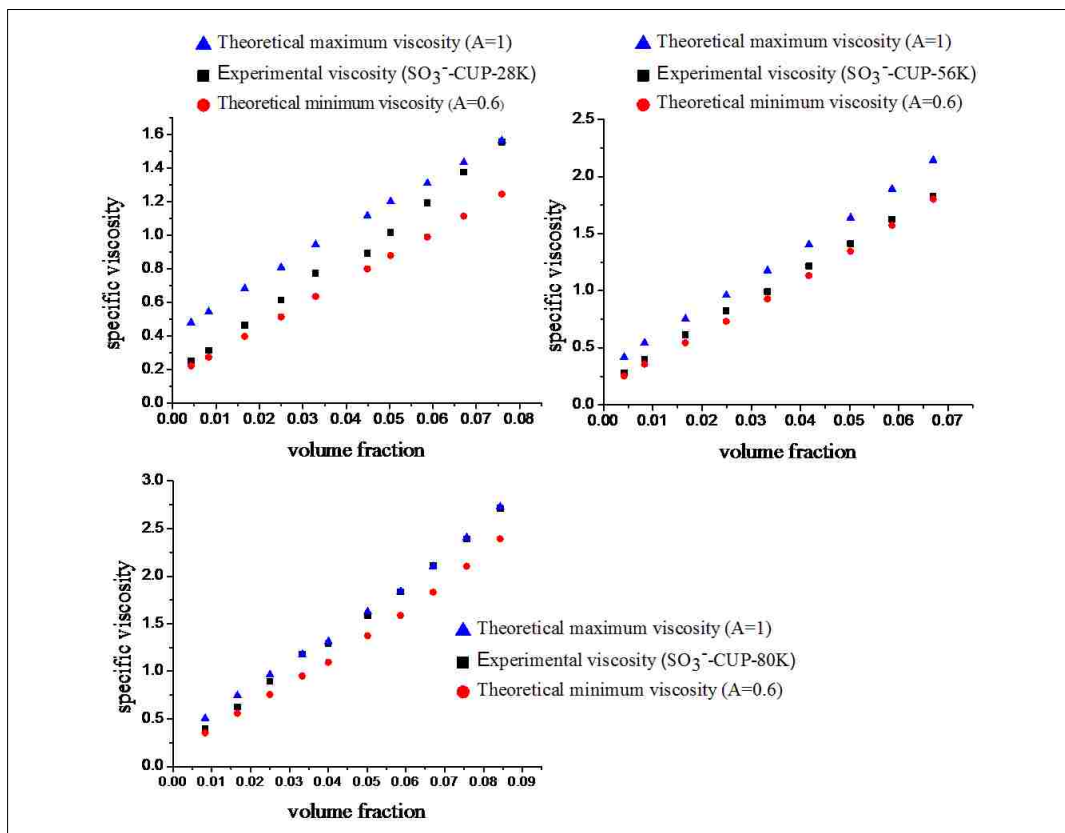
In equation 14, the first two terms include the contribution of primary electroviscous effect, tertiary electroviscous effect and hydrodynamic interaction. The second term contains a  $\phi^2$  term which is related with hydrodynamic interaction. The term  $\alpha$ , which is the ratio of electrorepulsion force to Brownian force, takes into consideration the contribution of secondary electroviscous effect. Thus the contribution from each electroviscous effect can be calculated and the theoretical viscosity was plotted with the experimental viscosity as shown in Figure 6.

Table 4 shows that the primary electroviscous coefficients decreased with increasing volume fraction. As the volume fraction of polymer was increased, the number of counterions also increased which shortened the electrical double layer. There was less distortion of the double layer and therefore less energy dissipation which reduced the contribution of the primary electroviscous effect to the viscosity. The effective collision diameter decreased with increasing volume fraction which indicated that the secondary electroviscous effect would become more prominent when the effective collision diameter became of the order of the actual CUP diameter.

**Table 4.** Effective Charge, surface potential, effective collision diameter, primary electroviscous coefficient and specific viscosity of CUP suspension at various volume fractions for carboxylate-CUP (28K) and the three sulfonate-CUPs

Polymer	Volume fraction	$Z_{\text{eff}}$	$\psi_s^c$	L (nm)	P	$\eta_{\text{sp}}^a$
CO <sub>2</sub> <sup>-</sup> -CUP (28K)	0.0189	9.21	0.079	11.1	0.16	0.25
"	0.0262	8.70	0.070	9.70	0.13	0.35
"	0.0352	8.29	0.062	8.61	0.11	0.44
"	0.0470	7.80	0.054	7.61	0.09	0.63
"	0.0589	7.42	0.047	6.90	0.08	0.79
"	0.0789	6.93	0.039	5.89	0.06	1.17
"	0.0964	6.61	0.034	5.32	0.06	1.56
SO <sub>3</sub> <sup>-</sup> -CUP (28K)	0.0043	11.9	0.122	23.8	0.38	0.25
"	0.0083	10.2	0.101	18.6	0.22	0.31
"	0.0166	9.90	0.085	14.6	0.16	0.46
"	0.0250	9.73	0.076	12.6	0.13	0.61
"	0.0330	9.55	0.071	11.5	0.12	0.77
"	0.0449	9.20	0.063	10.3	0.10	0.89
"	0.0503	8.91	0.060	9.91	0.10	1.01
"	0.0587	8.69	0.055	9.32	0.09	1.19
"	0.0671	8.40	0.052	8.79	0.08	1.37
"	0.0759	8.21	0.048	8.31	0.07	1.45
SO <sub>3</sub> <sup>-</sup> -CUP (56K)	0.0041	31.5	0.163	30.5	1.30	0.27
"	0.0083	29.8	0.146	24.2	0.91	0.40
"	0.0166	29.6	0.131	19.3	0.72	0.61
"	0.0249	29.5	0.124	16.9	0.65	0.82
"	0.0333	29.4	0.118	15.5	0.61	0.99
"	0.0418	29.1	0.113	14.5	0.59	1.21
"	0.0502	28.0	0.109	13.8	0.57	1.41
"	0.0587	28.5	0.105	13.2	0.53	1.62
"	0.0670	27.9	0.103	12.8	0.52	1.82
SO <sub>3</sub> <sup>-</sup> -CUP (80K)	0.0041	53.5	0.183	33.4	2.47	0.28
"	0.0083	47.3	0.163	26.9	1.58	0.40
"	0.0166	44.1	0.145	21.7	1.15	0.63
"	0.0250	43.7	0.137	19.1	1.05	0.89
"	0.0333	44.3	0.132	17.5	1.04	1.18

The theoretical relative viscosity obtained using Russel's model was converted into specific viscosity based on standard calculations and then plotted against volume fraction. Figure 6 shows that the theoretical viscosity predicted using Russel's model and the experimental viscosity gave a good correlation with each other. The theoretical viscosity varied from minimum to maximum values based on the value of coefficient A which varies from 0.6 to 1 in the equation for alpha, which is the ratio of electro-repulsion force to Brownian force. The experimental viscosity was within the calculated theoretical minimum and maximum viscosity.



**Figure 6. Comparison of experimental and theoretical specific viscosity for  $\text{SO}_3^-$ -CUP (28K, 56K and 80K)**

#### 4.6. Surface Tension Measurement

Figure 7 shows the plot of equilibrium surface tension behavior of the three sulfonate-functional CUPs versus the concentrations. For comparison, surface tension of carboxylate-functional CUP with molecular weight of 28K was also shown. Surface tension of all the suspensions decreased linearly with increasing concentration of CUPs. The reduction in surface tension was similar to that observed for typical surfactants; the higher the concentration of the surface active groups, the lower is the surface tension. Typical surfactants show a critical micelle concentration above which the surface tension does not decrease, but no such point was observed in the case of CUP particles in the concentration range evaluated.

Increasing the CUP concentration also increased the counter-ion concentration (sodium ions), some of which condensed on the CUP surface reducing its effective charge (Manning condensation [14]). The counterion condensation causes the effective charge to be lower than the bare surface charge and allows more number of CUP particles with better packing at the air-water interface. At the same time, the total number of charged groups at the air-water interface increased because only a small fraction of the charged groups on the CUP surface undergo Manning condensation. Therefore, the electrostatic repulsion increased at the air-water interface which reduced the surface energy of the system. The overall effect was a reduction in the equilibrium surface tension with increasing concentration of CUPs. The sulfonate functional CUPs showed greater surface tension reduction than the carboxylate functional CUPs.

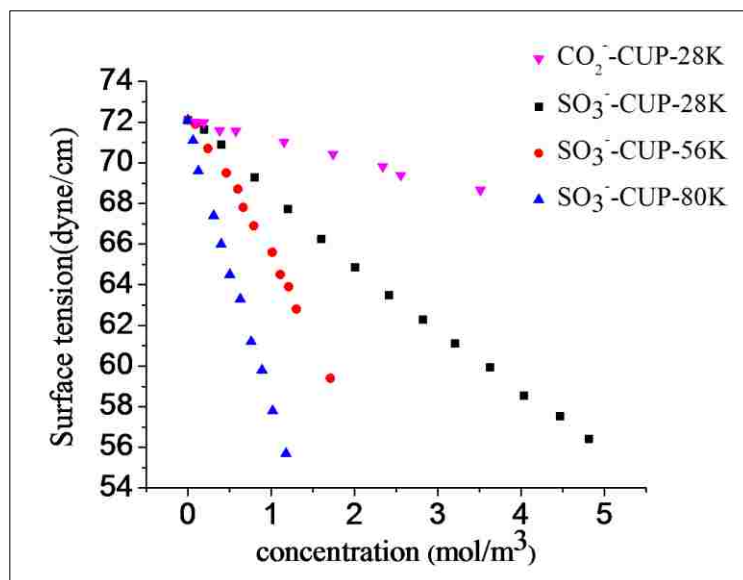


**Figure 7. Surface tension of CUP suspension as a function of concentration**

It is remarkable that the surface activity of CUPs increased with molecular weight. Okubo [44] observed similar behavior for the surface activity of methyl polyethylenimine which increased with molecular weight and was attributed to the increase in hydrophobicity of the backbone with increasing molecular weight. In the case of CUPs, the spherical nature of CUPs precludes any contribution from steric hindrance and rather it is the increasing surface charge per unit area which leads to increased surface activity. The individual polymer chain was composed of 9:1 ratio of MMA (M.W = 100): AMPS (M.W = 207) on an average. There was one AMPS group for every 1107 Da of polymer and therefore, the polymer with 28K, 56K and 80K molecular weight had on an average, 25, 51 and 72 AMPS groups respectively, per particle.

Particles at an interface can either have attractive (van der Waals) or repulsive forces (electrostatic) between them which determines the change in the surface energy. The surface energy increases due to van der Waals attractive force which in turn increases the

surface tension because increasing surface energy requires more work to distort the surface [45].

Vafaei et al. [46] have shown that Bismuth telluride nanoparticles with surface carboxylate groups reduced the surface energy via electrostatic repulsion and therefore reduced the surface tension. CUP particles with charged sulfonate groups repelled each other when adsorbed at the air-water interface and possibly reduced the surface energy of the system, therefore, lowering the surface tension. CUPs with higher molecular weight though slightly larger in size, had more charged groups per unit area on the surface and therefore had increased electro-repulsion which gave greater reduction in surface tension. The sodium counterion condensation at the air-water face also possibly resulted in better packing of the CUP particles at the interface. The sodium ion helps to align negatively charged CUPs at the interface.

The sulfonate-functional CUPs showed greater reduction in surface tension compared to carboxylate-functional CUPs mainly due to the higher effective charge of the sulfonate CUPs. As shown in Table 4, for similar molecular weight (28K), the  $\text{SO}_3^-$ -CUPs had higher effective charge than  $\text{CO}_2^-$ -CUPs at each volume fraction and therefore reduced the surface energy to a greater extent and helped to lower the surface tension to a higher degree.

Another influencing factor could be the contact angle reduction due to the particles at the interface. Typically as the surface tension is reduced, the contact angle of the adsorbed particle at the air-water interface also decreases [47, 48]. Okkema and Cooper [49] have demonstrated that the sulfonate group being more polar and hydrophilic than the carboxylate, gave lower contact angle at the air water interface. Therefore, the sulfonate-CUPs gave lower surface tension than the carboxylate-CUPs.



Figure 8 shows the plot of dynamic surface tension against surface age for the three  $\text{SO}_3^-$ -CUPs and  $\text{CO}_2^-$ -CUP (28K) at a concentration of  $0.5 \text{ mole/m}^3$ . Surface age is the time interval between the onset of bubble growth and the moment of maximum pressure. Therefore as the surface age was increased, the bubble rate reduced which gave the CUP particles more time to reach the air (bubble)-water interface.

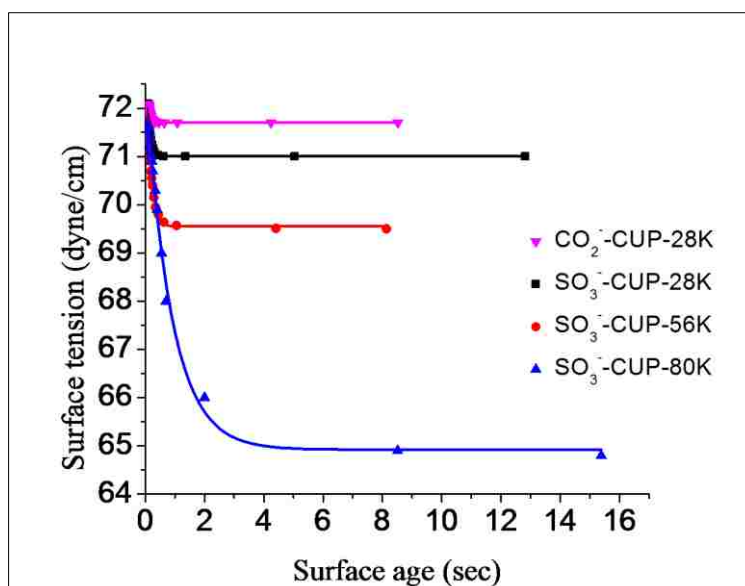


**Figure 8. Dynamic surface tension versus surface age for the three  $\text{SO}_3^-$ -CUPs and  $\text{CO}_2^-$ -CUP-28K**

The data gave a good exponential fit represented by the equation 35. The fitting parameters were shown in Table 5. The kinetic relaxation parameter corresponds to the time required for the surfactant to reach equilibrium surface tension value which is a function of different parameters.

$$y - y_0 = A * \exp(-t/\tau_k) \quad (35)$$

Figure 8 indicated that with increasing molecular weight, the CUP particles took longer time to reach the equilibrium surface tension. The exponential relaxation of surface tension is consistent with a kinetically limited adsorption (KLA) reported by Diamant et al. [50]. The relaxation time ( $\tau_k$ ) indicating the half-time in reaching equilibrium surface tension and obtained as a fitting parameter, increased with increasing molecular weight as shown in Table 5 and indicated a barrier to surface adsorption via electrostatic repulsion.

**Table 5.** Fitting parameters for DST versus surface age at 0.5 mole/m<sup>3</sup>

CUP system	$y_0$	A	B	R <sup>2</sup>
CO <sub>2</sub> <sup>-</sup> -CUP-28K	71.7	1.67	0.078	0.997
SO <sub>3</sub> <sup>-</sup> -CUP-28K	71.0	3.37	0.084	0.995
SO <sub>3</sub> <sup>-</sup> -CUP-56K	69.6	5.11	0.136	0.999
SO <sub>3</sub> <sup>-</sup> -CUP-80K	64.9	7.64	0.990	0.997

Van De Mark et al. [31] have shown that for accurate particle size measurement of CUPs using DLS, the viscosity of the solvent needs to be replaced by the viscosity of the solution because of electroviscous effects. The collective diffusion coefficient ( $D_c$ ) was approximated from the generalized Stokes-Einstein's expressed as equation 36, relating the collective diffusion coefficient to the radius of particle ( $r$ ) measured using DLS and the viscosity of the solution ( $\eta$ ) at 25 °C [51].

$$D_c = \frac{k_b * T}{6 * \pi * \eta * r} \quad (36)$$

Where,  $k_b$  is the Boltzmann constant and T is the absolute temperature of the solution.

The diffusion coefficients ( $D_c$ ) were calculated to be 1.30, 0.66 and 0.49 ( $10^{-6}$  cm<sup>2</sup>/s) for the 28K, 56K and 80K- SO<sub>3</sub><sup>-</sup>-CUPs (each at a volume fraction of 0.05) respectively. Therefore the SO<sub>3</sub><sup>-</sup>-CUP-80K taking more time to reach equilibrium surface tension could be explained by a slower diffusion of the higher molecular weight CUP to the air-water interface.

Figure 9 shows the dynamic surface tension data for the three sulfonate CUPs at different concentrations which was fit to the equation 34 and the kinetic relaxation time ( $\tau_k$ ) was shown in Table 6. The relaxation time required to reach equilibrium surface tension increased with increasing concentration of CUPs.

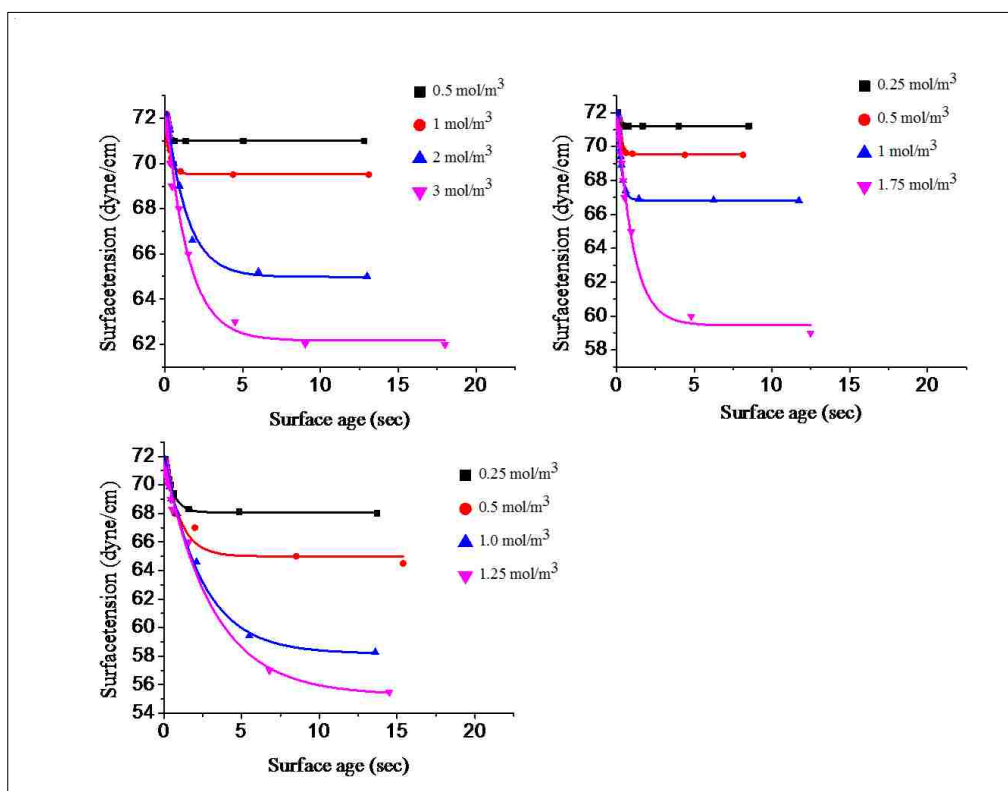


**Figure 9. Dynamic surface tension versus surface age at various concentrations for the three SO<sub>3</sub><sup>-</sup>-CUPs: a) 28K, b) 56K and c) 80K CUP**

**Table 6.** Relaxation time ( $\tau_k$ ) for the three sulfonate-CUPs at various concentrations

SO <sub>3</sub> <sup>-</sup> -CUP	Concentration (mole/m <sup>3</sup> )	$\tau_k$ (sec)	R <sup>2</sup>
28K	0.50	0.084	0.995
"	1.01	0.234	0.999
"	1.48	1.324	0.992
"	1.97	1.431	0.993
56K	0.25	0.083	0.997
"	0.50	0.136	0.999
"	1.04	0.242	0.999
"	1.76	1.007	0.997
80K	0.25	0.527	0.998
"	0.50	0.990	0.980
"	1.01	2.436	0.996
"	1.25	3.135	0.993

There are two factors at play in the case of CUP solutions: the viscosity of the solution and the distance required to travel to reach the air-water interface. As the concentration was increased, the viscosity of CUP solution also increased, slowing the diffusion of CUP particles to the air-water interface. Increasing the concentration also increased the probability of a CUP particle getting adsorbed at the air-water interface and decreased the distance needed to travel to reach the interface. The overall effect was an increase in the relaxation time to reach equilibrium which indicated that the CUP particles took longer time to reach the air-water interface. This observation is important from the point of view of applications for the CUP particles, where the rate of surface tension reduction is of prime importance.

## 5. CONCLUSIONS

The rheological and surface tension behavior of the strong-acid (sulfonic acid) containing CUP particles was studied and related with our previous work for the weak-acid (carboxylic acid) containing CUP particles. At similar molecular weight, the sulfonate functional CUP had a higher bound water fraction than the carboxylate functional CUP because of a higher surface charge density and higher hydrogen-bonding capability. The theoretical viscosity predicted by Russel's model gave a good fit to the experimental viscosity in the dilute concentration regime (volume fraction  $< 0.1$ ).

The sulfonate-functional CUPs showed higher surface activity than the carboxylate-functional CUPs which was attributed to greater surface energy reduction due to higher electrostatic repulsion and lower contact angle due to higher hydrophilicity. Dynamic surface tension studies revealed that the rate of surface tension reduction was a function of the molecular weight of the polymer and the surface charge density of the CUP particle. The understanding of rheology and surface tension behavior would be useful when one would specifically want to influence either one of the property without affecting the other. To increase the viscosity of a system without significantly affecting its surface tension the use of low molecular weight carboxylate functional CUPs at a higher concentration would be profitable. Similarly, to lower the surface tension of the system without significant increase in viscosity, the use of high molecular weight sulfonate functional CUPs at low concentration would be recommended. The surfactant free, zero-VOC nanopolymer systems have demonstrated excellent properties when used as film-formers [52, 53] and many more applications are currently being evaluated for the resins and coatings industry.

## 6. ACKNOWLEDGEMENTS

The authors would like to acknowledge the Coatings Institute and the Department of Chemistry of Missouri S&T for the financial support and resources. We thank Dr. Luc Belloni from Department of Molecular Chemistry Centre, d'Etudes de Saclay, 91191 Gif-sur-Yvette Cedex, France for the program to calculate effective charge. We thank Dr. Nicholas Leventis of Missouri S&T University for measuring the density of the dry polymers. We thank our fellow researchers: Sagar Gade, and Yousef Dawib for their help.

## 7. REFERENCES

- 1) Chang YH, Lee YD, Karlsson OJ, Sundberg DC. *Polymer* 2000;41:6741-6747.
- 2) Rattanakawin C, Hogg R. *Minerals Engineering* 2007;20:1033-1038.
- 3) Vinogradov SV, Bronich TK, Akabanov AV. *Adv Drug Deliver Rev* 2002;54:135-147.
- 4) James RO, Parks GA. *Surface and Colloid Science* 1982;12:119-216.
- 5) Russel WB, *J Fluid Mech* 1978;85:209-232.
- 6) Fritz G, Schadler V, Willenbacher N, Wagner NJ. *Langmuir* 2002;18:6381-6390.
- 7) Woods ME, Kreiger IM. *J Colloid Interf Sci* 1970;34:91-99.
- 8) Riddles CJ, Zhoa W, Hu H-J, Van De Mark MR. *Polymer Preprints* 2011;52:232-233.
- 9) Van De Mark MR, Natu AM, Gade SV, Chen M, Hancock C, Riddles C. *J Coat Technol* 2014;11:111-122.
- 10) Brader JM. *Journal of Physics: Condensed Matter* 2010;22:363101.
- 11) Chen M, Riddles CJ, Van De Mark MR. *Langmuir* 2013;29:14034-14043.
- 12) Evers M, Garbow N, Palberg T. *Physical Review E* 1998;57:6774-6784.
- 13) Grass K, Holm C. *Soft Matter* 2009;5:2079-2092.
- 14) Alexander S, Chaikin PM, Grant P, Morales GJ, Pincus P, Hone D. *J Chem Phys* 1984;80:5776-5781.

- 15) Manning GS. *J Phys Chem C* 1975;79:262-265.
- 16) Girifalco LA. *Statistical mechanics of solids*. Oxford University Press: 2003.
- 17) Ninham BW, Parsegian VA. *Journal of Theoretical Biology* 1971;31:405-428.
- 18) Belloni L. *Colloids and Surfaces A: Physicochem Eng Aspects* 1998;140:227-243.
- 19) Einstein A. *Annalen der Physik* 1906;14:289-306.
- 20) Simha R. *Journal of Applied Physics* 1952;23:1020-1024.
- 21) Hiemenz PR, Rajagopalan R. *Principles of colloid and surface chemistry*. 3<sup>rd</sup> ed.; MarcelDekker: 1997.
- 22) Smoluchowski M. *Theoretische Bemerkungen über die Viskosität der Kolloide*. *Kolloid Z* 1916;18:190-195.
- 23) Russel WB. *J Fluid Mech* 1978;85:673-683.
- 24) Booth F. *Proceedings of the Royal Society of London. Series A. Mathematical and Physical Sciences* 1950;203:533-551.
- 25) Watterson IG, White LR. *J Chem Soc Faraday Trans 2* 1981;77:1115-1128.
- 26) Ohshima H. *J Colloid Interf Sci* 2002;247:18-23.
- 27) Vaynberg AK, Wagner NJ. *J Rheol* 2001;45:451-466.
- 28) Jiang L, Chen SB. *J Non-Newton Fluid* 2001;96:445-458.
- 29) Nishida K, Kaji K, Kanaya T, Fanjat N. *Polymer* 2002;43:1295-1300.
- 30) Krieger IM. *Adv. Colloid Interface Sci* 1972;3:111-136.
- 31) Riddles CJ, Zhao W, Ju H-J, Chen M, Van De Mark MR. *Polymer* 2013;55:48-57.
- 32) Tanya C. Christensen, e. a. Patent 6085577 2000.
- 33) du Nouy PL. *J. Gen. Physio.* 1918;1:521-524.
- 34) Bohr N. *Roy. Soc. London, Phil. Trans., Ser. A* 1909;209:281-317.
- 35) Tornberg EA. *J. Colloid and Interface Sci.* 1977;60:50-53.
- 36) East GC, Margerison D, Pulat E. *Trans Faraday Soc* 1966;62:1301-1307.
- 37) Karlsson LE, Wesslén B, Jannasch P. *Electrochimica Acta* 2002;47:3269-3275.
- 38) Fedotova MV, Kruchinin SE. *J. Mol. Liq.* 2011;164:201-206.
- 39) Oncley, J. L. *Annals of the New York Academy of Sciences* **1941**, 41, 121-150.
- 40) Yan H, Guo X-L, Yuan S-L, Liu C-B. *Langmuir* 2011;27:5762-5771.
- 41) Lei Y, Child JR, Tsavalas JG. *Colloid Polym Sci* 2013;291:143-156.
- 42) Merzel F, Smith JC. *P Natl Acad Sci* 2002;99:5378-5383.
- 43) Chen M, Riddles C, Van De Mark MR. *Colloid Polym Sci* 2013;291:2893-2901.
- 44) Okubo T. *J Colloid Interf Sci* 1995;171:55-62.
- 45) Tanvir S, Qiao L. *Nanoscale Res Lett* 2012;7:1-10.

- 46) Vafaei S, Purkayastha A, Jain A, Ramanath G, Borca-Tasciuc T. *Nanotechnology* 2009;20:1-6.
- 47) Chaudhuri RG, Paria S. *J Colloid Interf Sci* 2009;337:555-562
- 48) Bennett MK, Zisman WA. *J Phys Chem* 1959;63:1911-1916.
- 49) Okkema AZ, Cooper SL. *Biomaterials* 1991;12:668-676.
- 50) Diamant H, Andelman HD. *J Phys Chem* 1996;100:13732-13742.
- 51) Kholodenko AL, Douglas JF. *Phys Rev E* 1995;51:1081-1090.
- 52) Mistry JK, Natu AM, Van De Mark MR. *J Appl Polym Sci* 2014;DOI10.1002/app.40916.
- 53) Mistry JK, Van De Mark MR. *J Coat Technol Res* 2013;10:453-463.



## 2. SUMMARY

This dissertation discussed the synthesis, characterization and application of a new type of aqueous, nano-particle dispersion system termed as colloidal unimolecular polymers (CUPs). CUPs with different surface functional groups, carboxylate, sulfonate and quaternary ammonium, were prepared by the process of water-reduction on the acrylic copolymers. The CUP particles were self-stabilized via electrostatic repulsion of the surface charged groups and hydrophobic chain association.

In PAPER I, a series of nine MMA-MAA copolymers were synthesized with molecular weight ranging from 3,000 to 160,000 to evaluate the effect of molecular weight of the copolymer on the CUP formation and stability. The particle size measurements of CUPs using DLS demonstrated that for polymers with molecular weight of less than 13,000, unimolecular collapse of polymer chains was not favored due to insufficient electrostatic stabilization. The CUP particles were not stable and aggregated to bigger particle size. For the polymers with molecular weight above 13,000, good agreement between the experimental and theoretical particle size was observed indicating the stability of the CUP particles.

In PAPER II, CUPs with sulfonate groups on the surface were prepared and utilized as an acid catalyst for crosslinking of acrylic-melamine resin systems. Unlike carboxylate functional CUPs, the sulfonate-CUPs were stable in the presence of water containing 50 ppm calcium ions, because, the calcium salt of sulfonic acid remained soluble. Carboxylate-functional CUPs on the other hand formed insoluble calcium salts and precipitated out of the solution. The sulfonate-CUPs effectively catalyzed crosslinking of hydroxyl and carboxyl functional acrylic latex resins with melamine resin and gave

mechanical properties comparable to that obtained using a commercial low molecular weight blocked sulfonic acid catalyst. The 4.5 nm particle size of the carboxylate-CUPs resulted in better availability of reactive groups and better coalescence than the 95 nm carboxylate functional latex, which was evident from better indentation hardness and MEK rubs. Leaching experiments using Soxhlet extraction showed that CUP catalyst became immobile possibly due to incorporation into the final cured film while the commercial catalyst leached out. Unlike conventional water reducible resins, CUP solutions offer a surfactant free, zero--VOC, high performance technology option for future coatings applications.

In PAPER III, synthesis of cationic functional CUPs based on quaternary ammonium groups was demonstrated. Compared to carboxylate-CUPs, the QUAT-CUPs displayed higher viscosity due to greater associated water fraction. The surface tension behavior of QUAT-CUPs was similar to carboxylate-CUPs. The surface tension decreased with increasing concentration and molecular weight of CUPs due to decreasing surface energy with increasing surface charge density.

In PAPER IV, the rheology and surface tension behavior of sulfonate-functional CUPs was evaluated. The sulfonate-CUP showed higher associated water fraction, surface water thickness and greater surface tension reduction than the carboxylate-CUP. Dynamic surface tension studies revealed a kinetically limited adsorption of CUPs to the air-water interface. The kinetic relaxation time increased with increasing concentration and molecular weight, indicating a barrier to adsorption of CUPs to the interface. It was demonstrated that similar to carboxylate-CUPs, Russel's model can also be used to predict viscosity of sulfonate-CUPs in the dilute region.

The development of acrylic colloidal unimoleuclar polymers (CUPs) has moved from the realm of laboratory investigation to the point today at which, they can be tested and developed commercially in numerous applications. Future research could involve studying the effect of concentration of polymer during water reduction on the unimolecular collapse and the evaluation of the solvent composition at the polymer chain collapse point.

**BIBLIOGRAPHY**

- 1) R.H. Fernando, *Nanotechnol. Appl. Coat.* 1008 (2009) 2-21.
- 2) M. Holman, *Nanopolymers*, Smithers Rapra Ltd., Berlin, Germany (2007).
- 3) B.V.N. Nagavarma, H.K.S. Yadav, A. Ayaz, H.G. Shivakumar, *Asian J. Pharm. Clin. Res.* 5 (2012) 16-23.
- 4) V. Balzani, *Small* 1 (2005) 278-283.
- 5) A.D. Ostrowski, E.M. Chan, D.J. Gargas, E.M. Katz, G. Han, P.J. Schuck, D.J. Milliron, B.E. Cohen, *ACS Nano* 6 (2012) 2686-2692.
- 6) K. Zhang, Z. Gui, D. Chen, M. Jiang, *Chem. Commun.* (2009) 6234-6236.
- 7) S. Lv, L. Liu, W. Yang, *Langmuir* 26 (2010) 2076-2082.
- 8) M. Chen, W. Yang, M. Yin, *Small* 9 (2013) 2715-2719.
- 9) C.J. Riddles, W. Zhao, H.J. Hu, M. Chen, M.R. Van De Mark, *Polymer* 55 (2014) 48-57.
- 10) J.K. Mistry, M.R. Van De Mark, *J. Coat. Technol. Res.* 10 (2013) 453-463.
- 11) A.V. Dobrynin, M. Rubinstein, *Prog. Polym. Sci.* 20 (2005) 1049-1118.
- 12) K.A. Dill, S. Bromberg, K. Yue, H.S. Chan, K.M. Ftebig, D.P. Yee, P.D. Thomas, *Prot. Sci.* 4 (1995) 561-602.
- 13) Q. Yang, S. Wang, P. Fan, L. Wang, Y. Di, K. Lin, F.S. Xiao, *Chem. Mater.* 17 (2005) 5999-6003.
- 14) Y. Zhou, W. Huang, J. Liu, X. Zhu, D. Yan, *Adv. Mater.* 22 (2010) 4567-4590.
- 15) X. Wang, X. Qiu, C. Wu, *Macromolecules* 31 (1998) 2972-2976.
- 16) V.O. Aseyev, H. Tenhu, S.I. Klenin, *Macromolecules* 31 (1998) 7717-7722.
- 17) J. Seixas de Melo, J., T. Costa, M.D.G. Miguel, B. Lindman, K. Schillén, *J. Phys. Chem. B* 107 (2003) 12605-12621.
- 18) L.J. Kirwan, G. Papastavrou, S.H. Behrens, *Nanoletters* 4 (2004) 149-152.
- 19) P. Kulkarni, K. Rajagopalan, D. Yeater, R.H. Getzenberg, *J. Cell Biochem.* 112 (2011) 1949-1952.
- 20) G. Li, J. Liu, Y. Pang, R. Wang, D. Yan, *Biomacromolecules* 12 (2011) 2016-26.
- 21) Y. Morishima, S. Nomura, T. Ikeda, M. Seki, M. Kamachi, *Macromolecules* 28 (1995) 2874-2881.
- 22) M. Mecerreyes, V. Lee, C. Hawker, J. Hedrick, A. Wursch, W. Volksen, *Adv. Mater.* 13 (2001) 501-510.
- 23) O. Altintas, J. Willenbacher, K. Wuest, K. Oehlenschlaeger, P. Krolla-Lidenstein, H. Gliemann, *Macromolecules* 46 (2013) 8092-8101.

- 24) X. Jiang, H. Pu, P. Wang, *Polymer* 52 (2011) 3597-3602.
- 25) J.W. Rosthauser, K. Nachtkamp, *Waterborne polyurethanes*, Stamford CT: Technomic Publ. (1987).
- 26) O. Sarvari, P. Phapant, V. Pimpan, *J. Appl. Polym. Sci.* 96 (2005) 1170-1175.
- 27) J.K. Mistry, A.M. Natu, M.R. Van De Mark, *J. Appl. Polym. Sci.* (2014).
- 28) Z.W. Wicks Jr., F.N. Jones, S.P. Pappas, A.D. Wicks, *Organic Coatings: Science and Technology*, 3<sup>rd</sup> Edition, John Wiley & Sons Publications, (2007).
- 29) M. Chen, C.J. Riddles, M.R. Van De Mark, *Colloid Polym. Sci.* 291 (2013) 2893-2901.
- 30) C.L. McCormick, D.L. Elliott, *Macromolecules* 19 (1986) 542-547.
- 31) M. Chen, C.J. Riddles, M.R. Van De Mark, *Langmuir* 29 (2013) 14034-14043.
- 32) A.V. Delgado, *Interfacial Electrokinetics and Electrophoresis*, Marcel Dekker Inc., NY, USA, (2002)
- 33) P. Hiemenz, R. Rajagopalan, *Principles of Colloid and Surface Chemistry*, 3<sup>rd</sup> Edition, Marcel Dekker Inc. NY, USA (1997).
- 34) H. Oshima, *J. Colloid Interface Sci.* 168 (1994) 269-271.
- 35) G.S. Manning, *J. Phys. Chem. C.* 79 (1975) 262-265.
- 36) L. Belloni, *Colloids and Surfaces A: Physicochem. Eng. Aspects* 140 (1998) 227-243.
- 37) R. Roa, F. Carrique, E. Ruiz-Reina, *Phys. Chem. Chem. Phys.* 13 (2011) 3960-3968.

## VITA

Ameya Manohar Natu was born on 14<sup>th</sup> January 1988 in Mumbai, India. He received his Bachelor's degree in Paints Technology with a First class, in May 2009 from the Institute of Chemical Technology (formerly known as UDCT) Mumbai, India. In August 2009, Ameya joined the Missouri University of Science & Technology and began his doctoral studies in Chemistry under the guidance of Dr. Michael R. Van De Mark and in the process received a Master's degree in Chemistry in August 2011. During the course of his doctoral study, Ameya has published 2 peer-reviewed papers out of which one was an Invited paper at the Journal of Coatings Technology and Research; 1 conference paper, 2 scientific industrial magazine articles and submitted 2 articles for publication in peer-reviewed journal. He presented his research work at 1 American Coatings Conference (2014), 1 American Chemical Society annual meeting (2014) and 1 Annual Waterborne Symposium. He has received Shelby F. Thames best paper award at the 40<sup>th</sup> Annual Waterborne Symposium for his research presentation as well as an Outstanding Graduate Teaching Assistant Award 2013 awarded by the Department of Chemistry at MST. Ameya joined Johns Manville in Littleton, Colorado as a Research Chemist following the completion of his Ph.D. in May 2015.